University of Stavanger

Faculty of Science and Technology

MASTER'S THESIS

Study program/Specialisation: Petroleum Geosciences Engineering	Spring, 2018 Open
Writer: Guro Laurentze Sætre Skarstein	(Writer's signature)
Faculty supervisor: Sverre Ekrene Ohm Alejandro Escalona	
Title of thesis: Geochemical Characterisation of Oils and Sediments from Cuba and Jamaica; Implications for the Northern Caribbean Petroleum System	
Credits (ECTS): 30	
Keywords: Cuba Jamaica Northern Caribbean petroleum system Hydrocarbon potential Geochemical characterisation	Pages: 129 Stavanger, 06.07.2018

Geochemical Characterisation of Oils and Sediments from Cuba and Jamaica; Implications for the Northern Caribbean Petroleum System

by

Guro Laurentze Sætre Skarstein

Master Thesis

Presented to the Faculty of Science and Technology

The University of Stavanger

The University of Stavanger

July, 2018

Abstract

The Caribbean plate has a complex tectonic history and its petroleum potential is relatively unexplored. Jamaica and a large part of Cuba were once part of the Great Arc of the Caribbean (GAC), which was later deformed as a result of two collisional events; Jamaica with the Chortis block during Latest Cretaceous and Cuba with the North American plate during the Paleocene. Due to the collision in the Paleocene, the stratigraphy of Cuba comprises rocks of both Caribbean and North American origins. The majority of the petroleum occurrences in northern Cuba are proposed to belong to a Gulf of Mexico (GOM) petroleum system.

This study presents detailed organic geochemical observations of fourteen crude oils and nineteen extracts from Cuba, as well as one crude oil, four extracts, and thirteen potential source rocks from Jamaica. The main goal is to investigate the petroleum system in the northern part of Caribbean. Analyses of oils and extracts by gas chromatography (GC), GC-mass spectrometry (GC-MS), GC-tandem mass spectrometry (GC-MSMS), and isotope analyses revealed alteration, facies, maturity, and age of the generating source rock. The geochemical results obtained were compared with published geochemical data from GOM and oils from the southern rim of the Caribbean plate (Barbados, Venezuela, and southeastern South America). In addition, Rock-Eval analysis gave information about source rock richness and maturity.

Organic geochemical data suggests that the Cuban and Jamaican oils can be divided into five oil families based on facies and age dependent biomarker ratios. Family I consists of oils derived from shales in northwestern Cuba, whereas Family II comprises oils originating from marls in the same area. The third (Family III) represents the oils generated by carbonates in central Cuba, Family IV includes the carbonate derived oils from southern Cuba, and Family V consists of the oils originating from marls in Jamaica. Furthermore, the presence of light oil fraction in biodegraded oils, as well as differences in maturity and facies between the oil fractions suggest the existence of at least two petroleum system in northwestern and central Cuba.

The regional geochemical comparison showed similarities in lithofacies and age with oils from GOM, suggests that the GOM petroleum system is working on northwestern Cuba. On the other hand, the Cuban and Jamaican oils appear to belong to different petroleum system than the oils

from the southern margin of the Caribbean plate. Finally, the potential source rocks collected from Jamaica showed to have petroleum potential when buried sufficiently deep to attain the temperatures needed to generate petroleum.

Acknowledgment

I would like to express my sincere gratitude to my supervisors Sverre Ekrene Ohm and Alejandro Escalona for their valuable guidance and support throughout this project.

Acknowledgement also goes to the Conjugate, Basin, Tectonics, and Hydrocarbons (CBTH) for providing essential economic support, Petroleum Cooperation in Jamaica (PCJ) and Union Cuba-Petróleo (CUPET) for facilitating oil samples necessary to develop this research. Per Erling Johansen for the valuable work on lab and training in organic geochemistry, and APT technologies for the engagement of the allowance to the technical visit and analysis runs.

Furthermore, a great thanks to my fellow students at the University of Stavanger, these two years of studying would not have been the same without you!

Lastly, I thank my family and friends for endless support through the duration of my studies. I could not have done this without you.

Table of Contents

Table of Figures

List of Tables

1 Introduction

The tectonically active Caribbean plate is less explored and understood compared to the neighbouring hydrocarbon-rich provinces to the north (Gulf of Mexico (GOM)) and the south (northern South America) (***Figure 1***). The tectonic complexity along with the diversity of depositional environments and the crustal characteristics of the region poses the main challenge for the evolution of the petroleum potential. Hence, its petroleum potential and the nature of the petroleum occurrences remain poorly understood. To the north of the Caribbean plate, the GOM is known to be sourced by Jurassic and Cretaceous source rocks (Galloway, 2009), whereas the northern margin of South America is known to be mainly sourced by Cretaceous source rocks (Talukdar et al., 1993).

Tectonic models indicate Jamaica and a large part of Cuba were once part of the same island arc, the Early Cretaceous Great Arc of the Caribbean (GAC) (Escalona and Norton, 2015). At present day, Jamaica is situated in the northeastern part of the Nicaraguan Rise within the Caribbean plate (Figure 1). On the other hand, Cuba has been thrusted over the southern part of the North American plate (Figure 2) and separated from the main lithospheric crust by the active Cayman trough (Figure 1) (Escalona and Norton, 2015). Thus, Cuba consist of rocks from both the GAC and the North American plate, whereas Jamaica comprises rocks from the Caribbean plate. The majority of the oil fields in Cuba are located in the north and are proposed to be related to the GOM petroleum systems (Moretti et al., 2003, Magnier et al., 2004). To date, no major fields have been discovered in the southern part of Cuba, neither in Jamaica, and petroleum occurrences in these areas are solely related to shows and seeps.

This study aims to improve the understanding of the petroleum system(s) in the Caribbean region as part of a major project initiated in 2017 by the Conjugate Basins Hydrocarbons and Tectonics (CBTH) consortium (Cedeno 2017). This project focuses on the northern margin of the Caribbean plate, namely Cuba and Jamaica, by preforming geochemical characterisation of oils and source rock samples. Rock-Eval, gas chromatography (GC), GC-mass spectrometry (GC-MS), GC-tandem mass spectrometry (GC-MSMS) are the main means of data. The results obtained will be compared to published data regarding oil composition from GOM and oils from northern South America and Barbados to evaluate possible similarities

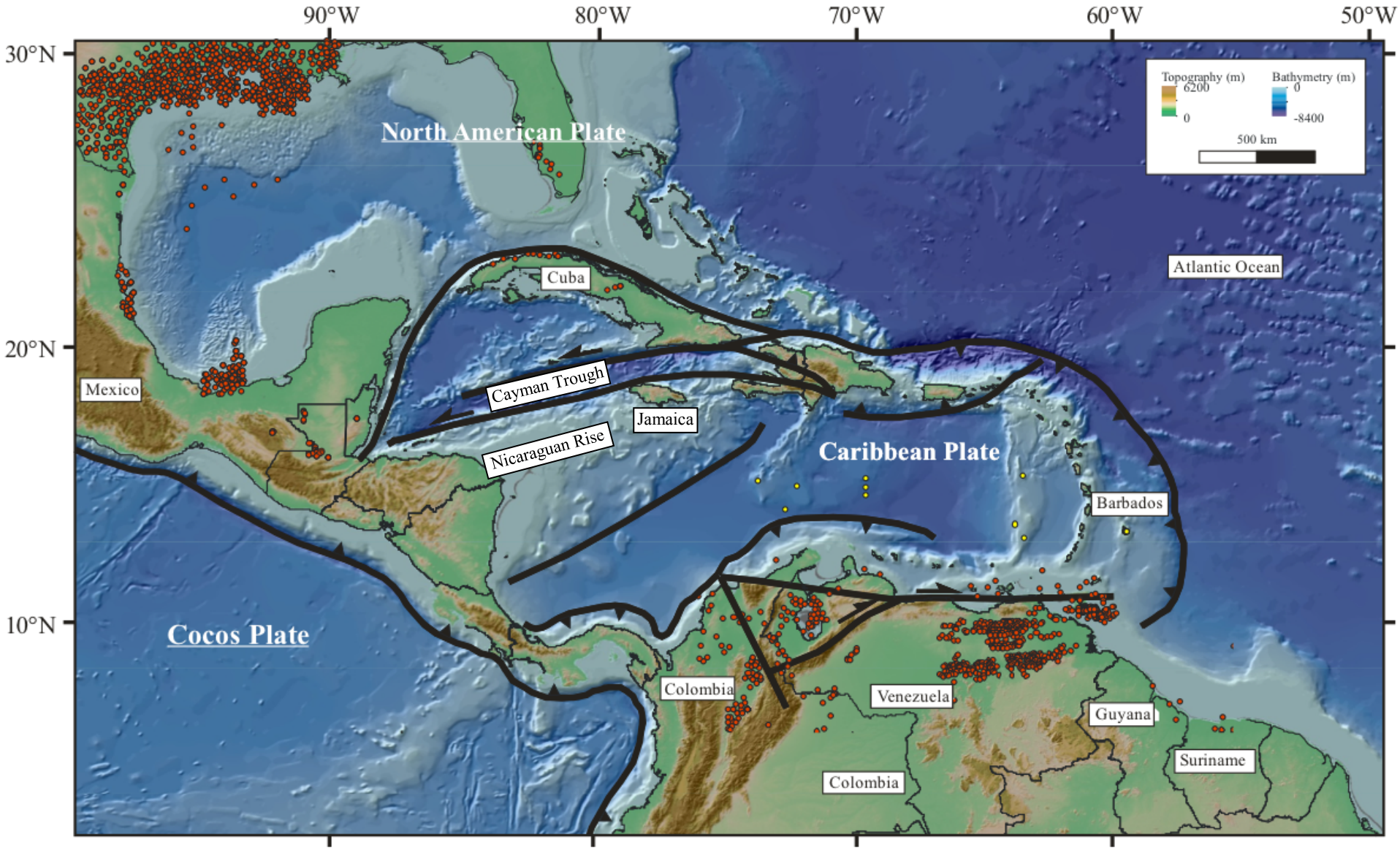

Figure 1 *Regional plate boundary map showing the margins to the north (Gulf of Mexico) and south (northern South America) of the Caribbean plate to very prolific for hydrocarbon, as the red circles represents oil fields (CBTH database, 2018). Jamaica is located on the Caribbean plate, whereas Cuba has been thrusted over the southern part of the North American plate and is separated from the Caribbean plate by the active Cayman trough.*

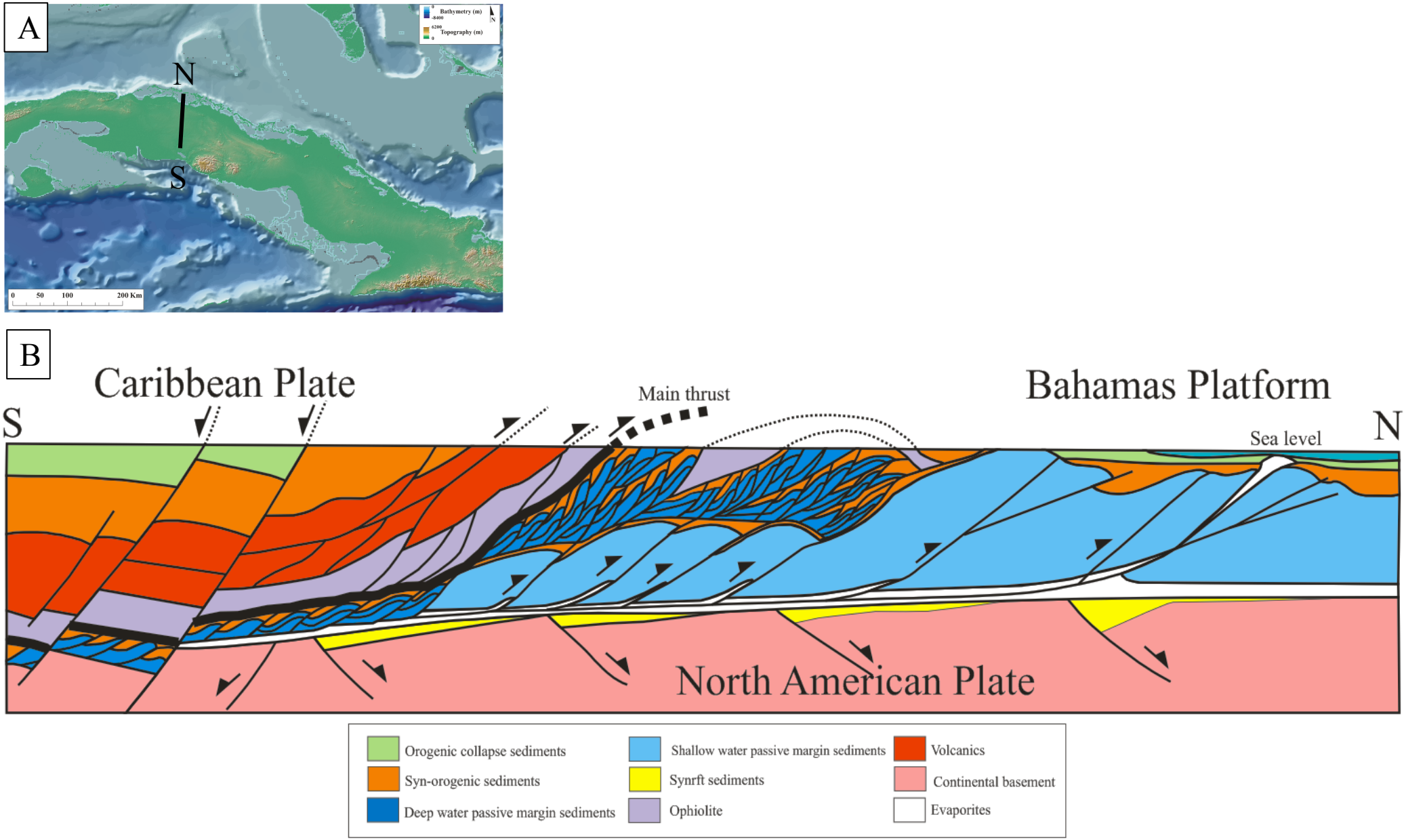

Figure 2 A *location of the cross section in Cuba,* ***B*** *Schematic geologic cross section illustrating the overthrusting of the Cuban island arc onto the North American plate and the complex structure of the fold and thrust belt, as well as the rift zone underlying the belt. Modified from Cubapetroleo (2002).*

2 Geological Setting

Cuba and Jamaica lie along a wide plate boundary of deformation formed by Cretaceous–Cenozoic tectonic interaction between the Caribbean and the southern North American plate (Mann et al., 1990). The present-day tectonic setting in the study area is controlled by the eastward motion of the Caribbean plate relative to North America plate at a rate of approximately 20 mm yr^{-1} (Mann, 1999, Weber et al., 2001).

2.1 Geological Evolution

Rifting between the North and South American plates during the breakup of Pangea (***Figure 3***A), from Late Triassic to Late Jurassic, resulted in the proto-Caribbean ocean with the formation of graben and half graben structures (Pindell and Dewey, 1982). These structures were later filled with synrift sedimentary facies (Haczewski, 1976). As the rifting progressed, a passive margin along the southern edge of the North American plate was developed. This margin was dominated by a carbonate build up platform during the Upper Jurassic (Schenk, 2008).

The end of the rifting of the proto-Caribbean ocean is unclear; however, a flooding event took place during the Berriasian, which submerged the graben and half graben structures (Denny et al., 1994). Due to a rapid subsidence, a second phase of carbonate deposition of stacked shallow water platforms established along the southern margin of the North American plate (Denny et al., 1994). To the west of the proto-Caribbean ocean (Figure 3B), an island arc, namely the Great Arc of the Caribbean (GAC) (Figure 3B), was developed due to the eastward subduction of the Farallon plate beneath the proto-Caribbean oceanic crust in the Aptian (Burke, 1988).

The collision between the GAC and a dense part of the Farallon plate (Figure 3C) called the Caribbean Large Igneous Province (CLIP) in Santonian times caused a switch in the direction of subduction in the Latest Cretaceous (Figure 3C). This led to the creation of the Caribbean plate (Burke, 1988, Sinton et al., 1998). In the Campanian, the newly created plate started to drift to the northeast with the GAC in the lead (Burke, 1988).

Two collisional events deformed the GAC and the leading edge of the proto-Caribbean plate. The first collision was with the Chortis block (Figure 3D) during the Campanian, resulting in the detachment of Jamaica from the GAC (Pindell, 1994). During the Paleocene, the second collision took place between the North American plate and the northernmost part of the GAC

(Figure 3E). As the Caribbean plate approached the Bahamian platform to the northeast, the proto-Caribbean crust of the North American plate was thrusted as imbricated slices (Allen and Allen 1990), resulting in the development of a foredeep basin (Iturralde-Vinent et al., 2008). The Caribbean plate further collided with the Bahamas platform during the Middle to Late Eocene, resulting in the ophiolites and volcanic rocks of the Cuban island arc to override the Bahamas platform (Iturralde-Vinent et al., 2008). By Late Eocene, the emplacement of Cuba onto the North American plate was completed (Figure 3F)(Iturralde-Vinent et al., 2008).

Jamaica, however, experienced northeast to southwest extension during the Paleocene until the Early Eocene. This resulted in the formation of a northwest-southeast graben system in eastern Jamaica (Draper, 2008), as well as north trending depocenters were developed in the southwest and southeast Jamaica (Mann and Burke, 1984). The rift event was followed by a time of quiescence with subsidence during Middle Eocene (Robinson, 1994, Draper, 2008). The period of quiescence ended in the Middle Miocene when Jamaica was uplifted due the development an east-west trending restraining bend (Mann et al., 1985, Mann et al., 2007).

In between Cuba and Jamaica, two southwest-northeast trending strike slip fault zones formed the Cayman trough during the Eocene (Leroy et al., 2000), related to the eastward movement of the Caribbean plate relative to the North American plate (Molnar and Sykes, 1969, Jordan, 1975). Cuba was then separated from the rest of the Caribbean plate by the active trough, whereas Jamaica was translated to the east due to the strike slip movement (Figure 3F-G)(Leroy et al., 2000).

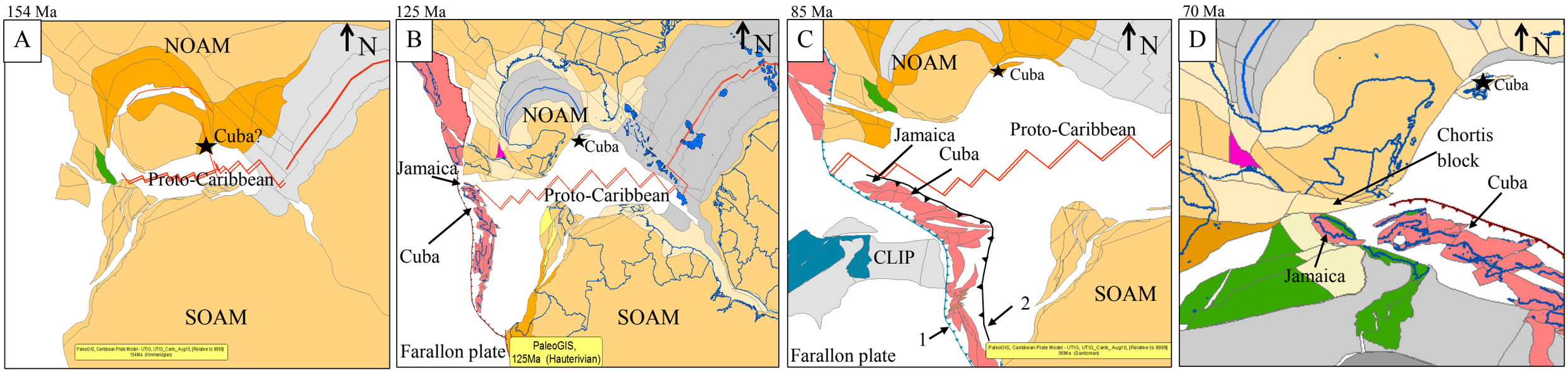

Figure 3 *Plate tectonic reconstruction model of the Caribbean region from the Late Jurassic to recent (Escalona and Norton, 2015).* ***A*** *Rifting between the North and South American plates during the Late Jurassic led to development of the proto-Caribbean ocean.* ***B*** *During the late Early Cretaceous the Great Arc of the Caribbean was developed due to the subduction of the Farallon plate.* ***C*** *The collision between the GAC and a dense part of the Farallon plate called the Caribbean Large Igneous Province (LIP) in the Late Cretaceous led to the switch in the direction of the subduction (from 1 to 2), resulting in the creation of the Caribbean plate.* ***D*** *During the Latest Cretaceous, the GAC collided with the Chortis block, which resulted in the detachment of Jamaica from the GAC.* ***E*** *The GAC collided with the North American plate in the Paleocene, which led to the Cuba being thrusted over the sourthern part of the North American.* ***F*** *During the Late Eocene, the emplacement of Cuba onto the North American plate was completed. Cuba was then separated from the Caribbean plate by the strike-slip movements of the Cayman trough, whereas Jamaica was translated to the east.* ***G*** *At present day, Cuba is located on the North American plate, consisting of rocks from both Caribbean and North American origin, whereas Jamaica is situated on the northeastern part of the Nicaraguan Rise.*

2.2 Lithostratigraphy

2.2.1 Cuba

The Cuban stratigraphy comprises rocks of both North American and Caribbean origins (Figure 5). Rocks related to the North American affinity are comprised of Lower Jurassic siliciclastic deposits, which are mainly followed by carbonate successions of Upper Jurassic to Upper Cretaceous ages (Pszczółkowski, 1999) (Figure 5). During the Paleocene to Lower Eocene, synorogenic foredeep sedimentary rocks of carbonate and olistostrome deposits derived from both the Cretaceous volcanic arc and the Bahamas Cretaceous carbonate platform were deposited (Bralower and Iturralde-Vinent, 1997, Iturralde-Vinent et al., 2008). These sediments are present in the northern foldbelt along the northern coast of Cuba (Iturralde-Vinent et al., 2008, van Hinsbergen et al., 2009) (Figure 4).

The Cuban island arc is, on the other hand, associated to the Caribbean plate. The basement of the arc complex was formed by high temperature amphibolites derived from the oceanic crust known as the Mabujina amphibolites (Draper and Barraos, 1994, Iturralde-Vinent, 1994) (Figure 5). In addition, igneous and volcanoclastic rocks were formed during the development of the Great Caribbean Arc system in the Cretaceous (Iturralde-Vinent, 1994) (Figure 5). During the collision with the North American plate, ophiolites were obducted onto the Caribbean arc and outcrop discontinuously for more than 1000 km along the northern margin of Cuba (Iturralde-Vinent et al., 2016) (Figure 4). Uppermost Cretaceous to Upper Eocene clastic deposits derived from Cretaceous igneous substrate and interbedded carbonates, unconformably overlie Cretaceous arc and ophiolite complexes (Iturralde-Vinent et al., 2016) (Figure 5). In eastern Cuba, rocks of Paleocene and Eocene ages are essentially of lavas and volcanoclastic rocks, associated with the formation of the east west trending submarine volcanic arc in southeastern part of Cuba (Iturralde-Vinent, 1994) (Figure 5 and Figure 4). Uppermost Eocene to recent rocks are characterised by post-orogenic carbonate and clastic rocks (Iturralde-Vinent and Lidiak, 2006) (Figure 5).

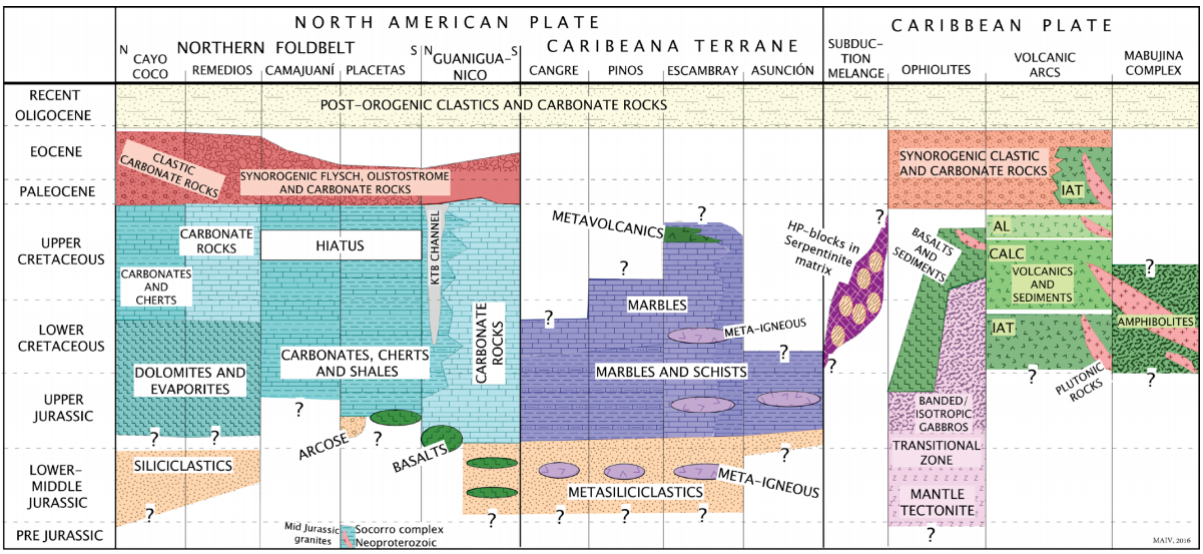

Figure 4 *Generalised stratigraphic chart of Cuba (Iturralde-Vinent et al., 2016).The abbreviations are described as followed:* ***IAT****: Island arc tholeiite;* ***AL****: alkaline suites;* ***CALC****: calc-alkaline suites;* ***KTB****: Deep erosional channel cut due to the Cretaceous-Tertiary boundary mass flows from the platform margins as a result of the impact.*

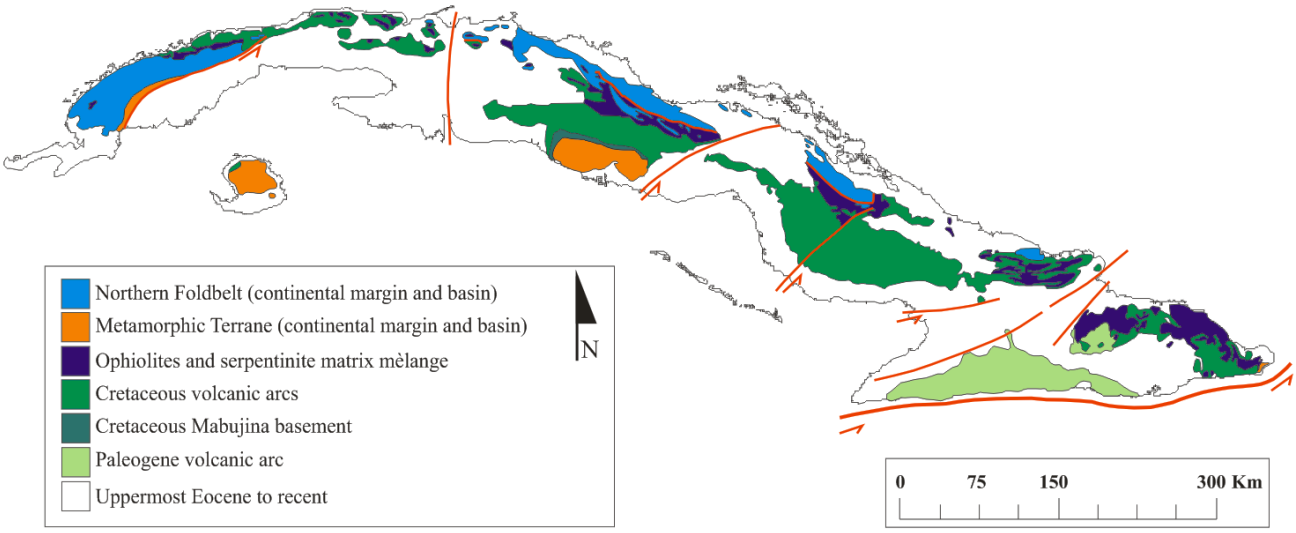

Figure 5 *Simplified geological map of Cuba showing the different outcropping units. Modified from Iturralde-Vinent et al. (2016).*

2.2.2 Jamaica

The Lower and Middle Cretaceous of the Jamaican island arc are characterised by volcanic activity associated with the extrusion of lavas and deposition of volcanically derived conglomerates and sandstones, as well as shales and limestones (Robinson, 1994, Mitchell, 2003). Rocks of Upper Cretaceous ages are comprised of deep-water shales with turbidites (Mitchell, 2006). These deep water sediments were followed by a shallowing event marked by the wide occurrence of limestone with the *Barrettia gigas* of Middle Campanian age (Mitchell, 2006). The Uppermost Cretaceous rocks in central Jamaica, represent a major transgressive-regressive cycle, consisting of mudstone, rudistbearing limestone, followed by a shallowing-upward succession of marine to terrestrial volcanoclastic sedimentary rocks (Mitchell, 2006) (Figure 7 Simplified geological map of Jamaica, showing the different outcropping geological units. Modified from Brown and *Mitchell (2010).*). In eastern Jamaica, these Cretaceous rocks are covered by synrift sediments mainly consisting of sandstones, conglomerates, mudstone, and limestones during the Paleocene to Middle Eocene (Figure 7 and Figure 6). Sediments of the Yellow and White Limestone groups unconformally overlie the Cretaceous rocks in western and central Jamaica, and the syn-rift rocks in eastern Jamaica (Mitchell et al., 2003) (Figure 6). The Yellow Limestone Group consists of clastic rocks, impure limestone, marlstone, and clean limestone of Middle Eocene age (Mitchell et al., 2003). The White Limestone Group is composed of shallow and deep water clean carbonates of Upper Eocene to Lower or Middle Miocene age, and covers two thirds of Jamaica (Mitchell, 2003, Mitchell et al., 2003) (Figure 7). These carbonate rocks were capped by rocks deposited in the Coast Group around the margin of Jamaica and alluvium (James-Williamson and Mitchell, 2012) (Figure 7 and Figure 6).

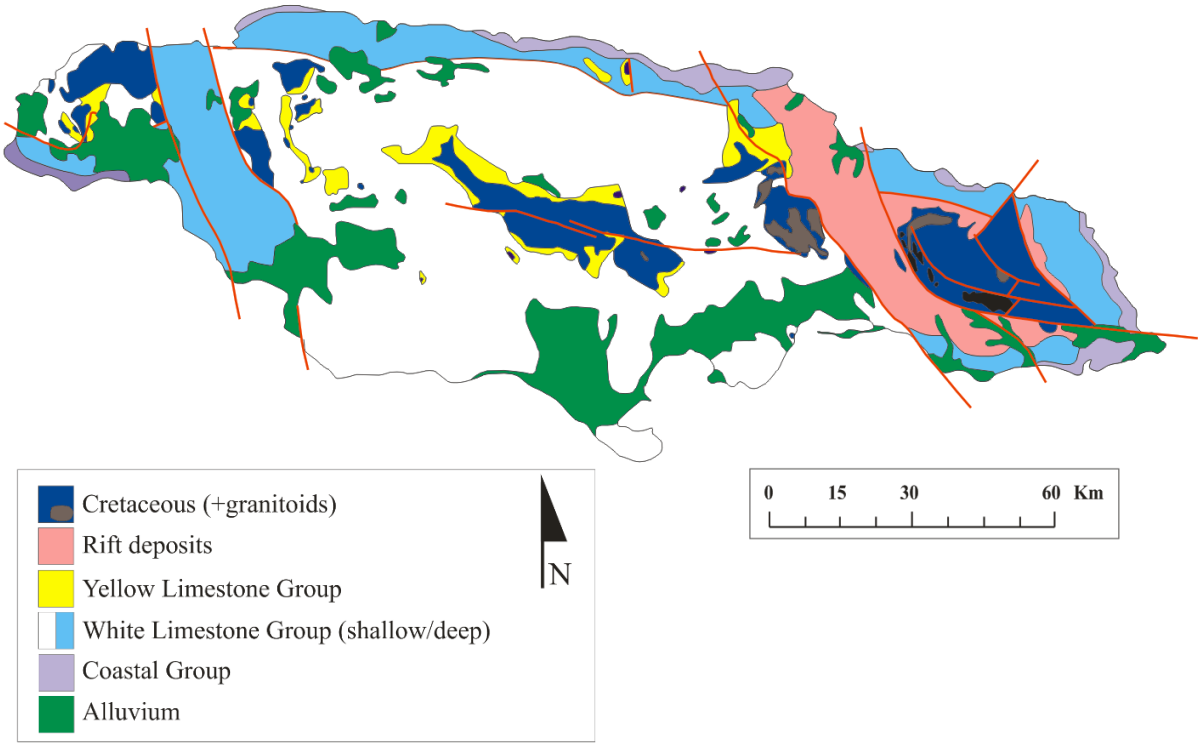

Figure 7 *Simplified geological map of Jamaica, showing the different outcropping geological units. Modified from Brown and Mitchell (2010).*

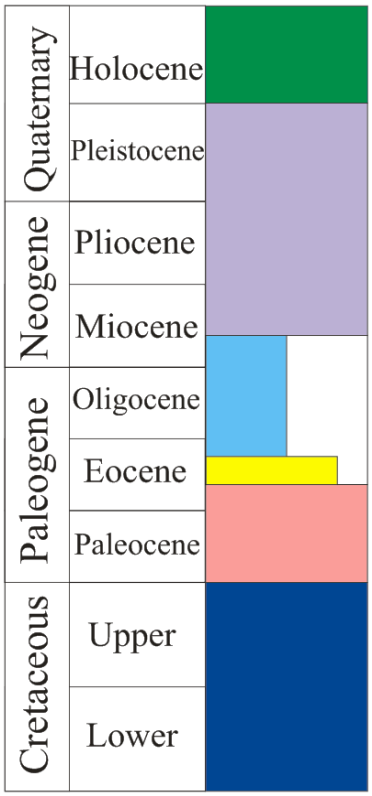

Figure 6 *Generalised stratigraphic column of Jamaica. Modified from (Brown and Mitchell, 2010).*

3 Methodology

3.1 Cuba

Fourteen crude oils, twelve extracts, and seven seepage samples were collected from different locations in Cuba (Figure 8) (Table 1). The crude oils (samples 1-14), and extracts (sample 15-26) were provided by Union Cuba-Petróleo (CUPET) in Cuba, whereas the seepage samples were collected during a field trip in January 2018 (samples X1, X2, Y1, A1, A2, A3, and C1).

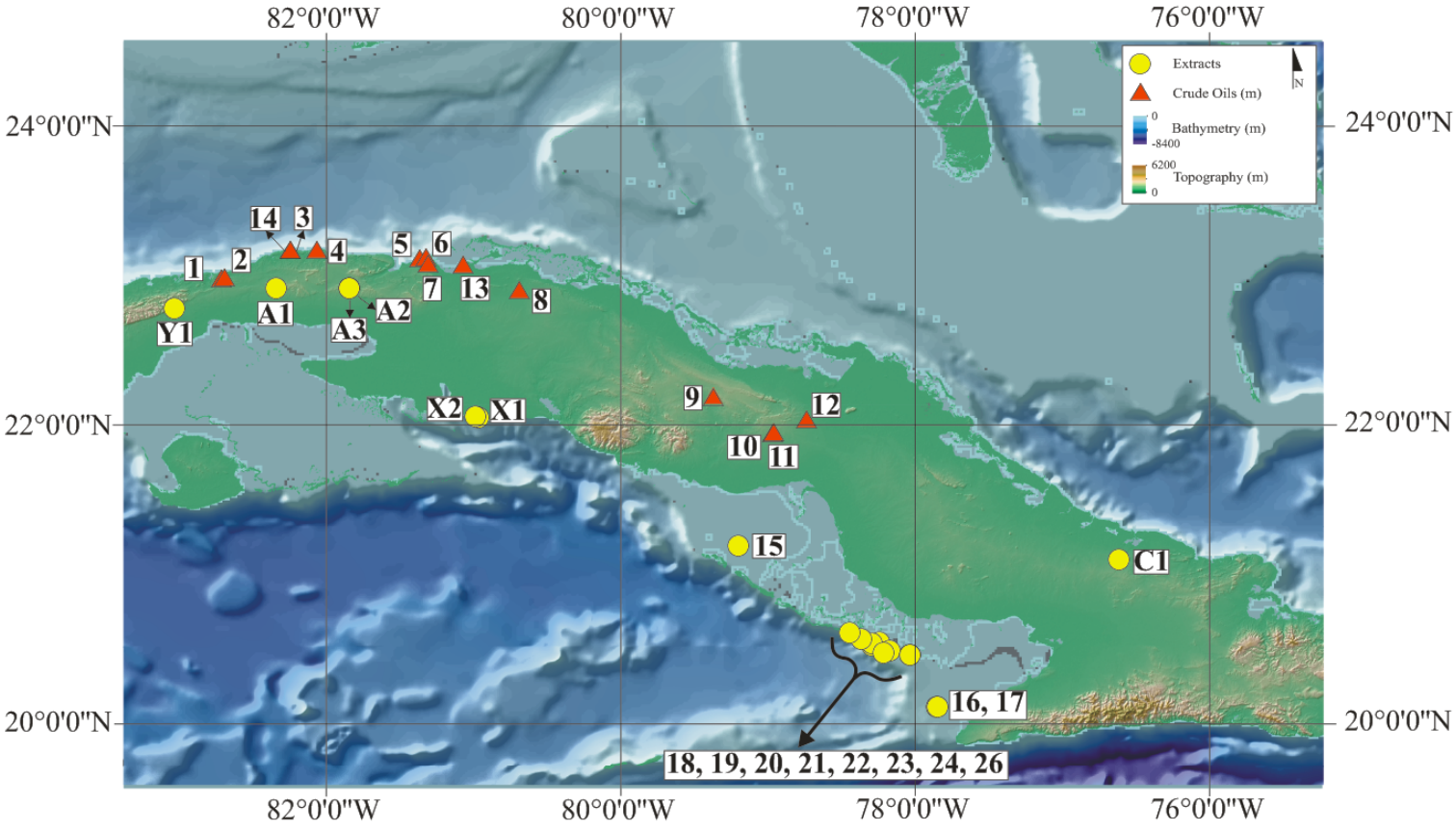

Figure 8 *Map of Cuba visualising the location of the crude oil (red triangles) and extract (yellow circles) samples included in this study.*

Table 1 *Location and description of the samples included in this study.* ***O****: crude oil;* ***OSS****: oil stained sediments;* ***OSC:*** *oil stained carbonate;* ***OS****: Oil seepage.*

Sample	Location/Well	Coordinates		Depth	Type	Description
		N	W			
1	Martin Mesa 7	82°41'15.7"	22°59'20.1"	1315	O	Black oil with low viscosity.
2	Martin Mesa 3	82°40'18.4"	22°59'48.9"	3425	O	Black oil with low viscosity.
3	Bacuranao L-300	82°14'41.8"	23°11'34.7	1000	O	Black oil with high viscosity.
4	Boca de Jaruco	82°02'56.5"	23°10'56.4"	1732	O	Black oil with low viscosity.
5	Varadero 1000	82°21'23.7	23°07'13.3"	1577	O	Black oil with high viscosity.
6	Varadero 604	81°18'42.5"	23°07'38.8"	745	O	Black oil with high viscosity.
7	Cantel 2000	81°17'59.9	23°05'30.2"	1300	O	Black oil with low viscosity.
8	Motembo 2X	80°41'03.2"	22°54'25.1"	1700	O	Condensate, clear in colour.
9	Jarahueca 34	79°21'58.1"	22°11'15.7"	1006	O	Light oil with an orange colour and low viscosity.
10	Cristales 100	78°58'22.6"	21°56'50.9	630	O	Black oil with low viscosity.
11	Cristales 69	78°57'56.1"	21°57'20.9"	645	O	Black oil with low viscosity.
12	Pina 134	78°44'41.0"	22°02'03.9"	1032	O	Black oil with low viscosity.
13	Majaguillar 1000	23°4'38.24''	81°3'39.18''	900.6-900.27	O	Black oil with high viscosity.
14	Bacuranao L-300	23°10'43.92"	82° 13' 44"	2203	O	Black oil with low viscosity and a strong smell of sulphur
15	Ana Maria	21° 10' 22.01"	79°11'54.98"	2625	OSS	Extract.
16	Sea bottom	20° 5' 19.32"	77°51'56.52"	16	OSS	Extract.
17	Sea bottom	20° 5' 9.24"	77°51'24.84"	16.7	OSS	Extract.
18	Sea bottom	20° 30' 45"	78°17'49.56"	23.2	OSS	Extract.
19	Sea bottom	20° 31' 45.12"	78°14'49.92"	4-10	OSS	Extract.
20	Sea bottom	20° 31' 17.4"	78°17'49.56"	17	OSS	Extract.
21	Sea bottom	20° 28' 8.76"	78°10'28.56''	8.3	OSS	Extract.
22	Sea bottom	20° 27' 41.4"	78°12'50.76''	10	OSS	Extract.
23	Cayo Carapacho	20° 26' 51.36"	78°2'24.72''	Outcrop	OSS	Extract.
24	Cayo Carapacho	20° 26' 51.36"	78°2'24.72''	Outcrop	OSS	Extract.
25	Cayo Caguama	20° 33' 12.96"	78°22'21.36''	Outcrop	OSS	Extract.
26	Cayo Caguama	20° 35' 24"	78°26'45.24''	Outcrop	OSS	Extract.
X1	Caleta Buena	22°2'39.23''	80°57'21.22''	Outcrop	OSC	Solidified oil sample from surface on a carbonate beach.
X2	Caleta Buena	22°2'51.95''	80°58'40.90''	Outcrop	OSC	Solidified oil sample from surface on a carbonate beach.
Y1	Soroa	22°46'77.91''	83°0'13.68''	Outcrop	OSC	Solidified oil sample along a fault.
A1	Bejucal	22°54'43.3"	82°19'20.8"	Outcrop	OSC	Solidified oil sample along a fault.
A2	Loma del Grillo	22°54'48"	85°49'30.098"	Outcrop	OS	Oil sample from the top of an active oil seep pond.
A3	Loma del Grillo	22°54'48.7"	85°49'30.098"	Outcrop	OSS	Solidified oil sample of the active oil seep taken from the edge of the pond.
C1	Manibón	21°05'12.0"	76°37'55.8"	Outcrop	OS	Oil sample from an active oil seep along a fault.

3.1.1 Crude Oils

The crude oils were collected from nine different oil fields in northwest and central Cuba (Figure 8). In general, the oils are black in colour with low viscosities (Figure 9A). However, four of these oils (samples 3, 5, 6, and 13) have relatively higher viscosities (Figure 9B). Nevertheless, the samples 8 (Figure 9C) and 9 (Figure 9D) are a condensate and a light oil, respectively.

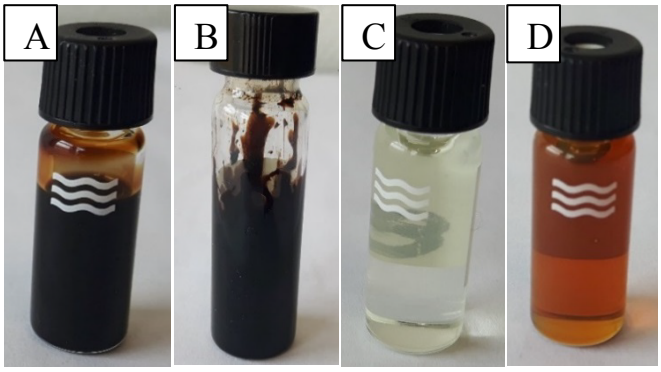

Figure 9 A *sample 11 an example of the low viscosity black crude oils,* ***B*** *sample 3 as an example of a black oil with high viscosity,* ***C*** *the condensate sample, and* ***D*** *the light oil sample 9.*

3.1.2 Extracts

The twelve extracts were collected from southeastern Cuba (Figure 8). Of these, sample 15 was gathered from the well Ana Maria (Figure 10A), the seven samples 16-22 were collected from the sea bottom, and the remaining four extracts (samples 23-26) were collected from the islands Cayo Carapacho (Figure 10C) and Cayo Caguama (Figure 10D). In addition, seven oil seep samples were collected from different locations on Cuba (Figure 8). Samples A2 (Figure 11A-B) and C1 (Figure 11C) were collected from active oil seeps, whereas the remaining samples (A1, A3, X1, and X2) were oil stained sediments (Figure 11 D-E).

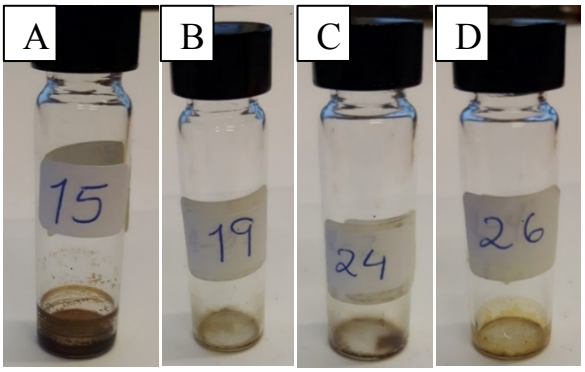

Figure 10 A *the extract sample from the well Ana Maria,* ***B*** *sample 19 as an example of the extract samples from the sea bottom,* ***C*** *sample 24 as an example of the extracts sampled from the island Cayo Carapacho, and* ***D*** *sample 26 as an example of the extracts collected from Cayo Caguama.*

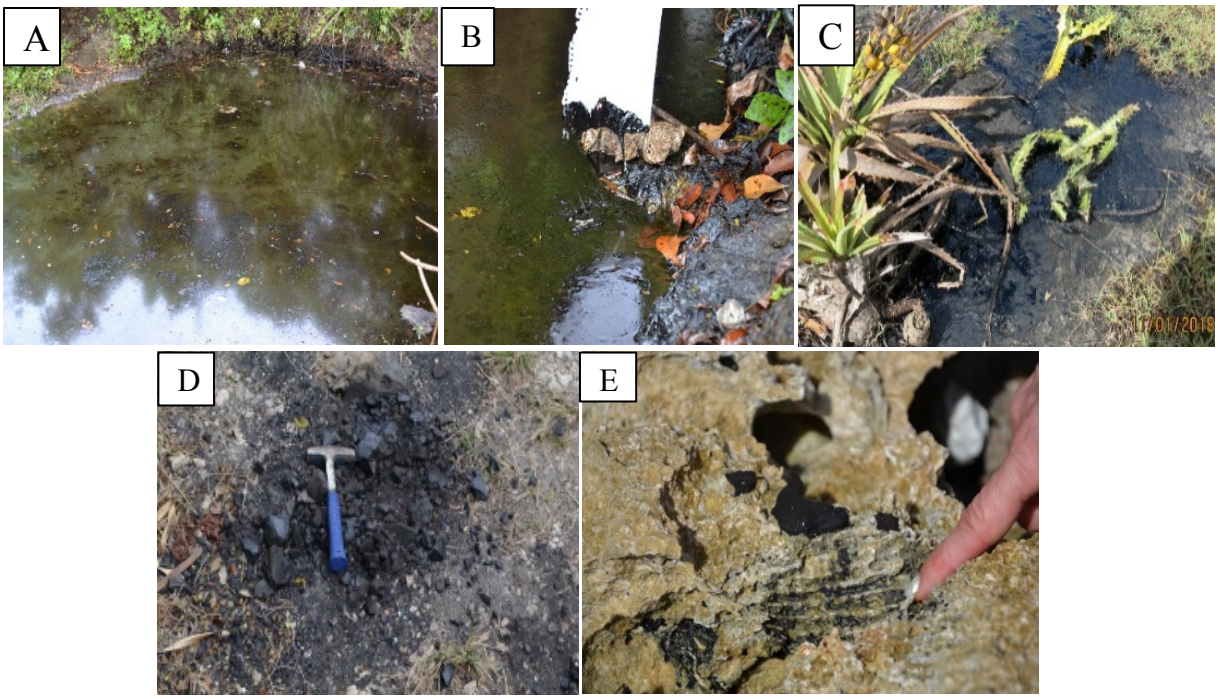

Figure 11 A *the active oil seep pond were sample A2 was collected,* ***B*** *high viscosity of the oil of the sample A2 shown on a paper dipped into the pond,* ***C*** *the active seep where the sample C1 was gathered* ***D*** *The fault zone where the bitumen sample A1 was collected,* ***E*** *Samples X1 and X2 were collected from this carbonate beach, where the samples were located at the surface as seen in the figure.*

3.2 Jamaica

The samples from Jamaica consists of one crude oil and twelve core samples provided by the Petroleum Cooperation in Jamaica (PCJ). In addition, one oil seep sample, as well as five organic-rich rocks were gathered from different locations on Jamaica during the field trip (Figure 12) (Table 2).

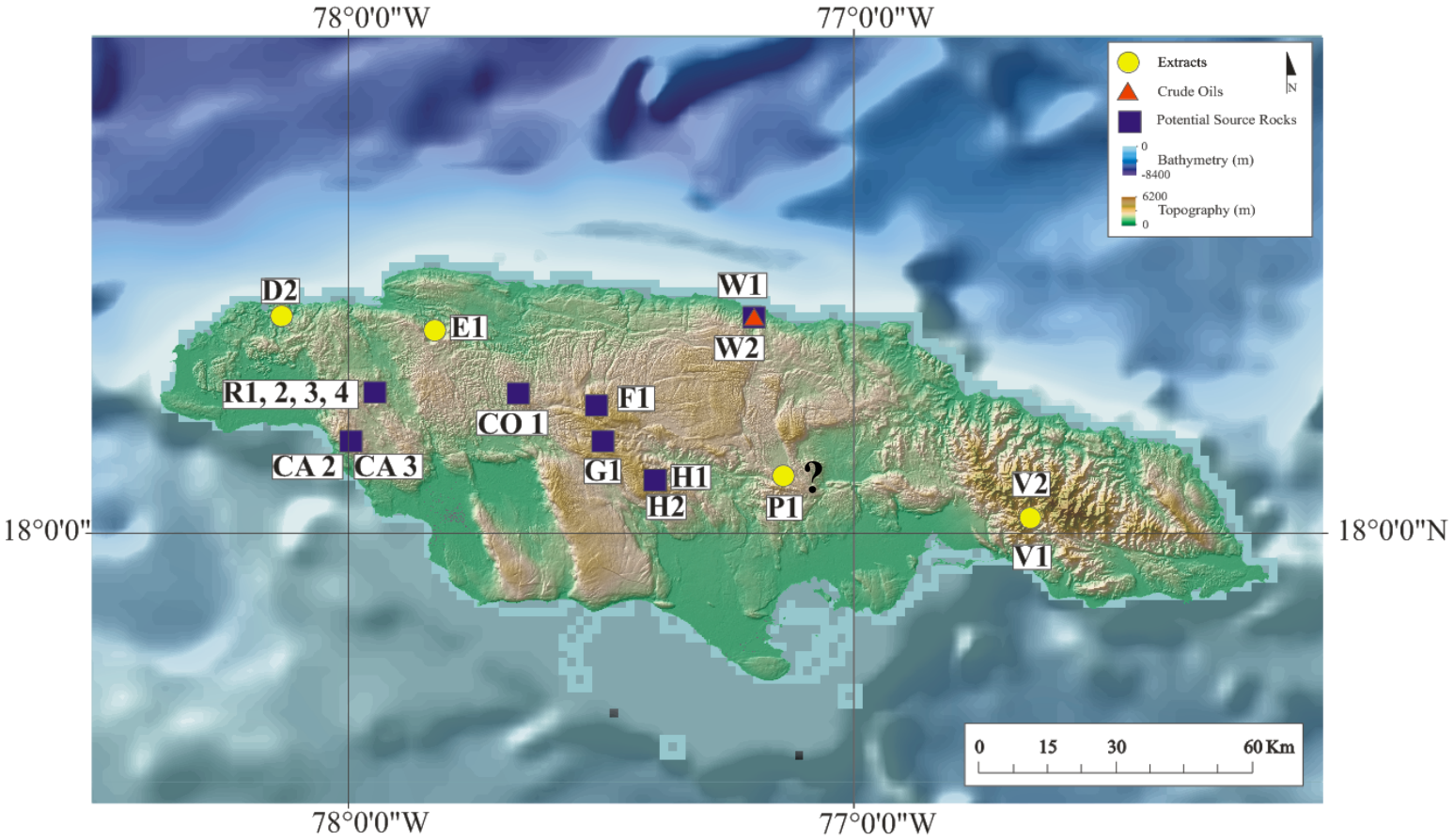

Figure 12 *Map of Jamaica illustrating the distribution of the extract, crude oil, and potential source rock samples included in this study.*

Table 2 *Location and description of the samples included in this study from Jamaica.* ***Sh****: shale;* ***OSC****: oil stained carbonate;* ***OSSil****: oil stained siltstone;* ***C****: coal;* ***O****: crude oil;* ***OSSs****: oil stained sandstone.*

Sample	Location/Well	Coordinates		Depth (m)	Formation	Age	Type	Description
		N	W					
D2	Outside Lucea Harbour	18°25'37.8"	78°07'48.0"	Outcrop	-	-	OSC	Oil stained carbonate sample, collected from an oil layer
E1	Johns Hall	18°23'56.0"	077°49'28.9"	Outcrop	-	Lutetian	OSSil	Oil impregnated siltstone from the field.
F1	?	18°15'3.92"	077°30'27.4"	Outcrop	Litchfield?	Lutetian	Sh	Black shale sample from the field.
G1	Alongside the Christiana road	18°10'39.9"	077°29'40.3"	Outcrop	Litchfield/ Chapelton contact	Lutetian	Sh	Grey shale sample.
H1	Broomwell, Clarendon	18°06'11.0"	077°23'33.1"	Outcrop	Litchfield	Lutetian	C	Coal sample form the top of the outcrop, were fossils of leafs were observed.
H2	Broomwell, Clarendon	18°06'11.0"	077°23'33.1"	Outcrop	Litchfield	Lutetian	Sh	Black shale sample from the bottom of
CO1	Cockpit 1	18°16'18"	077°39'36"	1081.4	Sunderland?	U. Campanian	Sh	Dark grey shale sample from core. The core has been exposed to high temperatures over time.
CA2	Content A	18°10'40"	077°59'32"	1488.6-1490.5	Litchfield	Lutetian	Sh	Dark grey shale sample from core. The core has been exposed to high temperatures over time.
CA3	Content A	18°10'40"	077°59'32"	1498.4-1502.4	Litchfield	Lutetian	Sh	Dark grey shale sample from core. The core has been exposed to high temperatures over time.
R1	Retrive 1	18°16'29.5"	077°53'223.5"	2032.4-2038.8	Seafield?	M. Albian	Sh	Dark grey shale sample from core. The core has been exposed to high temperatures over time.
R2	Retrive 1	18°16'29.5"	077°53'223.5"	2275.6-2276.8	Rio Nuevo	M. to U. Cenomanian	Sh	Dark grey shale sample from core. The core has been exposed to high temperatures over time.
R3	Retrive 1	18°16'29.5"	077°53'223.5"	2276.8-2277.9	Rio Nuevo	M. to U. Cenomanian	Sh	Dark grey shale sample from core. The core has been exposed to high temperatures over time.
R4	Retrive 1	18°16'29.5"	077°53'223.5"	2278.3-2279	Rio Nuevo	M. to U. Cenomanian	Sh	Dark grey shale sample from core. The core has been exposed to high temperatures over time.
W1	Windsor 1	18°25'25"	077°11'41"	990.6	Rio Nuevo	M. to U. Cenomanian	Sh	Dark grey shale sample from core. The core has been exposed to high temperatures over time.

W2	Windsor 1	18°25'25"	077°11'41"		-	-	O	Black oil with low viscosity. This sample has been kept in a bottle in a tropical environment which could have alter the oil.
V1	VBB4	18°1'40"	076°38'31"	42-45	-	-	OSSs	Oil impregnated sandstone sample from core, kept in a tropical environment which could have altered the oil.
V2	VBB4	18°1'40"	076°38'31"	63.25	-	-	OSSs	Oil impregnated sandstone sample from core, kept in a tropical environment which could have altered the oil.
P1	Pindars River BH3	?	?	55.6	-	-	OSSil	Oil impregnated siltstone sample from core, kept in a tropical environment which could have altered the oil.

3.2.1 Crude oil

The crude oil sample W2 (Figure 13) was black in colour with low viscosity, collected from the well Windsor 1 in northeastern Jamaica (Figure 12). This sample could have been exposed to evaporation, as the container the sample was kept in was not sealed.

Figure 13 *the black crude oil W2 with low viscosity collected from the well Windsor 1.*

3.2.2 Extracts

The extract samples consist of oil stained sandstones, siltstones and carbonates. Of these, two sandstones (samples V1 and V2, Figure 14A) and one siltstone (sample P1, Figure 14B) were collected from two wells (VBB4 and Pindars River BH3) originally drilled in search for water. The cores have been exposed to high temperatures over time. In addition, two samples were collected from the field; one carbonate (sample D2, Figure 14C) and one siltstone (sample E1, Figure 14D).

Figure 14 A *the oil stained sandstone sample V1 from the well VBB4,* ***B*** *the oil stained siltstone sample collected from the Pindars River BH3 well,* ***C*** *the oil stained carbonate sample D2,* ***E*** *the oil saturated siltstone sample E1.*

3.2.3 Organic-Rich Sedimentary Rocks

Nine organic-rich shales were collected from four different wells (Table 2). The formation from which these samples are gathered is uncertain for two of the shales (CO1 and R1) (Table 2), whereas the remaining samples are mainly collected from the Rio Nuevo (R2, R3, R4 (Figure 15A), and W1 (Figure 15B)) and Litchfield (CA2 and CA3 (Figure 15C)) formations with Middle to Upper Cenomanian (Upper Cretaceous) and Lutetian (Eocene) ages, respectively. In addition, five potential source rocks from different locations in Jamaica (Figure 12) were sampled from outcrops. One of these samples were a grey coloured shale (sample G1 (Figure 15E)), whereas the remaining samples were black in colour; two shales (samples F1 (Figure 15D) and H2 (Figure 15F)) and one coal (sample H1 (Figure 15F)). All samples collected from outcrops belong to the Litchfield Formation.

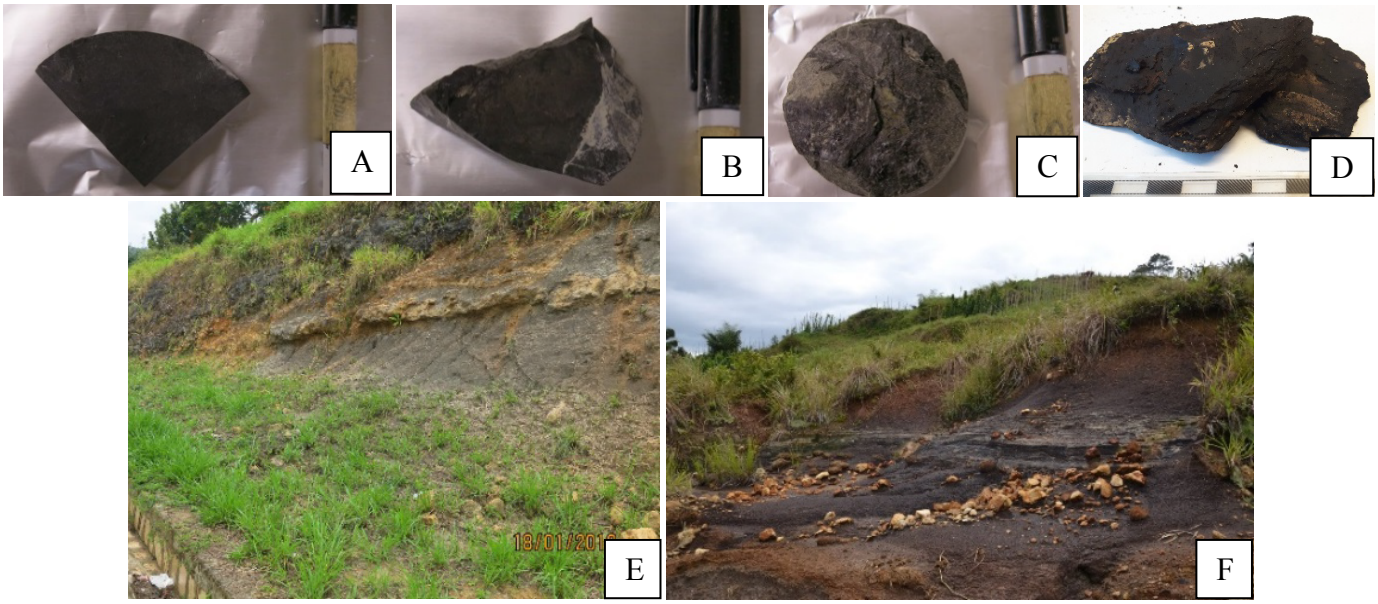

Figure 15 A *the black shale R3 as an example of the samples collected from the well Retrive 1,* ***B*** *the black shale sample W1 gathered from the well Windsor 1,* ***C*** *sample CA2 as an example for the black shale samples derived from the well Content A,* ***D*** *location were the samples H1 and H2 were collected,* ***E*** *sampling location for G1.*

3.3 Crude Oil, Condensate, and Extract Analyses

The extracts and the crude oils were analysed by gas chromatography (Table 3). This was done to get an indication of the level of biodegradation, and if possible, general indications of the degree of maturation, as well as the facies and depositional environment of the source rocks generating the oils. As the extracts are expected to be biodegraded in a greater extent than the crude oils, they were also analysed with Iatroscan to estimate the percentages of saturate, aromatic, and polar fractions. The extracts which contained a reasonable percentage of saturates, as well as all the oils that were not heavily biodegraded were further analysed by the Gas Chromatography-Mass Spectrometry (GC-MS).

Before the samples could be analysed by GC-MS, the saturate, aromatic, and polar fractions were separated using Medium Performance Liquid Chromatography (MPLC). For the crude oils, the percentage of saturate, aromatic, and polar fractions were measured with the quantitative version of the MPLC (QMPLC). The samples were analysed with GC-MS to reveal maturity and the depositional environment of the source rocks that generated and expelled the oils and organic matter type. The less degraded crude oil samples were also analysed for compound specific isotopes to correlate the different oils. In addition, all the samples were analysed for isotope of both saturate and aromatic fractions, except for all the extract samples, which were analysed by GC-MS, as there was not enough organic material to preform additional analyses. Furthermore, three crude oils (samples 2 (northwest Cuba), 12 (central Cuba), V1 and W2 (Jamaica)) from different facies and locations, which were not heavily biodegraded were chosen to be further analysed by gas chromatography-tandem mass spectrometry (GC-MSMS) in an attempt to better constrain the age of their source rocks.

3.4 Source Rock Analyses

The organic-rich sedimentary rocks collected from both the field and the cores were analysed for their hydrocarbon generation potential with Rock-Eval pyrolysis (R-E). In addition, the total organic carbon (TOC) were measured. Based on the TOC values, the samples with values above 1% were also analysed with marcel to indicate kerogen types.

Table 3 *an overview of the analyses preformed for each samples. The sample names are coloured after countries; Cuban samples are coloured blue, whereas Jamaican samples are coloured green.* ***R-E*** *– Rock-Eval pyrolysis;* ***TOC*** *– total organic carbon;* ***QMPLC*** *– quantitative medium performance liquid chromatography;* ***GC*** *– gas chromatography;* ***GC-MS*** *– gas chromatography-mass spectrometry;* ***GC-MSMS*** *– gas chromatography-tandem mass spectrometry;* ***CSIA*** *– compound specific isotope analysis;* ***δSAT+ARO*** *– stable carbon isotope analysis of the saturate and aromatic fractions.*

Sample	Analyses									
	R-E	TOC	Maceral	Iatroscan	QMPLC	GC	GC-MS	GC-MSMS	CSIA	δSAT+ARO
1					X	X	X		X	X
2					X	X	X	X	X	X
3					X	X	X			X
4					X	X	X		X	X
5					X	X	X			X
6					X	X	X			X
7					X	X	X			X
8					X	X	X			
9					X	X	X		X	X
10					X	X	X			X
11					X	X	X		X	X
12					X	X	X	X	X	X
13						X			X	X
14					X	X	X			X
15				X		X				
16				X		X				X
17				X		X				
18				X		X				
19				X		X				
20				X		X				
21				X		X				

22				X		X				
23				X		X				
24				X		X				
25				X		X				
26				X		X				
X1				X		X	X			X
X2				X		X				
Y1				X		X	X			X
A1				X		X				X
A2				X		X	X			X
A3				X		X	X			X
C1				X		X				X
D1	X	X								X
D2				X		X				
E1				X		X				X
F1	X	X	X							
G1	X	X								
H1	X	X	X							
H2	X	X	X							
CO1	X	X								
CA2	X	X	X							
CA3	X	X	X							
R1	X	X								
R2	X	X	X							
R3	X	X								
R4	X	X								
W1	X	X	X							
W2						X	X	X	X	X
V1				X		X	X	X	X	X
V2				X		X	X			X
P1				X		X				X

4 Analytical Methodology

Essentially, all the geochemical analyses presented in this thesis were performed by the Applied Petroleum Technology (APT). The procedures follow the Norwegian Industry Guide to Organic Geochemical Analysis (NIGOGA) fourth edition. For each tenth sample analysed in the different instruments, a standard test was used to quality check the results of the machine. The samples, which were analysed for maceral and mineral composition was sent to Thomas Demchuk, RPS Group Inc.

4.1 Rock-Eval Pyrolysis

The shale samples were crushed to powder with a mortar. Then the samples, as well as two samples of the standard test were weight in metal containers, the most presumable organic rich samples at 10 mg, and the less at 80 mg. A Rock-Eval 6 instrument was then used, where the samples were placed onto a rotational wheel in the instrument. Each of the samples were placed into a chamber which only contained nitrogen to have an atmosphere without oxygen. In the chamber, the samples were heated rapidly where the temperature began at 300 °C for 3 min, then the temperature increased with 25 °C/min until it reached 650 °C. When the samples are heated, the hydrocarbon chain structures begin to fracture, creating bitumen. A FID-detector (Flame ionization detector) records the volume of hydrocarbon the potential source rock can generate. Additionally, a second detector records the amount of CO2 (Carbon dioxide) and CO (Carbon monoxide) which was produced during the heating of the samples. The temperature at which the rock produces most of hydrocarbons (Tmax) was also registered.

4.2 Total Organic Content

Similar to the preparation for Rock-Eval Pyrolysis, the shale samples were crushed to powder with a mortar. Then a small part of the crushed samples, 100 mg or 200 mg depending on the samples presumable organic richness, was placed in ceramic containers and weight. The samples were then washed with HCl to remove carbonate. After the samples were dry, they were washed with distilled water to remove the chloride and further dried. The samples were heated in a Leco SC-632 instrument at a temperature of 1350 °C. During the heating of each sample, oxygen was pumped into the furnace where the sample was, and all of the carbon was converted to CO2. Then an infrared (IR) detector measured the CO2 as the amount of carbon in the sample.

4.3 Maceral

The rock samples were crushed to pass through a #16 sieve, and the resulting material was embedded in thermoplastic epoxy in 3.2 cm molds, which were left overnight to harden. These pellets were further ground and polished according to ASTM standards (ASTM, 2011). The samples were then investigated in white- and UV-light using a Zeiss Axio-Scope A1 at 500x (50x objective and 10x ocular) in immersion oil, where a total of 300 grains of both organic and mineral matter were counted for each sample.

4.4 Extracted Organic Matter

The samples were crushed into powder, where 20 grams were placed in pre-extracted containers. Extraction cups were filled with approximately 80 mL of dichloromethane (DCM) with 7 % (vol/vol) methanol. Then copper blades were added into the extraction cups after they had been activated in concentrated HCl. The copper blades were used to cause free sulphur to react with the copper. A Soxtec Tecator instrument was used to boil the thimbles containing the samples for one hour, and then rinse for two hours in the extracted cups. During this process, the organic matter is extracted from the crushed sample in the thimbles into the extracted cups. The mixture of extracted organic matter (EOM) and DCM from the extracted cups were then transferred into turbovap glasses used in a Turbovap instrument. In the Turbovap instrument, the turbovap glasses are heated in water with 40 °C, which is enough to evaporate the DCM and not the organic matter. When almost all the DCM has evaporated, the EOM was transferred to small bottles, where DCM was used to fill the bottles to 1.75 ml. Subsequently 10 % of the extract was transferred to pre-weighed bottles, left to dry before being weighed. The amount of extractable organic matter was calculated based on the difference in weight.

4.5 Gas Chromatography

Before the oil and extracted samples could be analysed in GC instruments, an internal standard was added to the samples to have a reference peak when integrating the Chromatograms. 100 mg of the crude oil samples were transferred to insert vials, where 1 ml of internal standard was added, whereas 30 mg of the EOMs were transferred to bottles. Then 100 ml of internal standard and DCM was used to fill the remaining volume until it reached 1.5 ml volume. The crude oil and extraction samples were introduced to Agilent 7890A instruments.

4.5.1 Whole Oil

The GC instrument used for the crude oils contain a 50 m HP PONA column with an inner diameter of 0.2 mm and film thickness of 0.5 µm. Initially, the temperature of the columns was 30 °C, which was maintained for 10 min. With a gradient of 2 °C/min, the temperature was increased until 60 °C was reached and maintained for 10 min. The temperature was further increased with the same gradient until 240 °C, which was maintained for 60 min. A FID recorded the amount of hydrocarbon compounds in the oils.

4.5.2 Extracted Organic Matter

The GC instrument used for the extractions had a 30 m CP-Sil- 5 CB-MS column with an inner diameter of 0.25 µm, and a film thickness of 0.25 µm. The initial temperature of the column was 50 °C, which was held for 1 min, then the temperature was increased to 320 °C with a gradient of 4 °C/m. A FID detected the combustion of molecules.

4.6 Iatroscan

The extracted samples were analysed in an Iatroscan MK-5 (TLC/FID Analyser) instrument to indicate the percentage of saturate-, aromatic- and polar fractions in the samples. Before the extracted samples could be analysed in the Iatroscan instrument, they had to be deasphaltened. Up to 100 mg of EOM were transferred to pre-weighed bottles, then evaporated to almost dryness. DCM was added, three times the amount of the EOM, and then pentane, 40 times the volume both the DCM and the EOM. The pentane is the reason for the asphalt being released from the solution, deasphaltening the sample. The solutions were stored for at least twelve hours in a dark room before the solutions were centrifuged, leaving the asphalt at the bottom of the glasses. Then 2 mL of extracts were spotted on Chromarod S-III rods, which were then eluted in hexane for 25 min to separate the saturated fractions, 8 min in toluene to separate the aromatic fractions, and at last in DCM with 7 % methanol (vol/vol) for 2 min for the polar fractions. The rods were heated in a heater chamber at 60 °C for 90 sec, before the rods were placed in the analyser, where the fractions are burned. A FID records the response when the different fractions are combusted and stored on a computer After the Iatroscan, the solutions were removed from the bottles leaving the asphalt, which was then dried and weighed.

4.7 (Quantitative) Medium Performance Liquid Chromatograph

The oils and EOMs were analysed in a medium performance liquid chromatograph (MPLC) instrument to separate the saturate-, aromatic- and the polar fractions in the oils and EOMs. 30 mg of the oils were weighed in bottles, whereas a percentage of the extractions equivalent 30 mg EOM were transferred into bottles. Then 100 mL of internal standard and 1.5 ml of hexane were added to the oils and EOMs, where the hexane was used to deaspahltene the samples. For approximately 12 hours the samples were left in a dark room, then centrifuged and separated in the MPLC instrument consisting of two HPLC pumps, sample injector, sample collector, pulse induction (PI) detector, ultraviolet (UV) detector, and two packed columns. The latter two columns were a pre-column filled with Kieselgel 100 and a main column, which is a LiChroprep Si60. The pre-column is heated at 600 °C for 2 hours to deactivate it, while the main column is heated at 120 °C for 2 hours to make it water free. For the crude oils and the condensate, a small part of the saturated, aromatic and polar fractions were dried and weight to register the percentages of each component.

4.8 Gas Chromatography-Mass Spectrometry

A Thermo Scientific DFS high-resolution instrument was used to analyse the different samples. The instrument was tuned to a resolution of 3000 and data was acquired in selected ion recording (SIR) mode. The instrument contains a 60 m CP-Sil-5 CB-MS column with an inner diameter of 0.25 μm and a film thickness of 0.25 μm. The column's initial temperature was 50 °C which was maintained for 1 min. Furthermore, the temperature was increased with a gradient of 20 °C/min until 120 °C was reached. The gradient was decreased to 2 °C/min until 320 °C was reached and maintained for 20 min. Both the saturated and aromatic fractions were analysed in the GC-MS.

4.9 Gas Chromatography-Tandem Mass Spectrometry

Both the saturate and aromatic fractions of the samples were analysed with a Thermo Scientific TSQ Quantum instrument tuned to a resolution of 0.7 mass units, where Argon was used as the collision gas at a pressure of 1.0 mTorr, with a collision energy of 15 V. A 60 m FactorFour VF-1ms column was used with an inner diameter of 0.25 mm and film thickness of 0.25 μm. The initial temperature of the column was 50 °C maintained for 1 min, then the temperature was increased to 225 °C with a gradient of 20 °C/min. Furthermore, with a gradient of 2 °C/min

the temperature was raised to 300 °C, and at last the temperature was increased to 320 °C with a gradient of 20 °C/min and maintained for 20 min.

4.10 Compound Specific Isotope Analysis

A Trace 1310 (Thermo Fisher Scientific) GC equipped with PTV (Programmed Temperature Vaporizing) Injector and TriPlus RSH autosampler (Thermo Fisher Scientific) was used. The n-alkane components of the oils were separated on a 60 m long Restek Rxi-1ms column, installed in the GC. Furthermore, the GC was interfaced to Delta V Plus IRMS (Thermo Fisher Scientific) via GC-Isolink II and conflo IV. For the calibration, NBS-22 (-30.031 vPDB) oil was used provided by IAEA.

4.11 Stable Carbon Isotope Analysis of Fractions

The samples were dissolved in DMC of a known amount, where 5 µl was transferred to 5X8mm tin capsules and was evaporated in an oven at 50 °C. Furthermore, the samples were loaded into an automatic sampler which dropped them into a combustion reactor (Thermo Fisher Scientific Elemental Analyser) held at 1000 °C. The temperature is raised to 1700 °C as a result of the excess supply of oxygen, which helps to flash combust the tin capsules. Magnesium Perchlorate trap the produced water, whereas the CO2 is separated by column and flashed into Delta V Plus Isotope Ratio Mass Spectrometer (IRMS) through Conflo IV.

4.12 Principal Component Analysis

Principal component analysis (PCA) was performed using SPSS V.12.02. The parameters used in this thesis were of different magnitudes and units, thus, the parameters had to be standardized in order to weight the variables equally when preforming the PCA. To standardise the parameters, the equation below was used.

$$Z_{ij} = \frac{X_{ij} - \overline{x}_i}{s_j}$$

X_{ij} = values for the parameter *j* in the unit *i*

x_j = mean for parameter *j*

S_j = standard deviation for parameter *j*

5 Results and Discussion

5.1 Source Rock Evaluation

Exploration for petroleum has so far not been successful on Jamaica. However, as ten of eleven wells drilled on Jamaica have hydrocarbon shows there obviously is or has been a working petroleum system. In this study thirteen potential source rocks were sampled (Figure 12) from cores (samples CO1, CA2, CA3, R1, R2, R3, and R4) and outcrops (F1, G1, H1, and H2) to investigate the richness, maturity (Table 4), and maceral composition (Table 5). The analysed samples are mainly collected from the Upper Cenomanian (Upper Cretaceous) Rio Nuevo Formation and the Lutetian (Eocene) Litchfield Formation in the Yellow Limestone Group (Figure 16).

Table 4 *Rock-Eval and total organic carbon (TOC) results for the potential source rocks in Jamaica. Samples with TOC values higher than 1 are marked in grey.* ***PI****: Production index (S1/(S1+S2));* ***HI****: Hydrogen index;* ***OI****: Oxygen index*

Sample	S1 (mg/g)	S2 (mg/g)	S3 (mg/g)	Tmax (°C)	PI (wt ratio)	HI (mg HC/g TOC)	OI (mg CO_2/g TOC)	TOC (%)
F1	0.71	11.6	12.38	399	0.06	67	72	17.2
G1	0.09	1.47	0.82	406	0.06	174	97	0.85
H1	0.55	41.88	22.45	384	0.01	96	52	43.5
H2	0.22	5.12	4.96	402	0.04	277	268	1.85
CO1	0.09	0.24	0.58	445	0.27	35	84	0.69
CA2	0.64	9.95	0.71	428	0.06	228	16	4.37
CA3	0.27	5.31	0.75	434	0.05	224	32	2.37
R1	0.03	0.26	0.42	455	0.1	53	86	0.49
R2	0.23	2.16	0.64	450	0.1	186	55	1.16
R3	0.08	0.41	0.26	457	0.16	127	80	0.32
R4	0.04	0.11	0.32	447	0.27	72	211	0.15
W1	0.74	33.56	0.71	435	0.02	512	11	6.56

Table 5 *Maceral and mineral-composition for the seven selected samples with total organic carbon (TOC) values higher than 1(Table 4).*

Sample	Mineral Matter			Solid Bitumen	Vitrinite	Liptinite	Inertinite
	Clay	Quartz	Other	Total	Total	Total	Total
F1	177	31	11	56	10	15	0
H1	25	27	16	0	215	17	0
H2	92	111	6	7	67	17	0
CA2	30	215	19	34	2	0	0
CA3	255	3	13	9	2	18	0
R2	29	227	8	26	0	9	1
W1	90	83	6	23	0	98	0

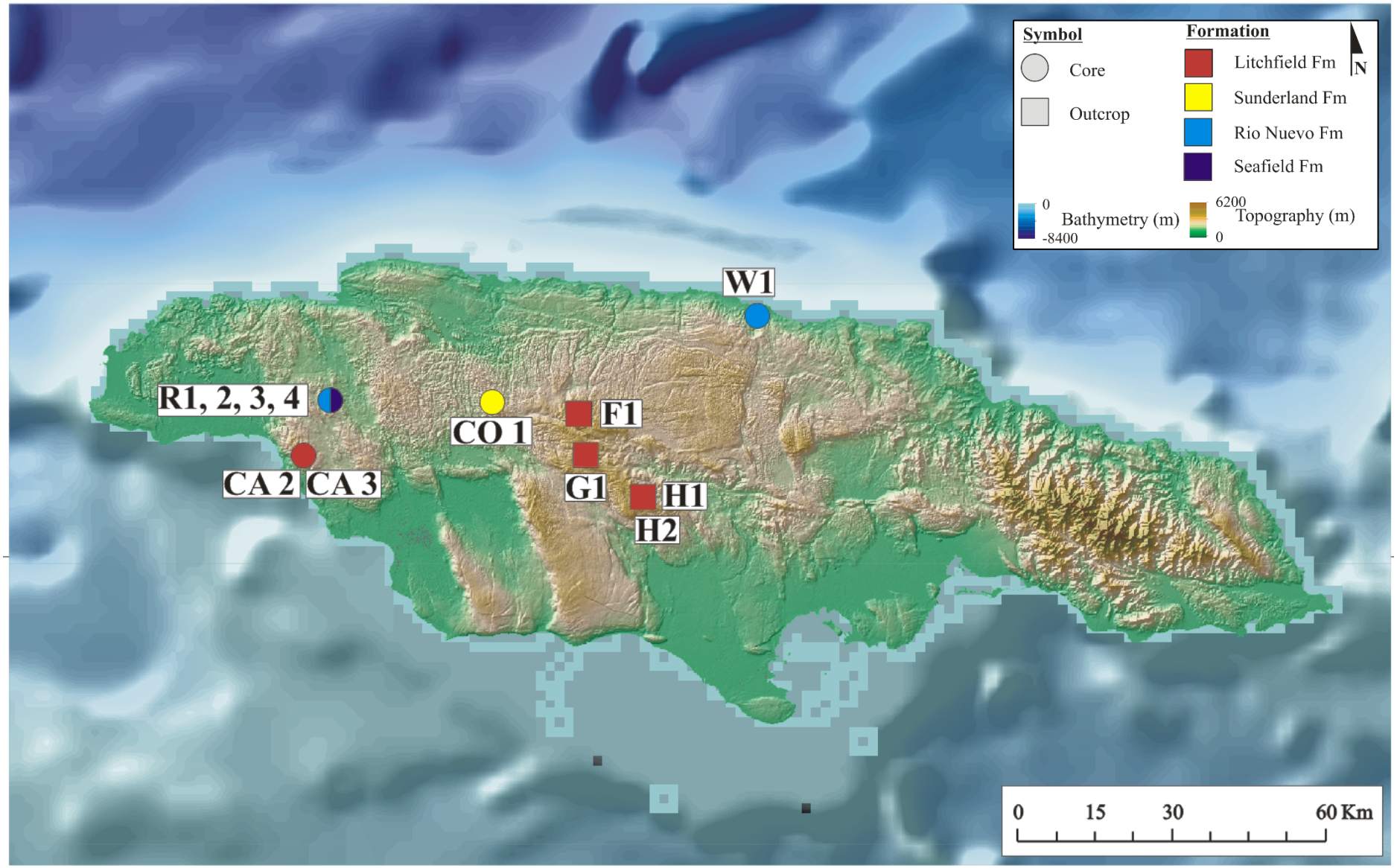

Figure 16 *Locations and formations of the different samples analysed. The samples are mainly collected from the Upper Cretaceous Rio Nuevo Formation and the Eocene Litchfield Formation.*

5.1.1 Total Organic Carbon

The results obtained from the TOC analysis revealed differences in organic richness (0.15 to 43.5 %) (Table 4), indicating poor to very good source rocks. Seven of the samples (F1, H1, H2, CA2, CA3, R2, and W1) showed TOC values above 1% (Table 4) and will further be evaluated for their source rock potentials. Of these, five samples (F1, H1, H2, CA2, and CA3) were collected from the Litchfield Formation (Figure 16), while two samples (R2 and W1) were gathered from the Rio Nuevo Formation (Figure 16).

5.1.2 Kerogen Type

5.1.2.1 Pseudo Van Krevelen

Kerogen type was classified by plotting hydrogen index (HI) against oxygen index (OI) on a pseudo van Krevelen diagram. Figure 17 show the samples H1, H2, and F1 to be mixed type III-IV kerogen. Sample R2 plot as type III kerogen, samples CA2 and CA3 are suggested to be kerogen type II, and sample W2 plot as a mixed type I-II kerogen.

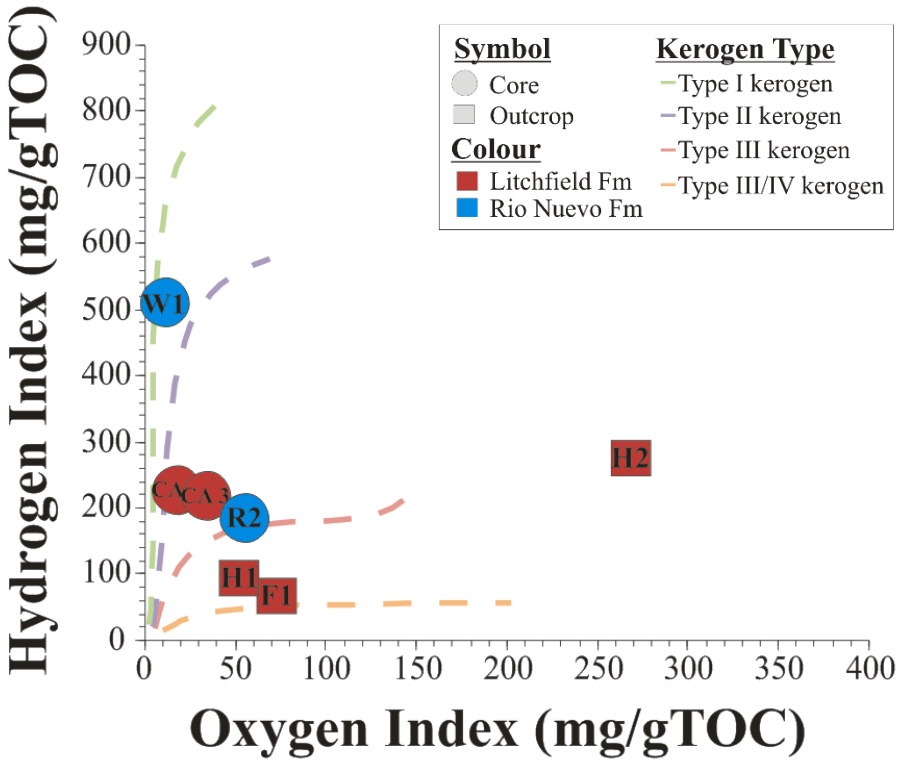

Figure 17 *Pseudo van Krevel diagram illustrating the kerogen types for the different samples. Samples H1, H2, and F1 appear to be of mixed type III-IV kerogen, sample R2 is suggested to be type III kerogen, samples CA2 and CA3 show to be of kerogen type II, and sample W1 plot as a mixed type I-II kerogen.*

5.1.2.2 Maceral Composition

The maceral composition of the samples was analysed and the results compared to those from the pseudo van Krevelen diagram (Figure 17). Liptinite rich samples with minor amounts of vitrinite and inertinite are normally linked to kerogen types I and II (Hakimi et al., 2012, Hakimi and Abdullah, 2013, Makeen et al., 2015), whereas samples with significant content of vitrinite are typed to kerogen type III (Baskin and Peters, 1992, Peters and Cassa, 1994, Sykes and Snowdon, 2002). Inertinite are related to kerogen type IV.

As illustrated in Figure 18, samples H1 and H2 show the highest content of vitrinite, implying high proportions of kerogen type III with minor amounts of kerogen types I and II. In contrast, sample W1 appear to contain the highest amount of liptinite, thus, indicating high proportions kerogen types I and II. This is in good agreement with the pseudo van Krevelen plot (Figure 17).

The remaining samples (F1, CA2, CA3, and R2) are seen to contain low amounts of the macerals. In these samples the content of solid bitumen generally dominates (Figure 18). Samples F1, CA3, and R2 display higher liptninte content compared to vitrinite and inertinite, while sample CA2 is seen to only contain vitrinite beside the solid bitumen. This would imply relatively higher proportions of kerogen types I-II for the samples F1, CA3, and R2, and kerogen type III for sample CA2.These interpretations does, however, not coincide with those obtained from the HI and OI values (Figure 17). The generally high content of solid bitumen could explain these differences as it is normally placed within the vitrinite maceral group. This suggests the samples contain higher proportions of kerogen type III than previously suggested, which correlates well with the interpretations based on the pseudo van Krevelen plot (Figure 17). The exception is sample CA2, interpreted to contain kerogen type II according to the HI and OI values (Figure 17). However, based on mineral content, samples CA2 and R2 have very high amounts of quartz (227 and 215 counted out of 300 grains) (Table 5), suggesting that these samples represent siltstones or fine-grained sandstones, and thus, that the organic content represents migrated hydrocarbon.

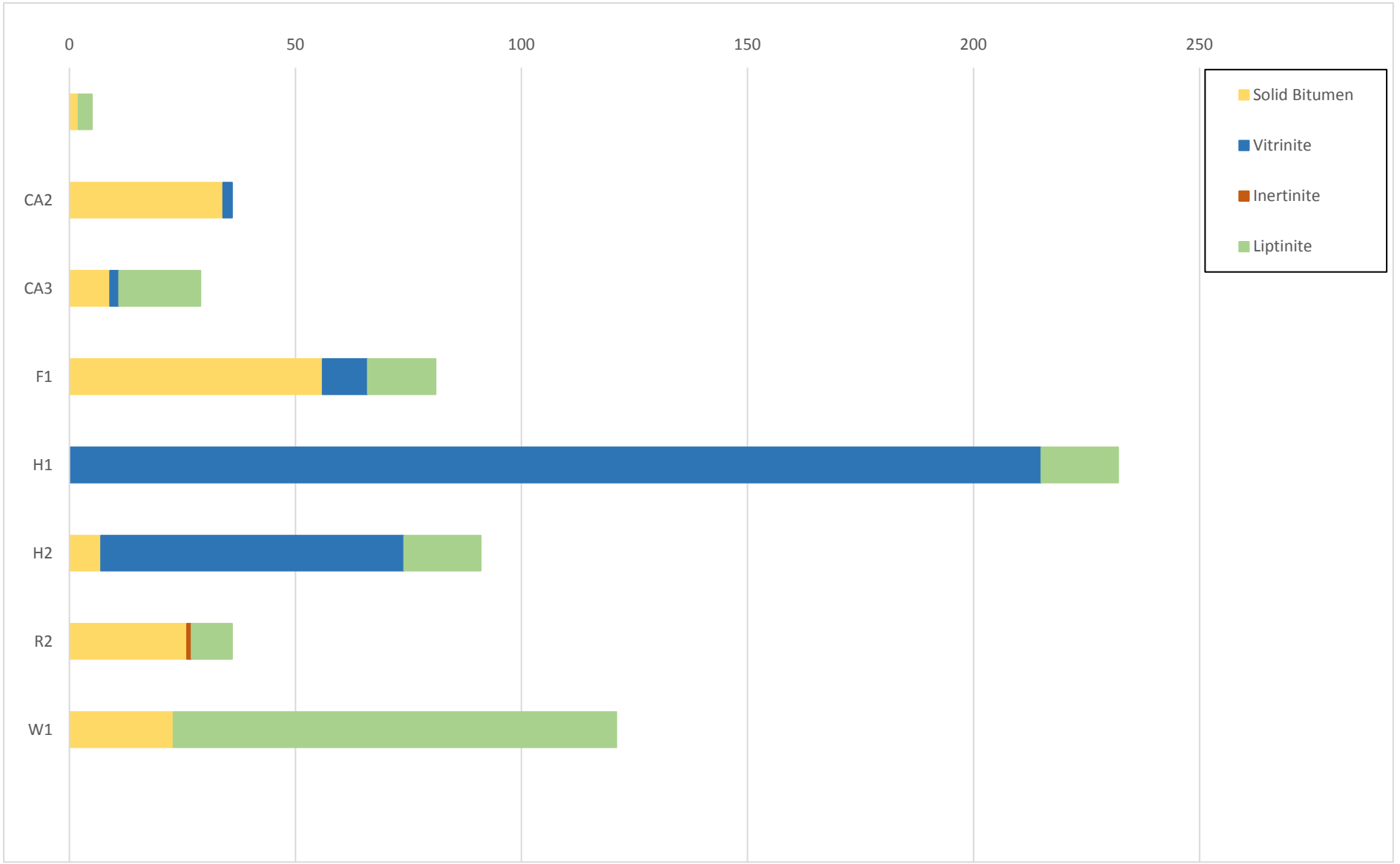

Figure 18 *The number of solid bitumen, vitrinite, inertinte, and liptinite grains out of 300 grains counted. The majority of the samples are seen to contain low amounts of macerals with relatively higher amounts of solid bitumen. This indicates higher content of kerogen type III, as the solid bitumen is usually placed within the vitrinite group. Sample H1 show the highest amount of vitrinite indicating high proportions of type III kerogen, whereas sample W1 appear to have the highest amount of liptinite suggesting mixed type I-II kerogen.*

5.1.3 Thermal Maturity and Production Index

In Figure 19 Tmax is plotted against the production index (PI) (S1/(S1+S2)). The samples gathered from cores (CA2, CA3, R2, and W1) display higher Tmax values (428 to 450 °C) than those collected from outcrops (samples F1, H1, and H2) (384 to 402 °C) (Table 4). These Tmax values indicates that only the samples from the cores (CA2, CA3, R2, and W1) have reached the oil window, whereas the outcrop samples F1, H1, an H2 are immature. Samples CA2, CA3, and W1 have Tmax values of 428, 434, and 435 °C (Table 4), respectively, suggesting that these samples are in the earliest oil window, while sample R2 has a Tmax value (450 °C) (Table 4) implying the sample is in peak oil window.

Furthermore, the majority of the samples appear to have low PI values, ranging from 0.02 to 0.06 (Figure 19)(Table 4), suggesting the samples have not reached the petroleum-generation stage. However, as the cores have been exposed to high temperatures over time at the core shed, low boiling petroleum fractions may have evaporated in low PI values. The exception is sample R2 with a PI value of 0.1, which indicates that this sample just has started generating petroleum (Hunt, 1996). As previously mentioned, this sample contain high amounts of quartz and the relatively high PI value could represent migrated rather than in-situ hydrocarbons. Furthermore, the high S2 values (5.12 to 41.88 g/mg) (Table 4) demonstrate that all the samples will generate petroleum when mature. The shale sample W1 (33.56 g/mg) and the coal sample H1 (41.88g/mg) have the highest source rock potential (Figure 20).

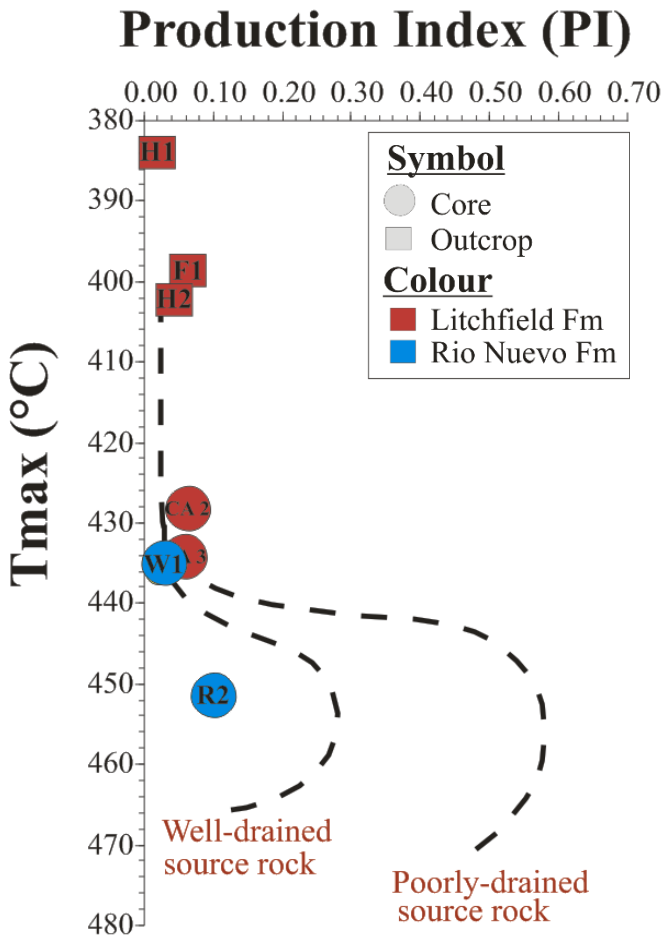

Figure 19 *Cross-plot of production index (PI: S1/(S1+S2)) versus Tmax shows the samples collected from outcrop to have lower maturity than samples gathered from cores. The low PI values suggest that the majority of the samples have not started to generate petroleum. Sample R2 show the highest value of 0.1, which indicates the sample has just started generating petroleum. However, high amounts of quarts (227 of 300 counted grains) (Table 5) suggest that the organic content represents migrated hydrocarbons.*

5.1.4 Petroleum Generation Potential

The analysed samples show to be dominated by high proportions of kerogen types II and III, with the exception of sample W1 which is characterised by higher proportions of mixed type I-II kerogens (***Figure 20***). The generally low thermal Tmax values (immature to very early oil window) show that the samples have not been buried sufficiently deep to attain the temperature needed to generate petroleum (Figure 19). Furthermore, high S2 values samples for the samples F1, H1, H2, CA3, and W1 (5.12 to 41.88 g/mg) (Figure 20)(Table 5) demonstrate that these samples have petroleum potential. Thus, in a more distal depositional setting, buried at a deeper depth, these source rocks could generate petroleum.

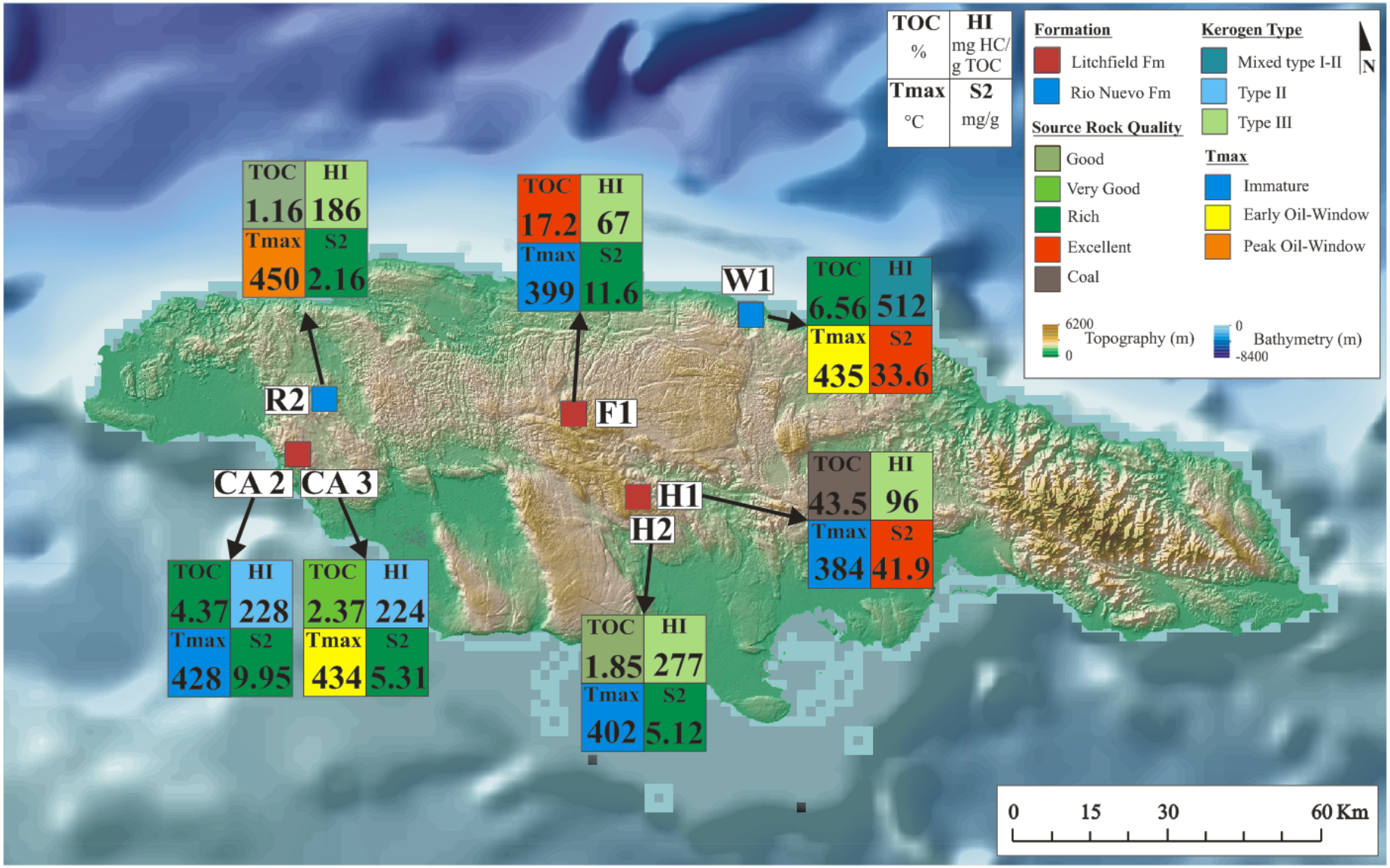

Figure 20 *Map illustrating the distribution of the petroleum generation potential for the analysed samples. The samples appear to be mainly contain kerogen types II and III and generally have low maturities. High relatively values of S2 (5.12-43.5 mg/g) demonstrate that these samples have potential and have not been buried sufficiently deep to attain the temperature needed to generate petroleum. Even though sample H2 show high values of hydrogen index (HI), this sample has been coloured to be dominated by type III kerogen, as the samples shows high values of oxygen index (OI) (Figure 17).*

5.2 Geochemical Evaluation

5.2.1 Alteration

5.2.1.1 Biodegradation and Water Washing

Biodegradation and water washing can affect the different biomarker ratios used to determine maturity, facies and depositional environment to source of the oils. The degradation of the petroleum is a selective process where bacteria usually attack the light fraction of the n-alkanes first, then proceed by attacking the isoprenoid after the n-alkanes are consumed. Furthermore, the steranes, hopanes, and aromatics are subsequently depleted with continued biodegradation (Peters et al., 2005).

Figure 21 show a ternary diagram illustrating the amount of saturate, aromatic, and polar components for each sample, these values can also be seen in Table 6. Most of the extract samples show low amounts of saturate and aromatic compounds, as well as high amounts of polar compounds, whereas the crude oils generally show an opposite trend. This suggests that the extracts experienced more severe biodegradation (Tissot and Welte, 1984). In addition, the low amount of aromatic compounds might be a result of water washing, which affects compounds soluble in water. Low concentration of thiophenes are observed in the fragmetograms (m/z) 184 and (m/z) 198 for all the samples, with the exceptions of samples 14 (northwest Cuba) and W2 (Jamaica) (Figure 23). This could indicate that the majority of the samples have experienced water washing, as the loss of dibenzothiophene is a good indication of water washing (LaFargue and Barker, 1988).

Furthermore, all the crude oils and extracts have n-alkane profiles that shows signs of biodegradation of different degrees (Table 7), whereas the condensate sample 8 (northwest Cuba) (Figure 22A) only consist of light components and is not biodegraded. The least degraded samples are the crude oils samples 1, 2, 4, 14 (northwest Cuba), 9, 11, 12 (central Cuba), and W2 (Jamaica) as mainly the light fraction is affected (Figure 22 B-C). These crude oil samples are ranked at level 1 for biodegradation according to Peters et al., (2005) (Table 7). On the other hand, the remaining crude oils (samples 3, 5, 6, 7, 13 (northwest Cuba), and 10 (central Cuba)) and all the extracts are depleted in n-alkanes and acyclic isoprenoids (Figure 22D-H), where some have pronounced unresolved complex mixture (UCM) humps (Figure 22D, G and H). This suggest the samples to have reached biodegradation level 4→5 (Peters et al., 2005). However, the steranes, hopanes, and aromatics are also affected in the extract samples Y1, A2,

A3 (northwest Cuba), C1 (northeast Cuba) where the steranes, as well as the hopanes are nearly removed and the aromatics are depleted. Thus, these samples are ranked at level 9→10 for biodegradation (Peters et al., 2005). Due to the high biodegradation level, these samples are discarded from this study.

From Table 7, the degradation level of the samples appears to be independent of the sampling depth. This is evidenced by sample 5 (level 4→5) collected at 1577 m depth, which is deeper than four of the lightly degraded crude oils (samples 11, 12, 9, and 1) with a biodegradation level of 1. In addition, samples 10 (level 4→5) and 11 (level 1) were gathered at 630 and 645 m depth, respectively, and have two very different levels of degradation. This could be a result of current charges of hydrocarbons or lack of bacteria in the reservoir. Alternatively, the reservoir could be pasteurised by previously having experienced temperatures exceeding 80-90 °C (Wilhelms et al., 2001). Although several oils are biodegraded, surprisingly high concentrations of light and medium fractions are seen in some oils, suggesting ongoing recharge (Figure 22D).

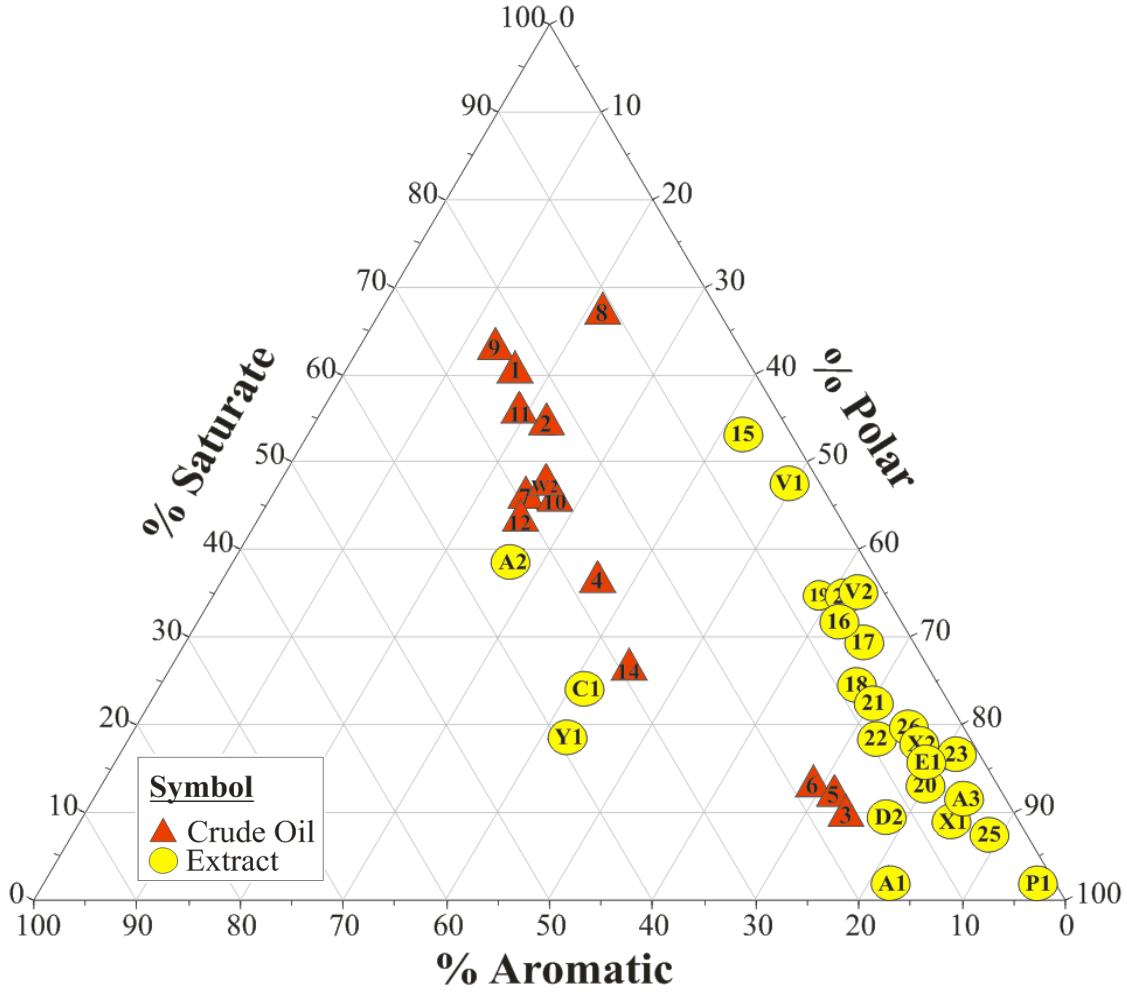

Figure 21 *Ternary diagram illustrating the amount of saturate, aromatic and polar components in the crude oils and the extracts. Most of the extract samples display low values of saturate and aromatic compounds.*

Table 6 *The amount of saturate, aromatic, and polar compounds in the oil samples. The sample names are coloured after countries; Cuban samples are coloured blue, whereas Jamaican samples are coloured green.*

Sample	% Saturate	% Aromatic	% Polar
1	60.7	23.2	16.1
2	54.5	23	22.5
3	9.6	16.4	74.1
4	36.3	27.2	36.4
5	11.6	17.1	71.4
6	12.6	18	69.4
7	45.8	29.2	25
8	66.7	11.1	22.2
9	63	23.3	13.6
10	45.9	27.1	27.1
11	55.9	25	19.2
12	44	31	25
14	27	28.8	44.2
15	53.2	4.6	42.3
16	31.9	6.1	62
17	29.6	4.8	65.7
18	24.8	7.7	67.4
19	34.7	6.6	58.8
20	13.4	6.7	79.9
21	22.5	7.5	70.1
22	18.6	9	72.5
23	16.8	2.3	80.9
24	34.8	4.6	60.5
25	7.5	3.6	88.9
26	19.8	5.4	74.8
X1	9	6.2	84.7
X2	17.1	6	77
Y1	18.7	38.7	42.6
A1	2.1	16	81.8
A2	39	34.2	26.9
A3	11.7	4	84.4
C1	24.3	34.5	41.1
W2	46.6	28.2	25.3
V1	47.9	3.3	48.9
V2	35.7	2.5	61.8
P1	2.1	1.6	96.3
D2	9.4	12.6	77.9
E1	14.5	6.2	79.2

Table 7 *Description of the preservation of the biomarkers analysed and the biodegradation according to Peters et al., (2005). The sample names are coloured after countries; Cuban samples are coloured blue, whereas Jamaican samples are coloured green.*

Sample	Light Fraction	n-Alkanes	Isopenoids	Steranes	Hopanes	Aromatics	Bio.degree	Depth (m)
1	Depleted	Intact	Intact	Intact	Intact	Intact	1	1315
2	Nearly intact	Intact	Intact	Intact	Intact	Intact	1	3425
3	Removed	Nearly removed	Nearly removed	Intact	Intact	Intact	4→5	1000
4	Depleted	Intact	Intact	Intact	Intact	Intact	1	1732
5	Nearly removed	Nearly removed	Removed	Intact	Intact	Intact	4→5	1577
6	Nearly removed	Nearly removed	Removed	Intact	Intact	Intact	4→5	745
7	Depleted	Nearly removed	Nearly removed	Intact	Intact	Intact	4→5	1300
8	Intact	Intact	-	-	-	-	0	1700
9	Nearly intact	Intact	Intact	Intact	Intact	Intact	1	1006
10	Very depleted	Removed	Removed	Intact	Intact	Intact	4→5	630
11	Nearly intact	Depleted	Intact	Intact	Intact	Intact	1	645
12	Intact	Nearly intact	Intact	Intact	Intact	Intact	1	1032
13	Removed	Removed	Removed	-	-	-	-	900.6-900.27
15	Removed	Depleted	Nearly removed	Intact	Intact	Intact	4→5	2625
14	Nearly intact	Intact	Intact	Intact	Intact	Intact	1	2203
16	Removed	Nearly removed	Nearly removed	-	-	-	-	2625
17	Removed	Nearly removed	Nearly removed	Intact	Intact	Intact	4→5	16
18	Removed	Nearly removed	Nearly removed	Intact	Intact	Intact	4→5	16.7
19	Removed	Nearly removed	Nearly removed	Intact	Intact	Intact	4→5	23.2
20	Removed	Nearly removed	Nearly removed	Intact	Intact	Intact	4→5	4-10
21	Removed	Nearly removed	Nearly removed	Intact	Intact	Intact	4→5	17
22	Removed	Nearly removed	Nearly removed	Intact	Intact	Intact	4→5	8.3

23	Removed	Nearly removed	Nearly removed	Intact	Intact	Intact	4→5	10
24	Removed	Nearly removed	Nearly removed	Intact	Intact	Intact	4→5	Outcrop
26	Removed	Nearly removed	Nearly removed	Intact	Intact	Intact	4→5	Outcrop
X1	Removed	Nearly removed	Removed	Intact	Intact	Intact	4→5	Outcrop
X2	Removed	Removed	Removed	-	-	-	-	Outcrop
Y1	Removed	Nearly removed	Nearly removed	Nearly removed	Nearly removed	Nearly removed	9→10	Outcrop
A1	Removed	Removed	Removed	-	-	-	-	Outcrop
A2	Removed	Removed	Removed	Nearly removed	Nearly removed	Nearly removed	9→10	Outcrop
A3	Removed	Removed	Removed	Nearly removed	Nearly removed	Nearly removed	9→10	Outcrop
C1	Removed	Removed	Removed	Nearly removed	Depleted	Depleted	9→10	Outcrop
W2	Removed	Depleted	Intact	Intact	Intact	Intact	2	1615.44
V1	Removed	Removed	Removed	Intact	Intact	Intact	4→5	42-45
V2	Removed	Removed	Removed	Intact	Intact	Intact	4→5	63.25
P1	Nearly removed	Nearly removed	Nearly removed	-	-	-	-	55.6
D2	Removed	Removed	Removed	-	-	-	-	Outcrop
E1	Removed	Nearly removed	Nearly removed	-	-	-	-	Outcrop

Figure 22 *GC-FID chromatographs of eight selected oil samples to represent the different levels of biodegradation.* ***A*** *is the condensate sample 8 which is not degraded.* ***B*** *and* ***C*** *are the samples 2 and 4, respectively, representing biodegradation level 1, as the isoprenoids (Pr: Pristane; Ph: Phytane) are intact.* ***D*** *(sample 5),* ***E*** *(sample 15), and* ***F*** *(sample 19) represents the biodegradation level 4→5, where sample 5 show a pronounced UCM (unresolved complex mixture). Additionally, sample 5 show higher concentration of light and medium fractions (<C20) than the heavy fraction (>C20).* ***G*** *(sample A2) and* ***H*** *(sample C1) represents the biodegradation level 9→10. These samples have high UCM humps.*

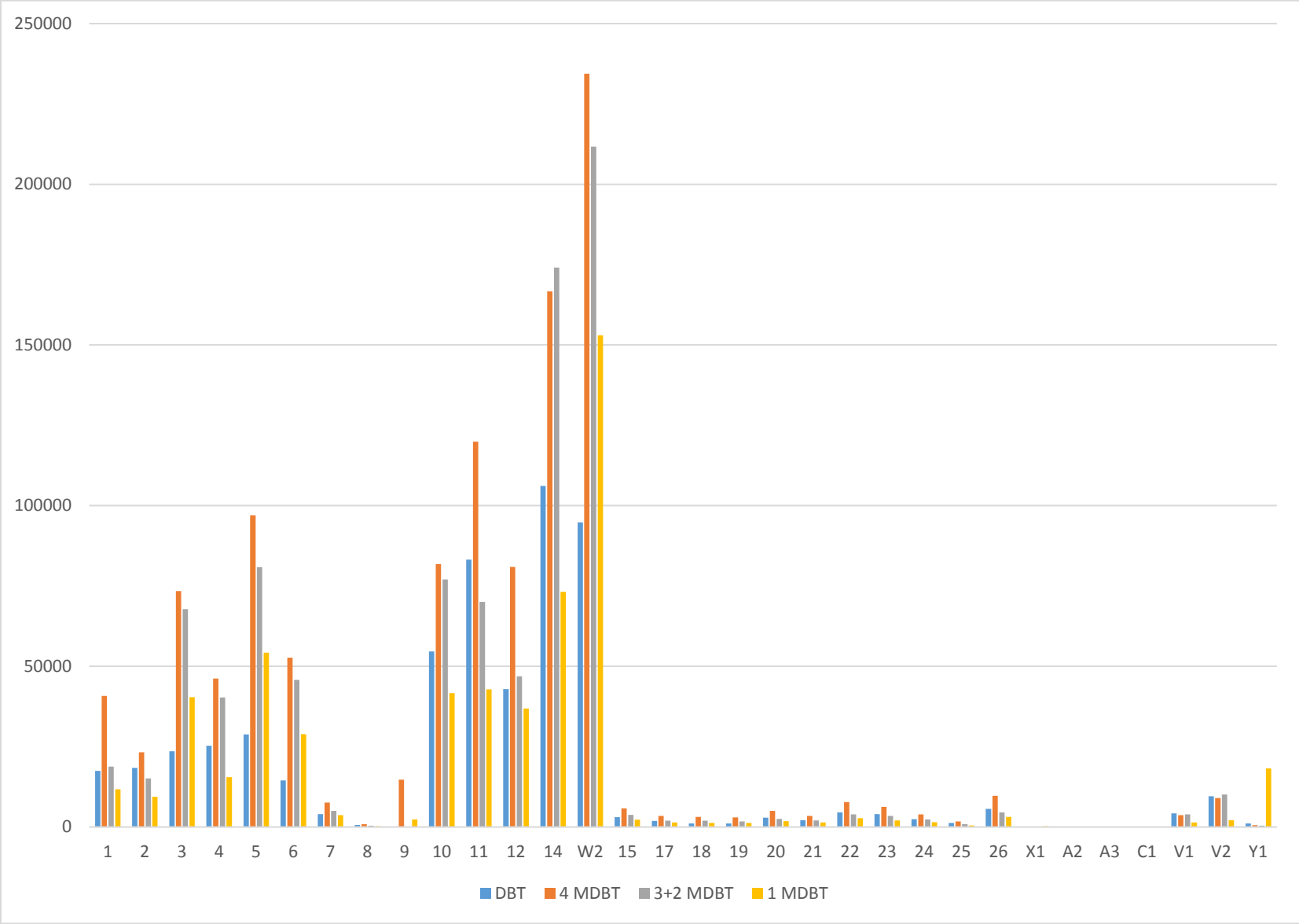

Figure 23 *Diagram illustrating the concentration of dibenzothiophene (DBT) and the methyldibenzothiophenes (MDBT) from the fragmetograms (m/z) 184 and (m/z) 198, respectively. All the samples show low concentration of the thiophenes, except samples 14 and W2, indicating the samples are water washed.*

5.2.1.2 Water Washing, and Biodegradation of the Light Oil Fraction

5.2.1.2.1 Toluene/Methylcyclohexane and Benzene/Cyclohexane

The oils generally have low concentration of benzene, which is the first aromatic compound to be removed during water washing (LaFargue and Barker, 1988) (Table 8). However, the concentration of toluene varies between the samples, suggesting the samples experienced different degrees of water washing. In Figure 24, benzene/cyclohexane is plotted against toluene/methylcyclohexane, where the samples 2, 5, 6, 7, 8 (northwest Cuba), 9, 10 (central Cuba), and W2 (Jamaica) plot as water washed. Samples 1 (northwest Cuba), 11, and 12 (central Cuba) show higher concentration of benzene and toluene, which implies these oils are less affected by water washing. The relatively high concentration of toluene compared to benzene seen in Figure 24 for the samples 4 and 14 from northwest Cuba, suggest these samples are influenced by biodegradation, as well as water washing.

Table 8 *Parameters used to evaluate water washing and transformation (TR) ratios for all the crude oils as defined by Halpern (1995). Sample names coloured in blue are collected from Cuba, whereas the Jamaican oil sample name is coloured in green.*

Sample	Tol/ MCyC6	Bz/ CyC6	Tr1	Tr2	Tr3	Tr4	Tr5	Tr6	Tr7	Tr8
1	0.29	0.48	53.25	33.96	6.85	3.75	10.60	0.00	2.28	3.89
2	0.06	0.15	2.11	6.92	4.10	2.86	6.96	0.00	2.21	1.93
4	0.06	0.76	63.68	28.72	7.67	4.46	12.13	0.00	1.94	3.11
5	0.00	0.26	2.86	1.60	3.72	1.23	4.95	0.00	1.29	1.15
6	0.03	0.19	1.54	2.79	6.00	2.28	8.28	0.00	1.72	1.45
7	0.01	0.03	0.35	2.53	2.14	1.31	3.44	0.00	1.01	1.38
8	0.05	0.06	1.39	11.72	6.00	6.01	12.01	0.00	1.51	3.63
9	0.10	0.07	1.90	11.45	5.10	4.38	9.48	0.00	1.54	2.93
10	0.12	0.20	1.64	1.63	3.83	1.68	5.51	0.00	1.32	0.78
11	0.21	0.44	7.83	11.92	6.24	4.66	10.90	0.00	1.41	1.80
12	0.29	0.38	7.45	19.80	9.27	7.42	16.69	0.00	1.56	2.41
14	0.28	1.09	25.77	40.04	16.65	11.92	28.57	0.00	2.00	3.04
W2	0.00	0.17	0.45	0.18	0.24	0.14	0.39	0.00	0.09	0.20

Tr1*: Toluene/1,1-dimethylcyclopentane;* ***Tr2****: n-heptane/1,1-dimethylcyclopentane;* ***Tr3****: 3-methylhexane/1,1-dimethylcyclopentane;* ***Tr4****: 2-methylhexane/1,1-dimethylcyclopentane;* ***Tr5****: (2-methylhexane+3methylhexane)/1,1-dimethylpentane;* ***T6****: 1-c-2-dimethylcyclopentane/1,1-dimethylcyclopentane* ***Tr7****: 1-t-3-dimethylcyclopentane/1,1-dimethylcyclopentane;* ***Tr8****: (2-methylhexane+3methylhexane)/(2,2-dimethylpentane+2,3-dimethylpentane+2,4-dimethylpentane+3,3-dimethylpentane+3-ethylpentane).*

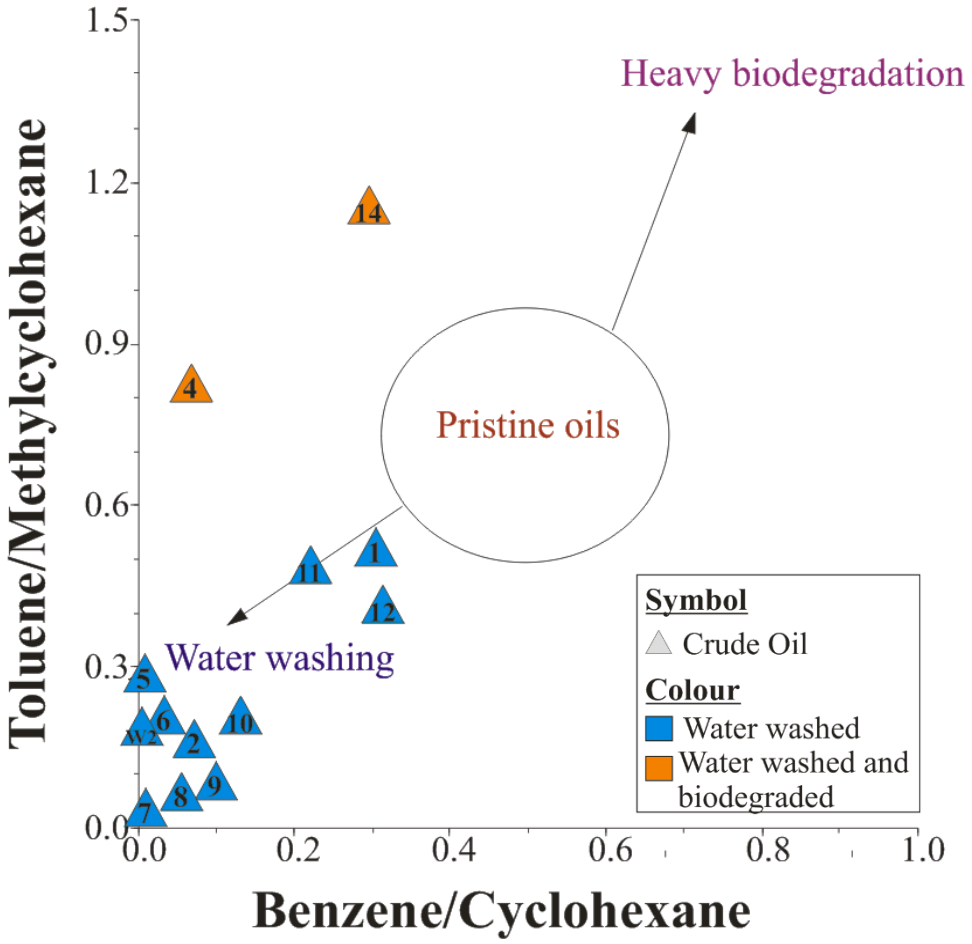

Figure 24 *Cross-plot of the toluene/methylcyclohexane and benzene/cyclohexane ratios, indicating water washing effects for the samples 2, 5, 6, 7, 8 (northwestern Cuba), 9, 10 (central Cuba), and W2 (Jamaica). Samples 1 (northwestern Cuba), 11, and 12 (central Cuba) have experienced less degree of water washing, whereas samples 4 and 14 (northwestern Cuba) could also be affected by biodegradation.*

5.2.1.2.2 C7 Transformation star-diagram (C7-OSTD)

Figure 25 illustrate the C7 transformation star-diagram (C7-OTSD) of Halpern (1995), where the samples show different levels of transformation. The numerator in the transformation ratios Tr2 through Tr7 are typically affected by biodegradation in decreasing degree, whereas the Transformation ratio Tr8 is the most stable ratio (Halpern, 1995). The Tr1 ratio (toluene/ 1.1-dimethylcyclopentane) can also be used to compare the degree of water washing between the samples. The samples 2, 5, 6, 7, 8 (northwestern Cuba), 9, 10, 11 (central Cuba), and WIN2 (Jamaica) show the lowest values (Table 8). This suggests water washing, which complies with the results previous discussed (Figure 24). Less affected are samples 1, 4, and 14 (northwestern Cuba), which have the highest values of the Tr1 parameter (Table 8). From the transformation star-diagram (Figure 25), sample 14 seems to be the least affected by bacterial attack compared to the other samples, whereas W2 has experienced high level of biodegradation.

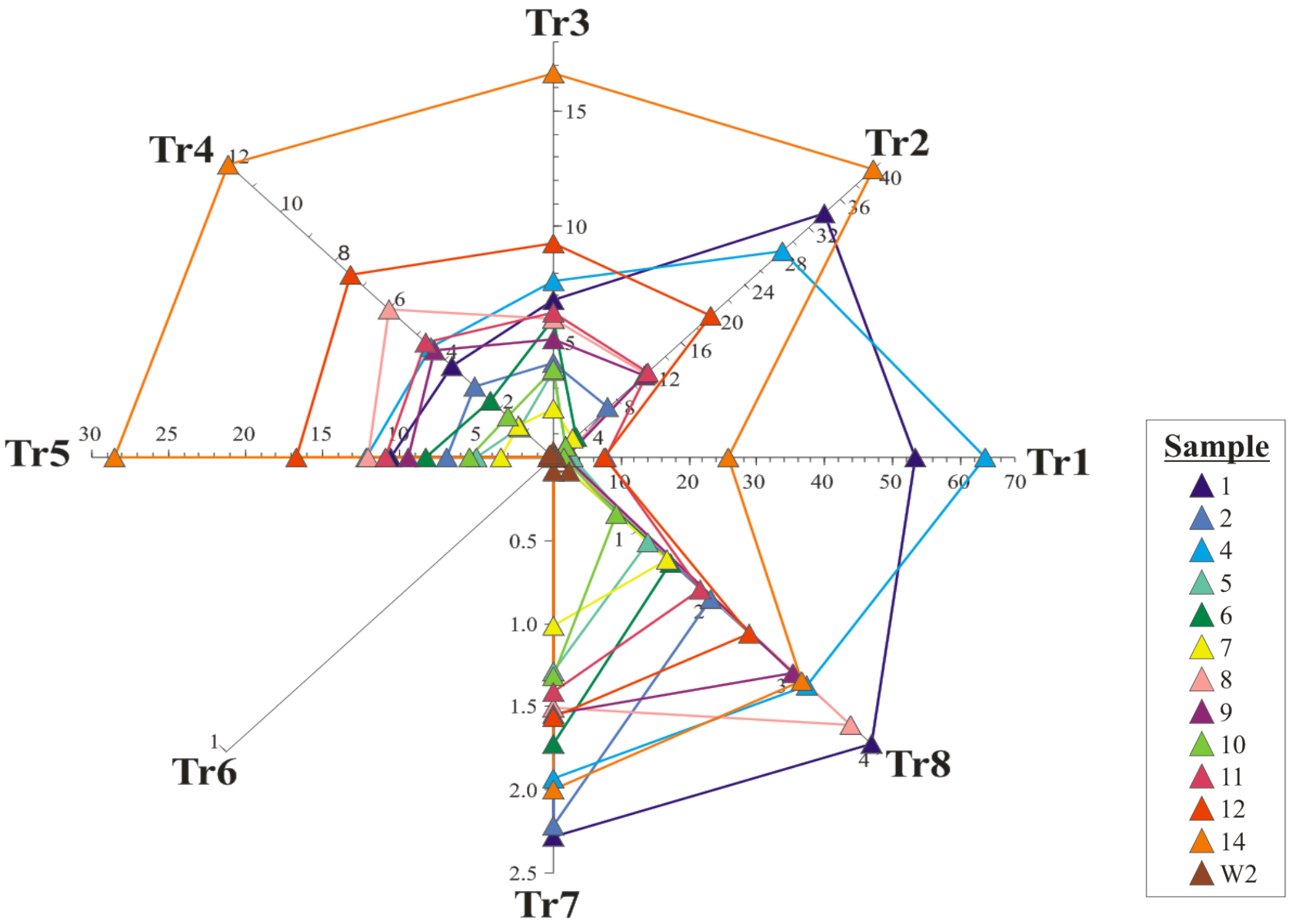

Figure 25 *Transformation (Tr) star-diagram illustrating the different levels of transformation for the crude oil samples. Sample W2 show to be the most affected by biodegradation compared to the other samples, whereas sample 14 seems to have experienced relatively low level of transformation.*

5.2.2 Thermal Maturation

5.2.2.1 Heavy Oil Fraction

5.2.2.1.1 Aromatisation

The aromatic steroids are typically the last compounds to be affected by bacterial attack and are, in addition, more reliable than biological markers at relatively high levels of maturity (Radke, 1988). Originally, the triaromatic (TA) and monoaromatic (MA) steroids used as maturity parameters were interpreted to be the result from the cracking of the long-chained hydrocarbons compared to short-chained homologues during maturation (Peters et al., 2005). However, the change in the ratios are now suggested to be more a thermodynamic stability effect, as the short-chained hydrocarbons survive destruction better than the long-chains. Thus, to use the TA and MA as the maturity parameters, values higher than 0.5 are required for the two ratios TA(C20-21/(C20-21+C26-28)) and C26-28TA/(C26-28TA+C27-29MA). The stability effect would have more influence on the ratios with higher maturities than organofacies related variabilities with higher values (Killops pers. Comm.). None of the samples have values exceeding 0.5 for both the two ratios (Table 9), which does not reach the requirement to use the aromatisation as maturity parameters.

5.2.2.1.2 Steranes Isomerisation

Steranes isomerisation can be used to assess the thermal maturity of the different samples. By comparing the concentration of the S configuration against the R configuration in the sterane ratio ααS/(ααS+ααR) of the C29 steranes, the maturity can be evaluated. Only the ααR configuration is present in living organisms, which is converted to the other three configurations during maturation (Mackenzie and McKenzie, 1983, Beaumont et al., 1985). The ratio reaches its equilibrium at 0.52 – 0.55 equivalent to the vitrinite reflectance (% Ro) value of 0.8-0.9 (Seifert and Moldowan, 1986). Similar, the ββ/(ββ+αα) ratio of C29 is also affected by maturation, where the ββ-isomer will increase compared to the αα-isomer with increasing maturity, due to the ββ-isomer being more thermally stable (Mackenzie et al., 1985). This ratio equilibrates at 0.67-0.71, which correspond to % Ro of 0.9 (Seifert and Moldowan, 1986).

In Figure 26, the sterane ratios ααS/(ααS+ααR) and ββ/(ββ+αα) are cross-plotted. The crude oil samples 4, 5, 6, and 7 from northwestern Cuba, as well as the extract samples from southeastern Cuba (samples 17-24 and 26) show low values indicating oil generation in the early oil window

(<0.9%Ro). Furthermore, samples 3 (northwestern Cuba), 9 (central Cuba), and X1 (southern Cuba) show comparatively higher maturities close to the equilibrium of the ααS/(ααS+ααR) ratio with values of 0.50, 051, and 0.51, respectively (Table 9), suggesting the oils were generated in the peak oil window. Additionally, the seven remaining samples (samples 1, 2, 14 (northwestern Cuba), 10, 11, 12 (central Cuba), and 15(southern Cuba)) have reached the equilibrium (Figure 26) for this ratio, which makes this maturity assessment uncertain. None of the samples have reached the ββ/(ββ+αα) equilibrium, indicating %Ro below 0.9 and oil expulsion during the peak oil window. A maturity of approximately 0.9 is inferred based on discrepancy in isomerisation.

5.2.2.1.3 Hopane Isomerisation

Figure 27 compares the hopane maturity ratio C30 diahopane/(C30 diahopane + C29 moretane) with the hopane isomerisation ratio C31S/(C31S+C31R). Most of the oils are close to or have reached the isomerisation equilibrium value (0.6) and, are thus, suggested to be early mature. The C30 diahopane/(C30 diahopane+C29moretane) shows variation in maturity of the samples (Figure 27). These values are, however, not coincide with the interpretations derived from the steranes isomerisation (Figure 26). As will later be discussed in the lithofacies chapter (5.2.3.1), the samples show to plot in three clusters according to lithofacies. The blue circle represents oils derived from carbonate, whereas oils originating from shales are marked with a green circle. Furthermore, the majority of the oils encircled in orange colour are sourced by marly source rocks (Figure 27). Thus, this maturity assessment is greatly influenced by facies. The maturity determination of the heavy oil fraction is, therefore, solely based on the sterane isomerisation.

5.2.2.1.4 Distribution

The interpreted maturities of the source rocks that generated and expelled the analysed oils on Cuba and Jamaica are shown in Figure 28 and Figure 29, respectively. The oil samples from Cuba appear to be derived from source rocks in the early to peak oil window, whereas the extracts from southeastern Cuba and Jamaica only demonstrate an early mature signature.

Table 9 *Biomarker ratios used to interpret the maturities for the heavy, medium, and light fractions of the analysed samples.* ***TA****: Triaromatic;* ***MA****: Monoaromatic;* ***D****: Diahopane;* ***M****: Moretane;* ***%Rc****: Calculated vitrinite reflectance;* ***MPR****: methylphenanthrene ratio;* ***MPI 1****: Methylphenanthrene index 1;* ***MPDF****: Methylphenanthrene distribution fraction;* ***MDR****: Methyldibenzothiphene ratio;* ***%Rc-ave****; average of the calculated vitrinite reflectance values;* ***H****: Heptane value; F: heptane/methylcyclohexane ratio.*

	Heavy Fraction					Medium Fraction					Light Fraction	
Sample	**TA(C20-21/ (C20-21+C26-28))**	**C26-28 TA/ (C26-28TA+C27-29MA)**	**C29 ααS/ (ααS+ααR)**	**C29 ββ/ (ββ+αα)**	**C30D/ (C30D+C29M)**	**%Rc - MPR**	**%Rc - MPI 1**	**%Rc - MPDF**	**%Rc - MDR**	**%Rc-Ave**	**H**	**F**
1	0.29	0.48	0.51	0.55	0.88	0.78	0.71	0.71	0.76	0.79	20.04	0.31
2	0.15	0.53	0.53	0.43	0.86	0.76	0.77	0.77	0.69	0.80	15.66	0.48
3	0.32	0.11	0.50	0.55	0.93	0.81	0.78	0.78	0.64	0.84		
4	0.14	0.31	0.34	0.41	0.96	0.86	0.86	0.86	0.73	0.89	20.9	0.34
5	0.19	0.14	0.48	0.49	0.86	0.76	0.71	0.71	0.64	0.78	5.93	0.14
6	0.19	0.14	0.48	0.50	0.84	0.77	0.71	0.71	0.64	0.77	9.02	0.34
7	0.09	0.47	0.45	0.46	0.96	0.88	0.85	0.85	0.66	0.90	9.09	0.19
8	0.12	0.49	0.46	0.48	1.16	0.88	1.09	1.09	0.79	1.05	19.24	0.49
9	0.11	0.01	0.51	0.56	0.23	0.63	0.32	0.32	0.96	0.39	17.81	0.44
10	0.35	0.44	0.53	0.55	1.04	0.85	0.93	0.93	0.65	0.94	6.98	0.2
11	0.36	0.44	0.53	0.55	0.98	0.84	0.86	0.86	0.71	0.89	22.89	0.67
12	0.29	0.46	0.54	0.58	1.17	0.81	0.95	0.95	0.67	0.97	28.9	1.02
14	0.37	0.17	0.57	0.56	0.89	0.79	0.69	0.69	0.68	0.79	36.15	1.69
15	0.20	0.54	0.61	0.50	1.04	0.88	0.90	0.90	0.70	0.94		
17	0.14	0.33	0.46	0.54	1.21	0.94	1.16	1.16	0.68	1.11		
18	0.15	0.27	0.43	0.53	1.20	1.05	1.13	1.13	0.69	1.13		
19	0.15	0.28	0.47	0.55	1.21	1.07	1.15	1.15	0.69	1.15		
20	0.17	0.33	0.48	0.53	1.18	0.90	1.12	1.12	0.72	1.07		
21	0.09	0.37	0.45	0.53	1.24	0.94	1.18	1.18	0.69	1.12		
22	0.16	0.29	0.44	0.54	1.24	0.94	1.17	1.17	0.72	1.12		
23	0.18	0.25	0.47	0.54	1.15	0.87	1.05	1.05	0.73	1.02		
24	0.17	0.24	0.41	0.52	1.23	0.93	1.16	1.16	0.70	1.11		
25	0.20	0.40	0.52	0.54	1.18	0.84	1.13	1.13	0.79	1.05		
26	0.15	0.29	0.45	0.52	1.24	0.89	1.16	1.16	0.73	1.10		
X1	0.20	0.52	0.51	0.57	0.71	0.66	0.56	0.56	0.54	0.65		
W2	0.28	0.50	0.48	0.54	0.89	0.83	0.69	0.69	0.62	0.80	3.76	0.07
V1	0.04	0.80	0.46	0.49	1.01	0.75	0.87	0.87	0.70	0.88		
V2	0.05	0.83	0.46	0.48	1.11	0.77	1.01	1.01	0.82	0.96		

%Rc-MPR *= 1.1 x log10 MPR + 0.95 (Radke, 1988), MPR =2-MP/1-MP;* ***%Rc-MPI 1*** *= 0.60 x MPI1 + 0.40 (Radke, 1988), MPI 1 = 1.5 x (3-MP + 2-MP)/(P + 9-MP + 1-MP);* ***%Rc-MPDF*** *= 2.242 x MPDF - 0.166 (Kvalheim et al., 1987), where methylphenanthrene, MPDF = (3-MP + 2-MP)/ (3-MP + 2-MP + 1-MP + 9-MP);* ***%Rc-MDR*** *= 0.073 x MDR + 0.51 (Radke, 1988), MDR = 4-MDBT/1-MDBT;* ***H*** *=100*n-heptane/cyclohexane+2-methylcyclohexane+3-methylcyclohexane+c-1,3-dimethylcyclopentane+t-1,2-dimethylcyclopentane+n-heptane+methylcyclohexane (Thompson, 1979);* ***F****= n-heptane/ methylcyclohexane (Thompson, 1979).*

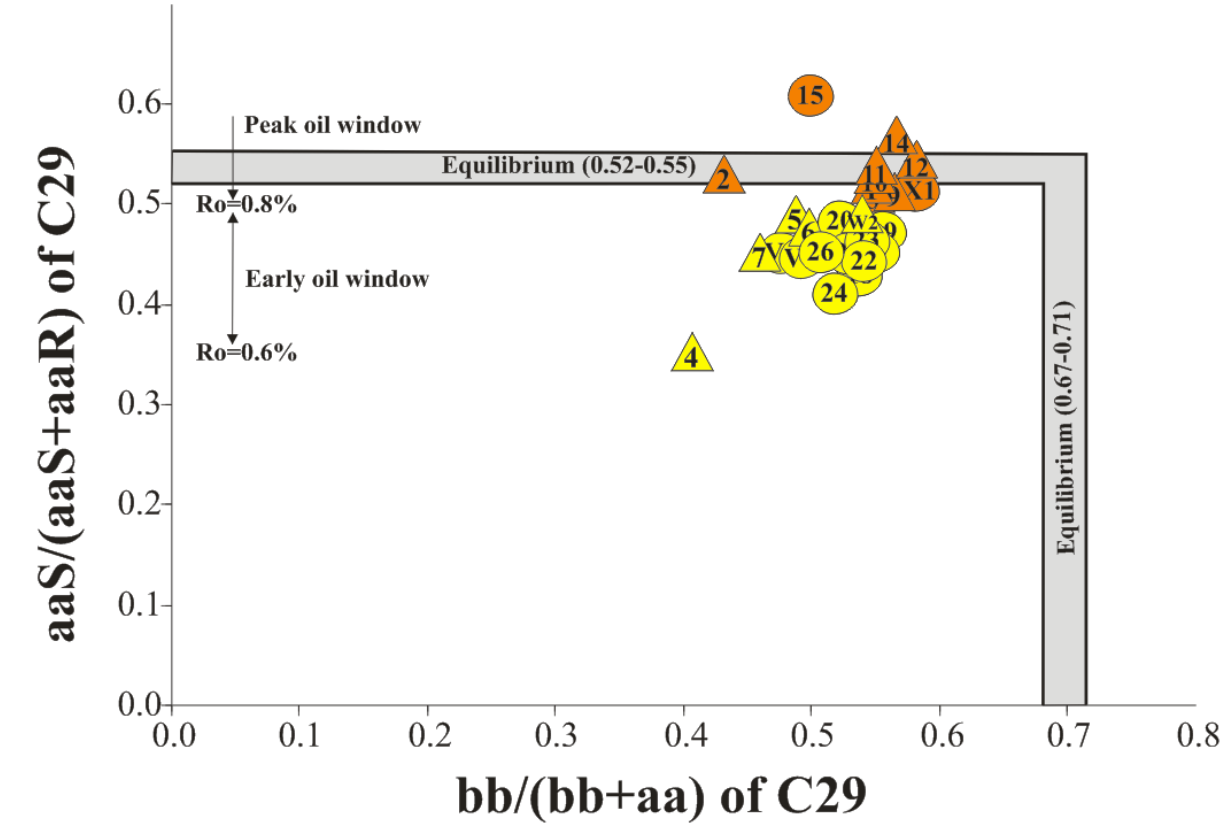

Figure 26 *Cross-plot of the steranes isomerisation maturation parameters (ββ/(ββ+αα) versus aaS/(ααS+αα R) of the C29 steranes).The extract samples show to be, generally, generated in the early oil window, whereas most of the crude oils plot as derived from source rocks in the peak oil window.*

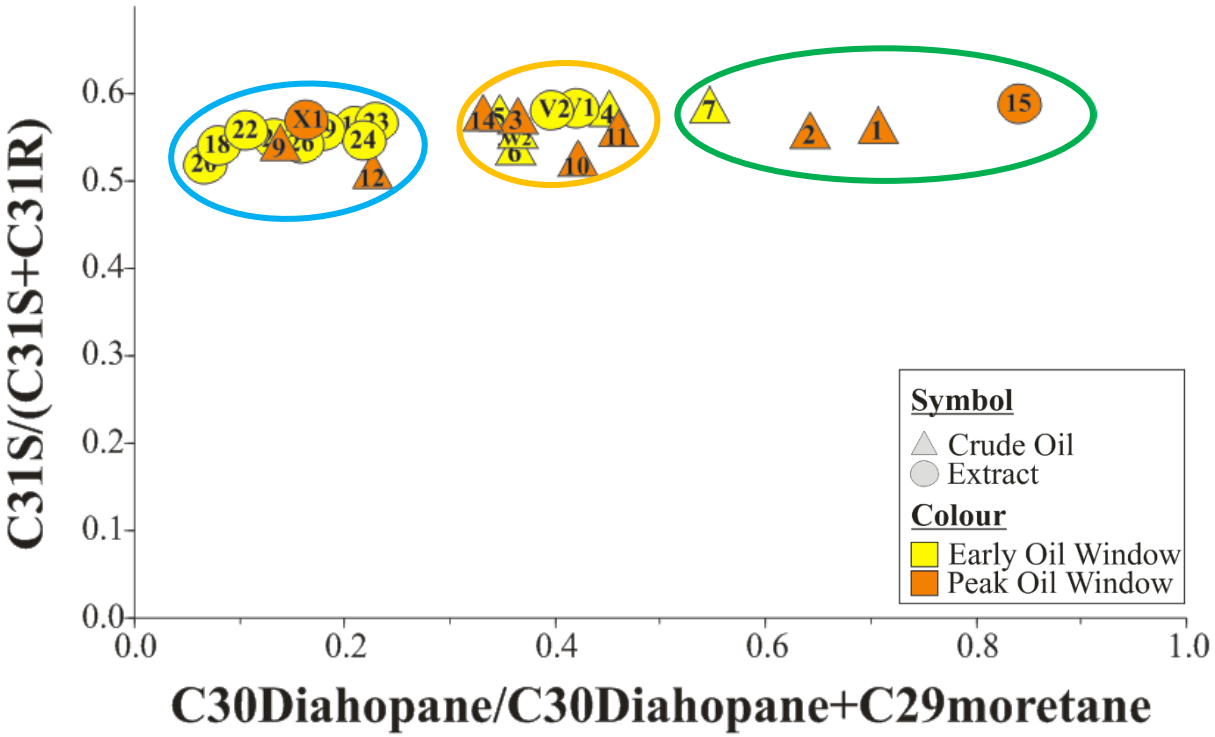

Figure 27 *Hopane isomerisation (C31S/(C31S+C31R)) plotted against C30 diahopane/(C30 diahopane+C29moretane) indicating the maturity of the heavy oil fraction. The maturity values derived from the terpanes does not show similarities to the interpretations gained from the sterane isomerisation. However, the terpane ratios show to be influenced by facies (Figure 25), the samples in the blue circle are derived from carbonates, most of the samples in the orange circle originate from marls, and the samples in the green circle were generated by shales.*

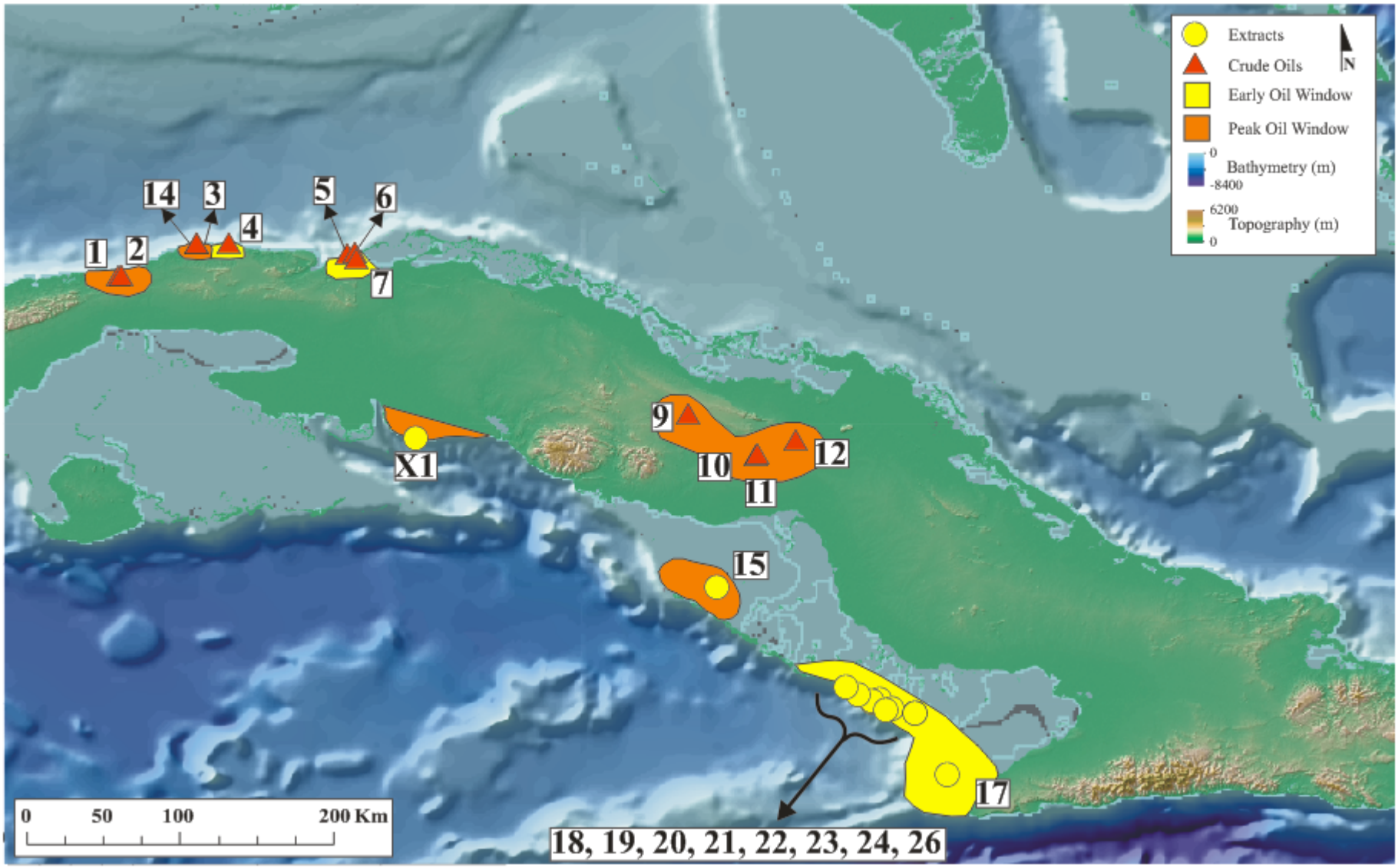

Figure 28 *Map of Cuba, illustrating the interpreted maturities of the source rocks generating the oils based on the heavy fraction. The samples show to mainly be derived from source rocks in the peak oil window in Cuba, whereas southeast Cuba appear to only originate from early mature source rocks.*

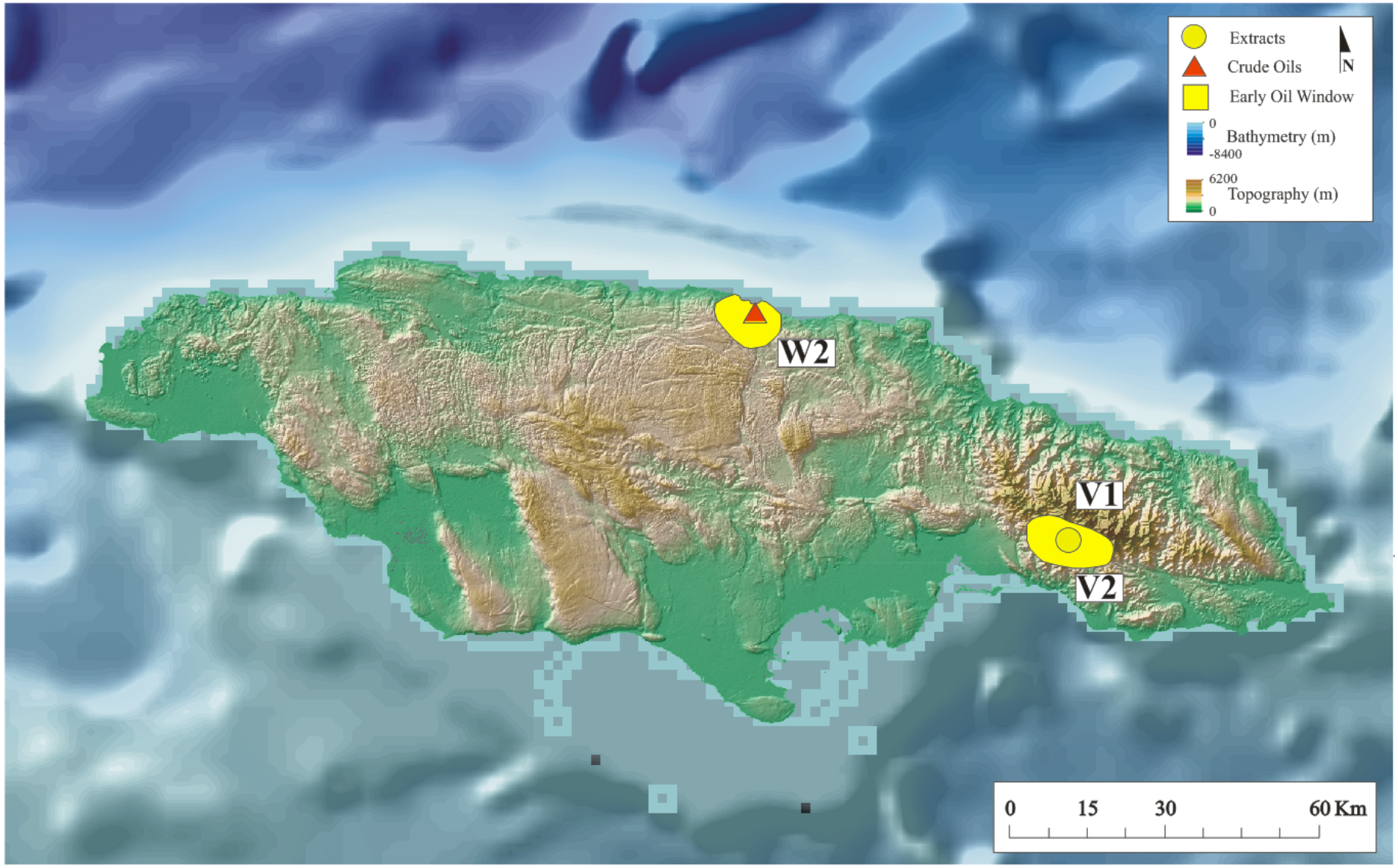

Figure 29 *Map of Jamaica where the interpreted maturities are shown, where all the samples show to originate from early mature source rocks.*

5.2.2.2 Medium Fraction

5.2.2.2.1 Calculated Vitrinite Reflectance

The methylphenanthrene (MP) and methyl-dibenzothiophene (MDBT) can be used as maturity indicators for the medium fraction of an oil. During maturation, the 3-MP and 2-MP are more stable compared to 9-MP and 1-MP. Thus, an increase in maturation will result in relatively higher concentration of the 3-MP and 2-MP, as well as the 4-MDBT (Radke, 1988). Maturities were calculated (%Rc, Table 9) based on: methylphenanthrene ratio (MPR) (Radke, 1988), methylphenanthrene distribution factor (MPDF) (Radke, 1988), methylphenanthrene index (MPI) (Radke, 1988), and methyldibenzothiophene ratio (MDR) (Kvalheim et al., 1987). The maturities calculated from the various ratios were summed and averaged (%Rc-ave) (Table 9). However, as was discussed in the alteration chapter, most of the samples have low concentrations of the various thiophenes. This makes the %Rc-MDR unreliable. This ratio is, therefore, excluded from the calculation of the %Rc-ave.

The calculated vitrinite reflectance values based on two of the phenanthrene ratios (MPR and MPDF) are illustrated in the Figure 30. The two parameters are seen to correlate well and the samples are suggested to be in the maturity range 0.8 to 1.3 %Rc. These values are, in general, consistent with the %Rc-ave shown in Table 9. Samples from southeastern Cuba (samples 17-24 and 26) have the highest maturities with values of 1.10-1.15 %Rc-ave (Table 9), indicating expulsion at the late oil window. The remaining samples (samples 1, 2, 3, 4, 7, 14 (northwestern Cuba), 10, 11, 12 (central Cuba), 15 (southern Cuba), V1, and V2 (Jamaica)) have values ranging from 0.79 to 0.97 %Rc-ave, suggesting oil generation at the peak oil window. Samples 5 and 6 from northwestern Cuba, as well as the sample X1 in south Cuba have lower values (0.78, 0.77, and 0.65 %Rc-ave) indicating that the oils were generated in the early oil window. Furthermore, sample 9 from central Cuba has the lowest maturity of all the samples.

The maturity interpretation of the medium ranged oil fraction illustrated in Figure 31 and Figure 32 shows that the medium oil fraction, with the exception of samples 5 and 6 in northwestern Cuba, have higher maturity than the heavy oil fraction. The highest maturity is seen in the extracts (samples 17-24 and 26) from southeastern Cuba.

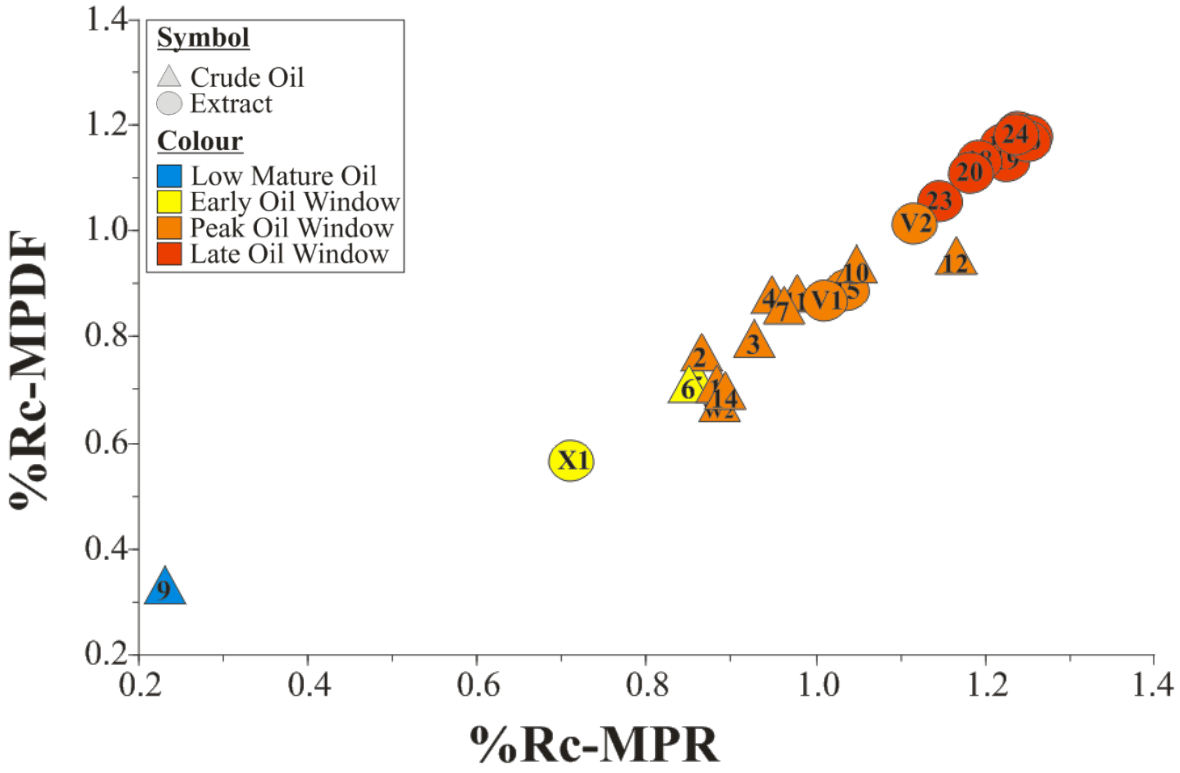

Figure 30 *Cross plots of maturity parameters using the vitrinite reflectance (%Rc) calculated from medium range aromatics based on the methylphenanthrene ratio (MPR) and the methylphenantherene distribution factor (MPDF). In general, the samples show to have high maturities in the 0.8-1.3 %Rc range. Sample 9 plot as the least mature oil in the sample set. The maturities of the samples are coloured after the %Rc-ave values.*

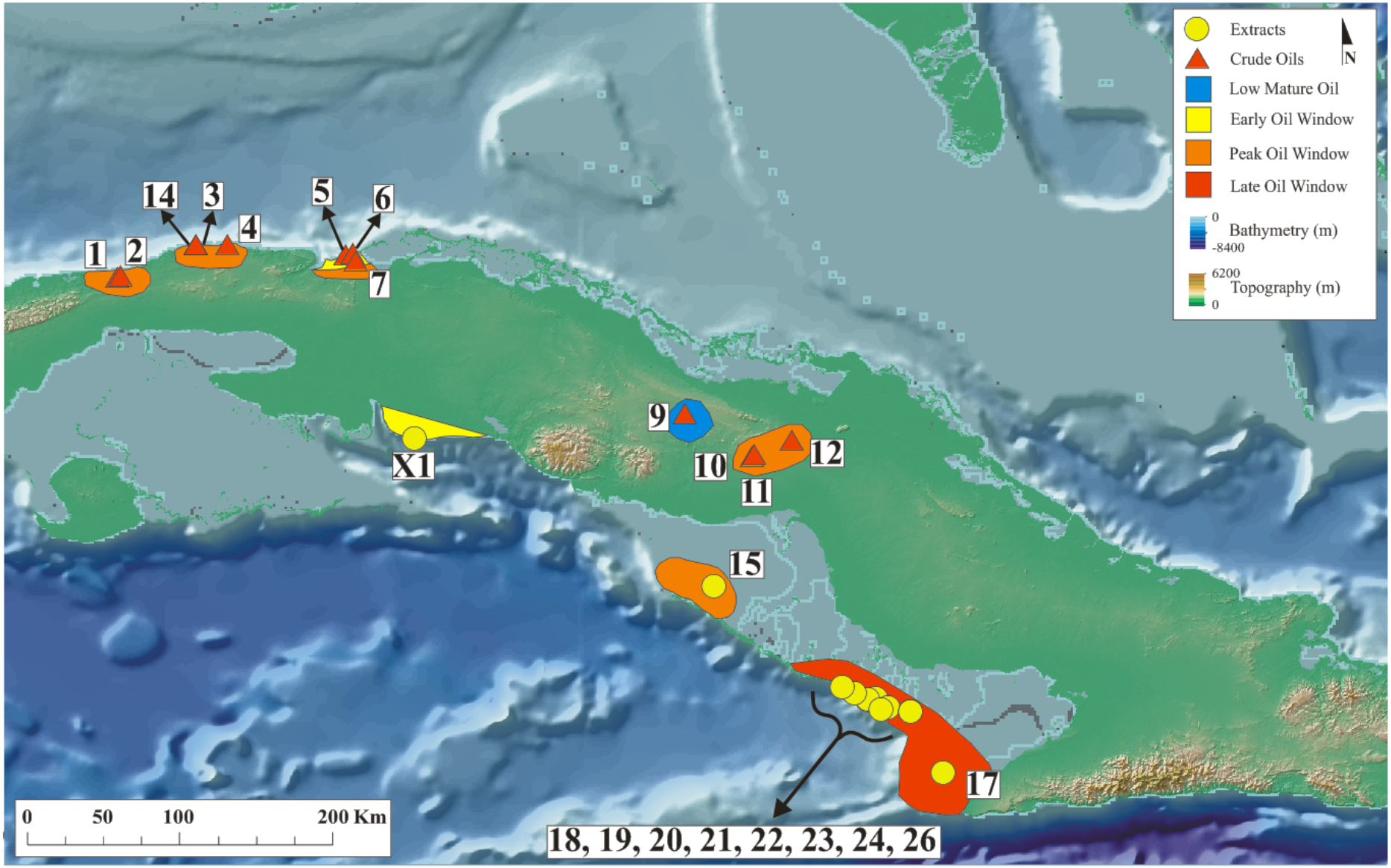

Figure 31 *Map of Cuba illustrating the interpreted maturities based on the average calculated vitrinite reflectance (%Rc-ave) values. The extract samples in the southeast show to have the highest maturities relative to the other samples.*

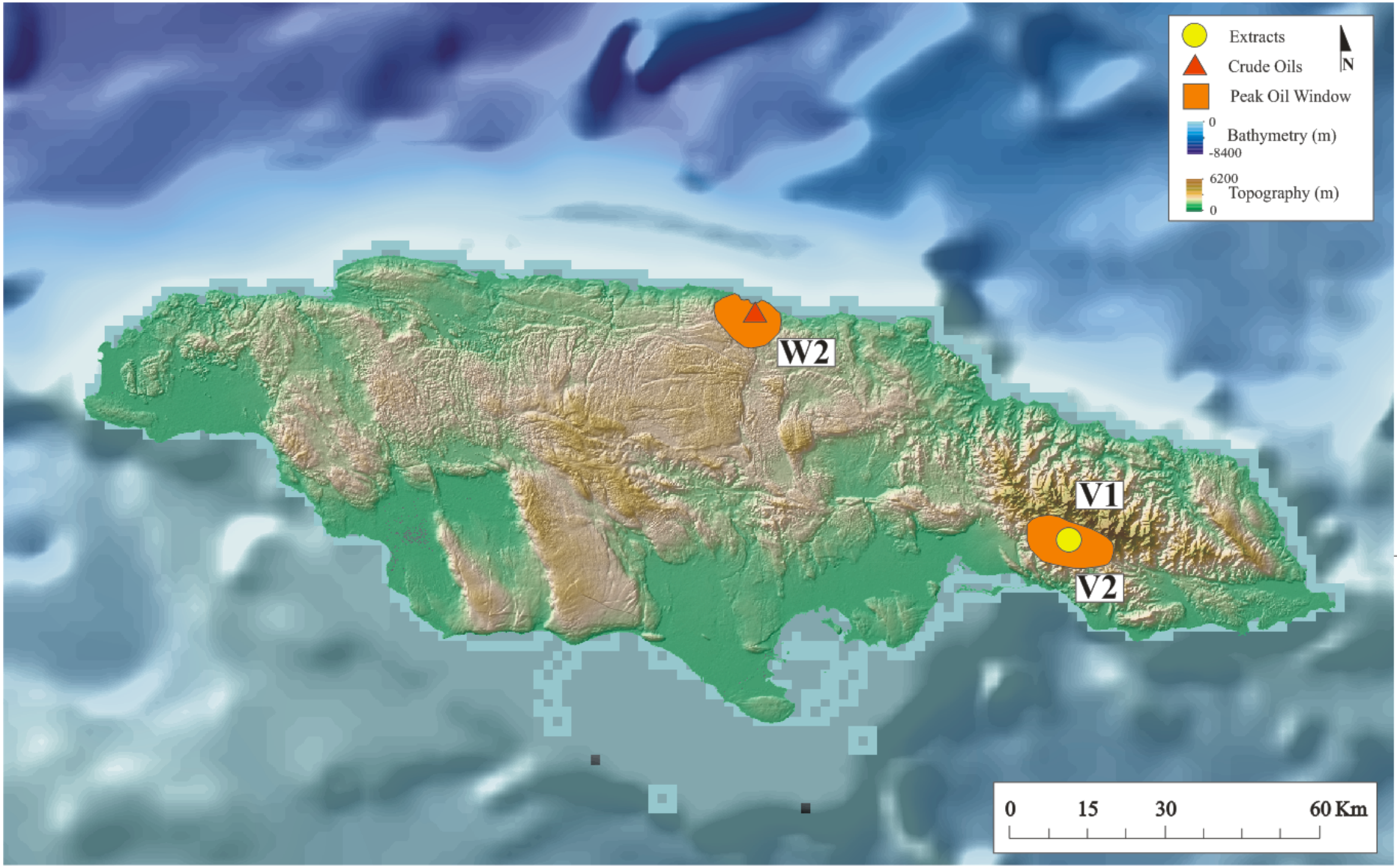

Figure 32 *Map showing the interpreted medium oil fraction maturities of the samples from Jamaica based on the average calculated vitrinite reflectance (%Rc-ave) values. All the samples show to be generated from source rocks in the peak oil window.*

5.2.2.3 Light Oil Fraction

5.2.2.3.1 Thompson H-F diagram

Paraffinicity (paraffins-to-naphthenes) is shown to increase during thermal maturation (Philippi, 1975, Philippi, 1977), consequently maturity assessments of the light oil fraction can be based on the Heptane value (H) and n-heptane/methylcyclohexane ratio (F) (Thompson, 1979) (Table 9). In Figure 33 most of the undegraded oils (samples 1, 2, 4, 8 (northwestern Cuba), 9 (central Cuba)) plot as normal mature (%Ro in the 0.8-0.9 range). Samples 11 and 12 from central Cuba (Figure 34) plot with higher maturity (Figure 33) and sample 14 from northwestern Cuba (Figure 34) displays the highest maturity of the oils. The degraded oils (samples 5, 6, 7 (northwestern Cuba), 10 (central Cuba), and W2 (Jamaica)) plot as expected with the lowest ratios (Figure 33), as the normal-paraffins are preferentially attacked by bacteria (Peters et al., 2005).

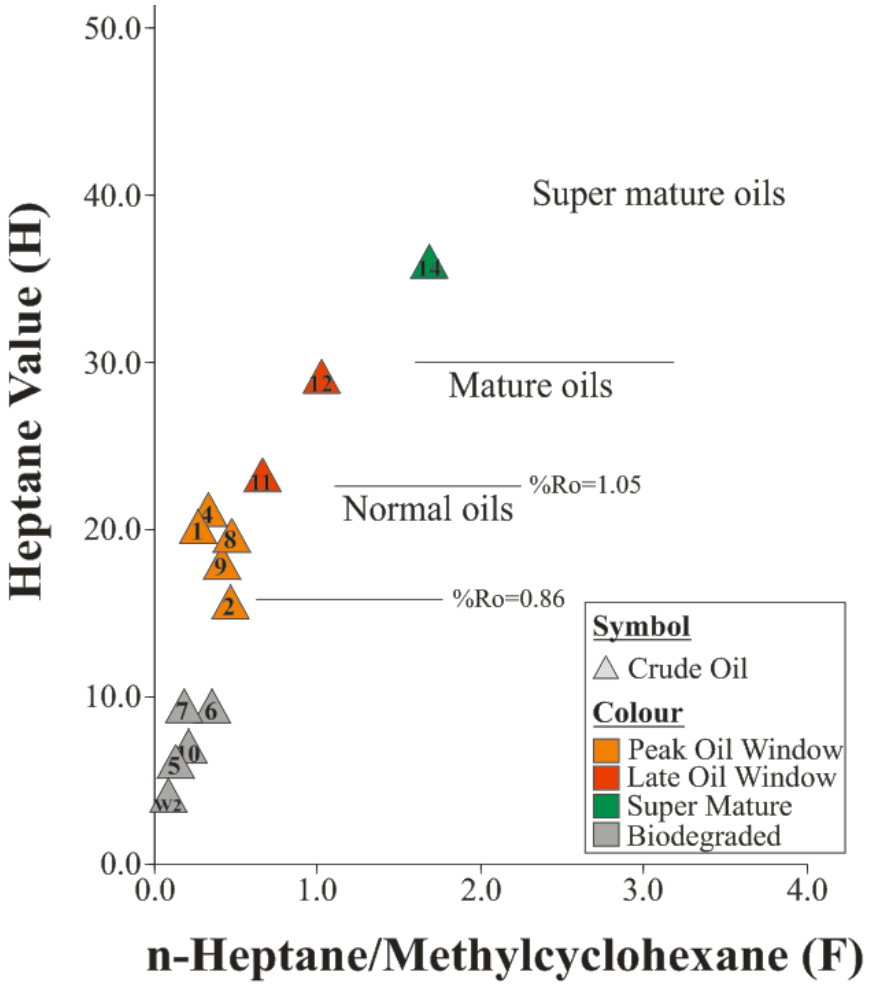

Figure 33 *Maturity evaluation of the source rocks from which the oils originate. The Heptane value (H) is plotted against the n-heptane/methylcyclohexane ratio (F), indicating most of the samples (1, 2, 4, 8 (northwest Cuba), and 9 (central Cuba)) were generated in the peak oil window.*

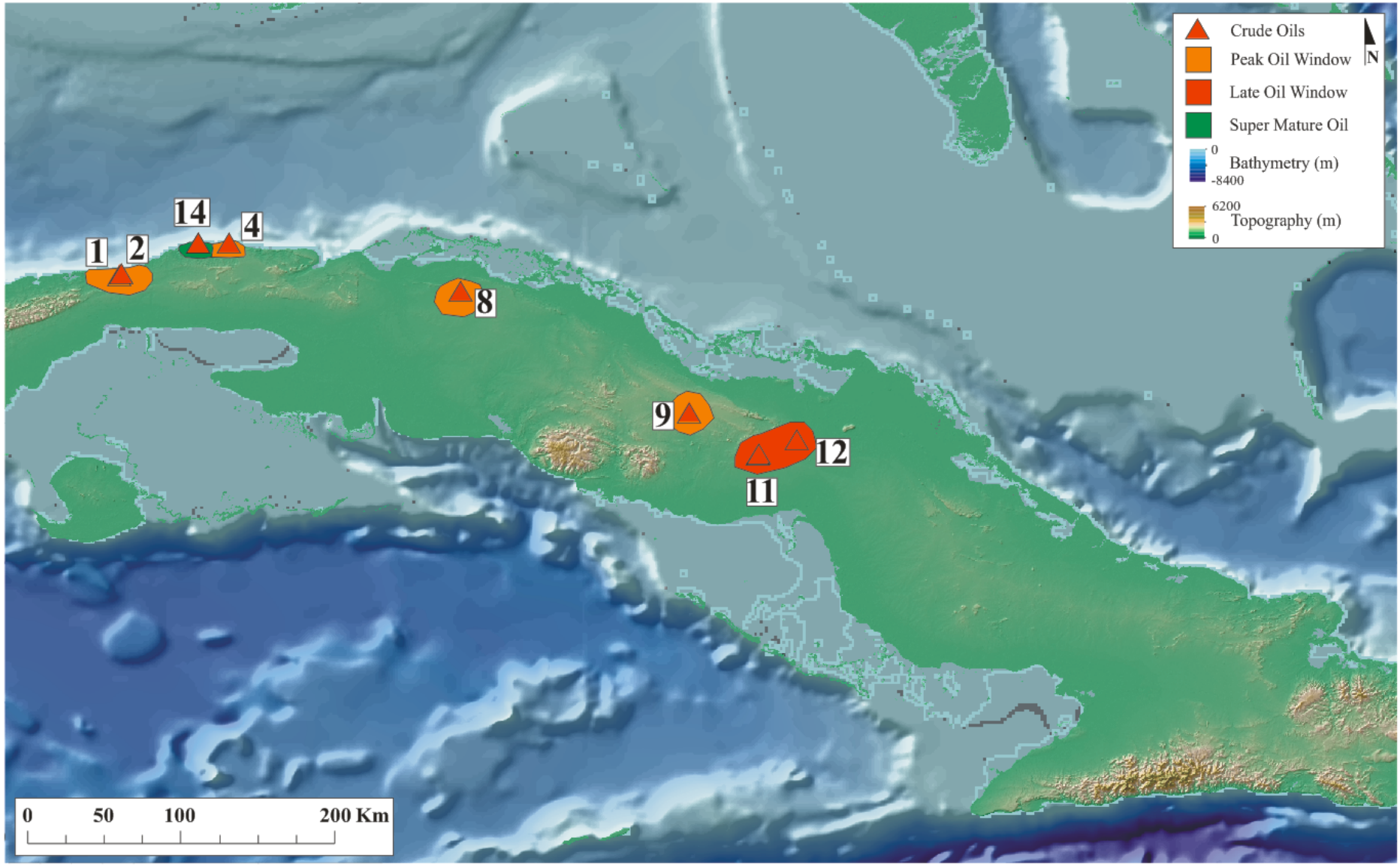

Figure 34 *Map of Cuba illustrating the maturity of the light oil fraction for the crude oils that are not biodegraded. All the samples have relatively high maturities, where sample 14 show the highest maturity as a super mature oil.*

5.2.3 Lithofacies and Depositional Environment

5.2.3.1 Heavy Oil Fraction

5.2.3.1.1 Diasteranes/(Diasteranes+Regular Steranes)

The diasteranes/(diasteranes+regular steranes) ratio can be used to distinguish petroleum derived from carbonate and clastic source rocks (Mello et al., 1988b). Low values generally imply petroleum originating from clay-poor (carbonate) source rocks (Hughes, 1984, Mello et al., 1988a, Mello et al., 1988b), whereas high values are typical for petroleum derived from clay-rich source rocks (Rubinstein et al., 1975, Sieskind et al., 1979). The crude oil and extract samples have low values ranging from 0.11 to 0.38 (Table 10), except for the samples 1, 2, 7 (northwestern Cuba), 15 (southern Cuba), and W2 (Jamaica) with values in the 0.42 to 0.52 range. Thus, based on this lithofacies assessment, most of the oils are interpreted to be derived from carbonates. Five samples (1, 2, 7, 15, and W2), however, are suggested to originate from clastic source rocks.

High concentrations of diasteranes can also be a result of the depositional environment, as formation of diasteranes is favoured by oxic (high Eh) and acidic (low pH) conditions during diagenesis (Moldowan et al., 1986). This suggests that the oil samples 1, 2, 7 (northwestern Cuba), 15 (southern Cuba), and W2 (Jamaica) originate from source rocks deposited in a more oxic and acidic environment relative to the interpreted carbonate derived oils. In addition, high maturity can increase the concentration of diasteranes relative to the regular steranes as diasteranes are thermally more stable (Seifert and Moldowan, 1978, Moldowan et al., 1986). However, as discussed in the maturity chapter, none of the samples show maturities levels exceeding the peak oil window for the heavy oil fraction (Chapter 5.2.2.1).

Table 10 *Biomarker ratios used to evaluate the lithofacies and depositional environment of the source rocks generating the oils. The Cuban sample names are coloured in blue and the Jamaican sample names are coloured in green* ***Dia****: Diasteranes;* ***Ster****: Steranes;* ***D****: Diahopane;* ***M****: Moretane;* ***HH****: Homohopanes;* ***TT****: Tricyclic terpanes;* ***C****: Correlation ratio.*

Sample	Heavy Fraction						Light Fraction				
	Dia/ (Dia+Ster)	C29/C30 hopanes	C30D/ C30D+C30M	C35/C34 HH	C24/C23 TT	Gammacerane index	C1	C2	C3	C4	C5
1	0.46	0.68	0.53	0.76	0.79	0.11	0.00	0.71	0.00	0.00	0.29
2	0.44	0.53	0.41	0.79	0.71	0.08	0.05	0.60	0.17	0.04	0.13
3	0.11	0.79	0.28	1.32	0.66	0.32					
4	0.25	0.73	0.34	1.09	0.66	0.25	0.00	0.61	0.04	0.07	0.28
5	0.13	0.67	0.25	1.33	0.71	0.33	0.03	0.61	0.07	0.07	0.21
6	0.13	0.67	0.25	1.38	0.65	0.34	0.05	0.59	0.12	0.05	0.18
7	0.42	0.52	0.35	0.64	0.76	0.03	0.07	0.59	0.12	0.09	0.14
8	0.43	0.47	0.33	1.52	0.48	0.00	0.11	0.43	0.22	0.13	0.11
9	0.20	1.37	0.17	1.22	0.40	0.08	0.07	0.57	0.15	0.09	0.12
10	0.34	1.04	0.41	1.12	0.73	0.05	0.07	0.58	0.14	0.09	0.12
11	0.35	0.94	0.40	0.96	0.74	0.05	0.07	0.58	0.14	0.09	0.11
12	0.26	1.45	0.32	1.55	0.56	0.09	0.04	0.64	0.11	0.07	0.14
14	0.22	0.93	0.29	1.28	0.61	0.20	0.03	0.62	0.11	0.05	0.19
15	0.38	0.40	0.59	0.64	0.86	0.11					
17	0.29	1.01	0.23	1.01	0.46	0.09					
18	0.27	1.07	0.16	1.06	0.48	0.09					
19	0.27	1.00	0.22	1.07	0.46	0.10					
20	0.28	0.98	0.13	1.05	0.45	0.07					
21	0.28	1.00	0.23	0.99	0.55	0.12					
22	0.26	0.98	0.17	1.06	0.48	0.07					
23	0.27	1.05	0.25	1.01	0.57	0.11					
24	0.26	1.00	0.21	1.00	0.48	0.09					
25	0.25	0.94	0.21	1.10	0.67	0.09					
26	0.27	1.09	0.20	0.96	0.51	0.08					
X1	0.17	1.19	0.20	1.13	0.42	0.09					
W2	0.52	0.71	0.32	0.68	0.79	0.07	0.14	0.53	0.07	0.19	0.07
V1	0.32	0.67	0.29	1.12	0.58	0.11					
V2	0.33	0.74	0.28	1.07	0.61	0.11					

Diasteranes/(diasteranes+regular steranes): *C27 diasterane/C27(diasteranes+regular steranes);* ***Gammacerane index****: C30 gammacerane/C30 hopane;* ***C1****: 2,2-dimethylpentane/ (2,2-dimethylpentane+2,3-dimethylpentane+2,4-dimethylpentane+3,3-dimethylpentane+3-ethylpentane);* ***C2****: 2,3-dimethylpentane/(2,2-dimethylpentane+2,3-dimethylpentane+2,4-dimethylpentane+3,3-dimethylpentane+3-ethylpentane);* ***C3****:2,4-dimethylpentane/(2,2-dimethylpentane+2,3-dimethylpentane+2,4-dimethylpentane+3,3-dimethylpentane+3-ethylpentane);* ***C4****: 3,3-dimethylpentane/(2,2-dimethylpentane+2,3-dimethylpentane+2,4-dimethylpentane+3,3-dimethylpentane+3-ethylpentane);* ***C5****: 3-ethylpenatne/(2,2-dimethylpentane+2,3-dimethylpentane+2,4-dimethylpentane+3,3-dimethylpentane+3-ethylpentane)*

5.2.3.1.2 C35/C34 Homohopanes

Clark and Philp (1989) showed that high ratios of the C35 to C34 homohopanes (~1) often are associated with oils sourced by carbonates. High values are seen in the oil samples 3, 4, 5, 6, 14 (northwestern Cuba), 9, 10, 11, and 12 (central Cuba), as well as in the extract samples from southern Cuba (samples 17-24, 26, and X1) and Jamaica (V1 and V2), which have values of 0.96 to 1.37, further indicating that these oils are derived from carbonate source rocks. Values greater than 1 are also reported by Peters and Moldowan (1991) to be typical for oils derived from source rocks deposited under anoxic conditions, suggesting that the carbonate derived oils were deposited under anoxic conditions. Samples 1, 2, 7 (northwestern Cuba), and 15 (southern Cuba) have values ranging from 0.64 to 0.79 (Table 10), indicating that the associated source rocks were deposited under oxic to dysoxic conditions (Peters and Moldowan, 1991). This correlates well with interpretation of the relatively high concentrations of diasteranes compared to regular steranes, indicating deposition under oxic conditions.

5.2.3.1.3 C24/C23 Tricyclic Terpanes

Low values of the C24/C23 tricyclic terpanes ratio are indicative of carbonate derived oils, whereas higher values are typical for oils originating from clastic source rocks (Waples and Machihara, 1991). In Figure 35, the C24/C23 tricyclic terpanes ratio is cross-plotted versus the C35/C34 homohopanes ratio, showing two different cluster of samples. A first cluster includes the oil samples 3, 4, 5, 6, 14 (northwestern Cuba), 9, 10, 11, 12 (central Cuba), as well as the extract samples X1, 17-24 and 26 (southern Cuba). These samples show the lowest values of the C24/C23 tricyclic terpanes ratio and the highest for the C35/C34 homohopanes ratio, indicating that these oils are derived from carbonate-rich source rocks deposited under anoxic conditions. The second cluster show relatively higher values of the C24/C23 tricyclic terpanes ratio and lower values of the C35/C34 homohopanes ratio, suggesting that these oils originate from shaly source rocks deposited under dysoxic to oxic conditions.

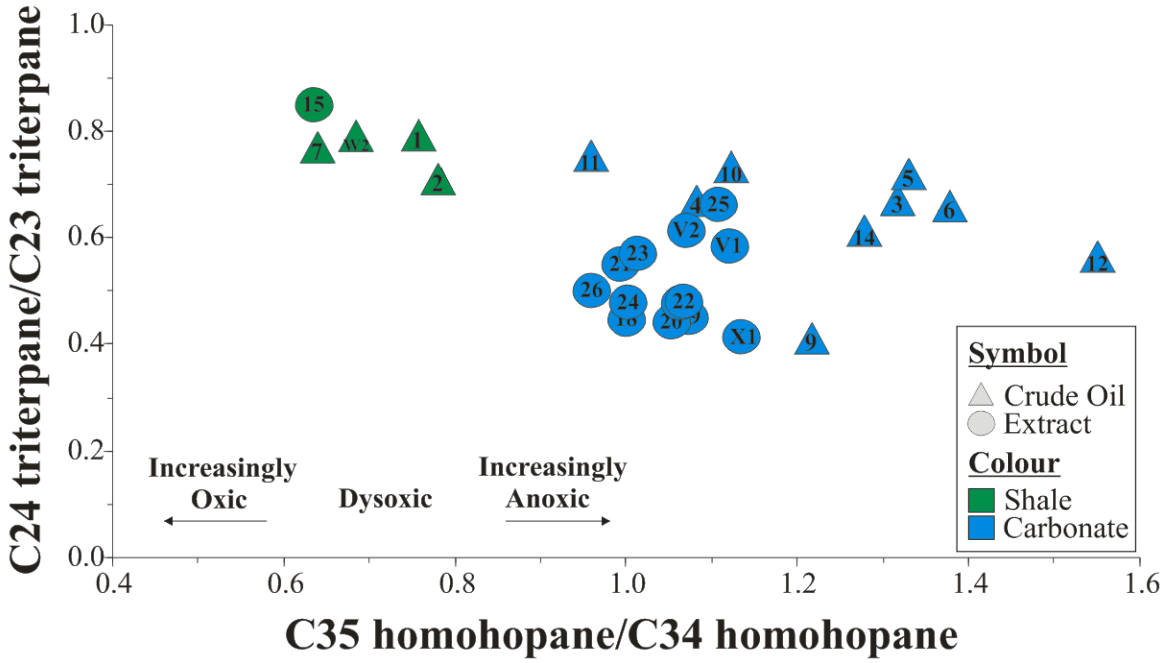

Figure 35 *The C24/C23 tricyclic terpanes ratio plotted against the C35/C34 homohopanes ratio in a cross-plot. The samples can be group into two groups; carbonate derived oils, deposited under anoxic conditions, and oils originating from shales deposited under oxic to dysoxic conditions in accordance to Waples and Machihara (1991), and Peters and Moldowan (1991) .*

5.2.3.1.4 C29/C30 Hopanes and C30 Diahopane/C30 Moretane

In Figure 36, the C29/C30 hopanes ratio is compared to the C30 diahopane/C30 moretane ratio in an attempt to further differentiate the lithology between the sources generating the different oils. High values of C30 diahopane/C30 hopane ratio are indicative of clastic input (Peters and Moldowan, 1993), whereas high values of the C29/C30 hopanes ratio are indicative of more carbonate input (Zumberge, 1987, Mello et al., 1988a, Clark and Philp, 1989). Samples 1, 2, 7 (northwestern Cuba), and 15 (southern Cuba) show high values of the C30 diahopane/C30 moretane, as well as low values of the C29/C30 hopanes further indicating these oils were derived from clastic source rocks. The extracts from southern Cuba (samples 17-24 and 26 and X1), as well as the oil samples 9, 10, 11, 12 (central Cuba), and 14 (northwestern Cuba) have low values of the C30 diahopane/C30 hopane ratio and high values of the C29/C30 hopanes, which suggests that these oils originate from carbonate source rocks, coinciding with the previous interpretations (Figure 35). Sample 14 in northwestern Cuba has a distinctive smell of sulphur which favour this interpretation as carbonate derived oils often show elevated sulphur concentrations.

Samples 3, 4, 5, 6 (northwestern Cuba), W2, V1, and V2 (Jamaica) plot in between the interpreted carbonate and clastic derived oils. This suggests that the oils were generated by a shaly carbonate. Sample W2 has, however, previously been suggested to originate from a clastic source rock. As will later be discussed in the organofacies chapter (Chapter 5.2.4) sample W2 shows terrestrial enrichment in the organofacies. This could explain the relatively high values of the C29/C30 hopanes, as oils derived from source rocks consisting of terrestrial organic matter can give high values of C29/C30 hopanes (Ramanampisoa et al., 1990).

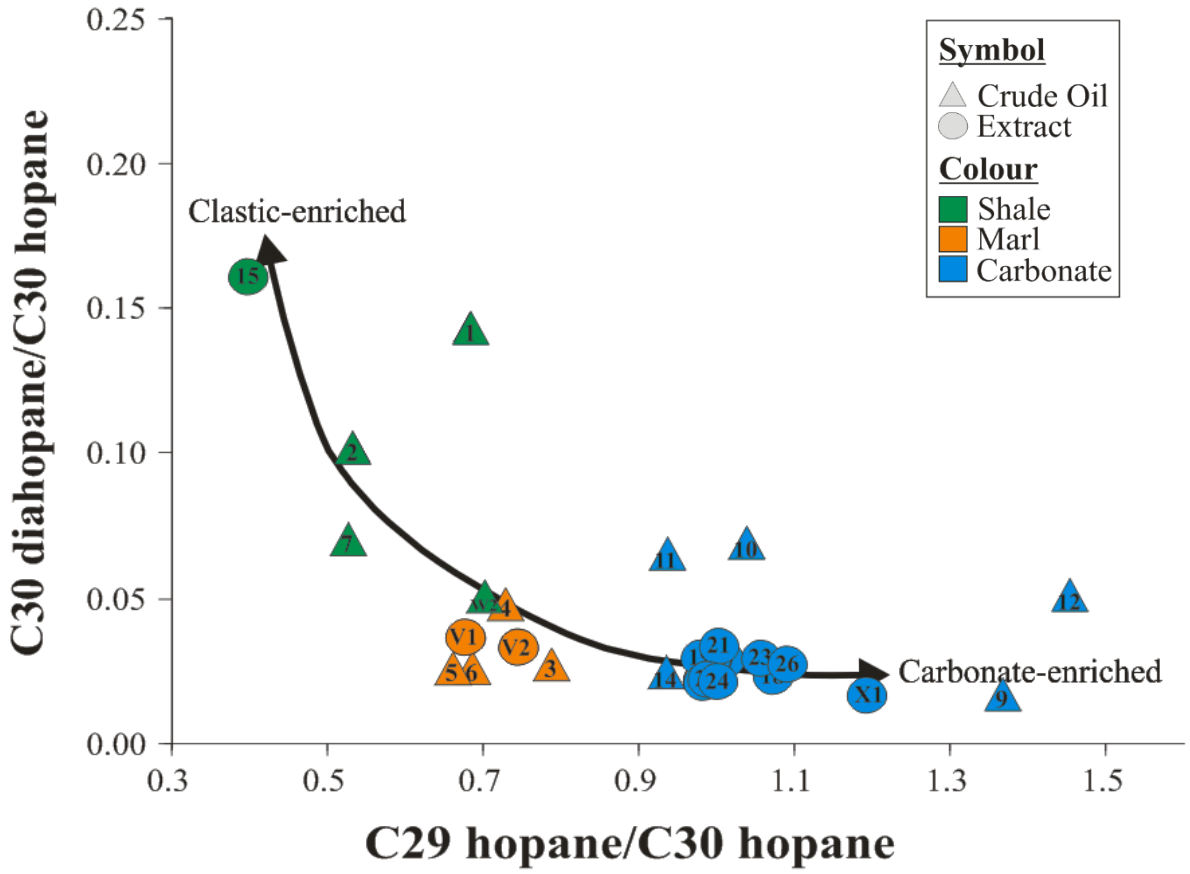

Figure 36 *Cross-plot of the C29/C30 hopanes ratio against the C30 diahopane/C30 hopane separating the samples according to lithofacies of the source rocks generating the oils; carbonates, marls, and shales. The shale derived oil sample W2 plot with values similar as the oils derived from marly source rocks. This could be due to high content of terrestrial input (Ramanampisoa et al., 1990).*

5.2.3.1.5 Gammacerane Index

High content of this compound is commonly associated with a reducing and hypersaline depositional environment of the source rock (Moldowan et al., 1985). However, all the samples have low values ranging from 0.03 to 0.25, which indicates the source rocks were deposited under normal saline conditions.

5.2.3.1.6 Distribution

The interpreted lithofacies are shown in Figure 37 and Figure 38. The oil samples in central and southern Cuba are, essentially, interpreted to originate from carbonates. Sample 15 in the south plot, however, as an outlier with the interpreted shaly source. The "outlier characteristics" of this sample will be discussed in a later chapter (Chapter 5.2.7). The oils from northwestern Cuba appear to come from source rocks of various lithofacies (Figure 37). In Jamaica, the samples V1 and V2 are suggested to derive from marly source rocks, whereas sample W2 appear to originate from a shaly source rock (Figure 38).

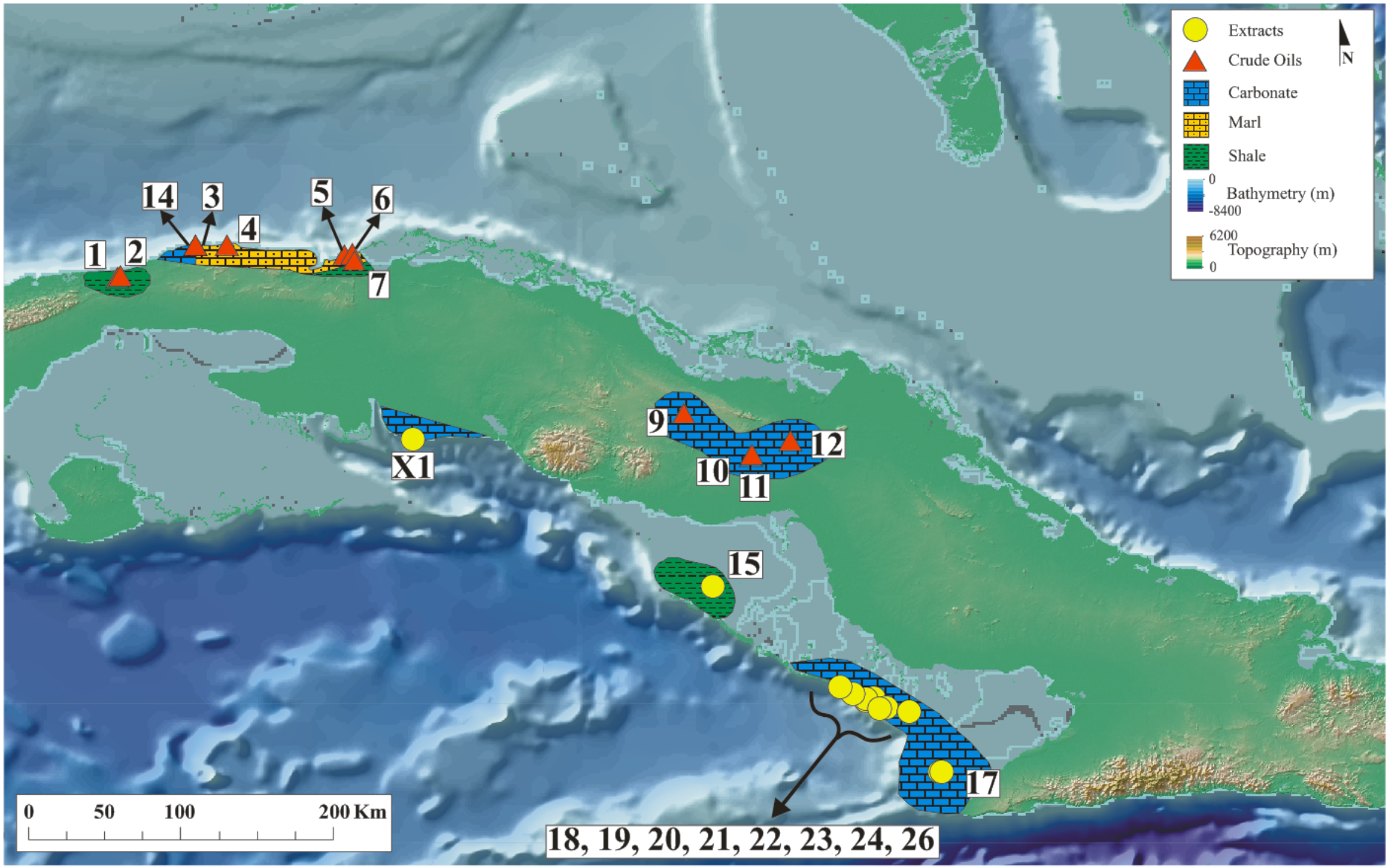

Figure 37 *Map of Cuba illustrating the interpreted lithofacies of the source rocks generating the oils. The samples in the southern and central Cuba show to, generally, be derived from carbonates, whereas the oils in northwestern Cuba show to originate from a mix of carbonate, shales, and marls.*

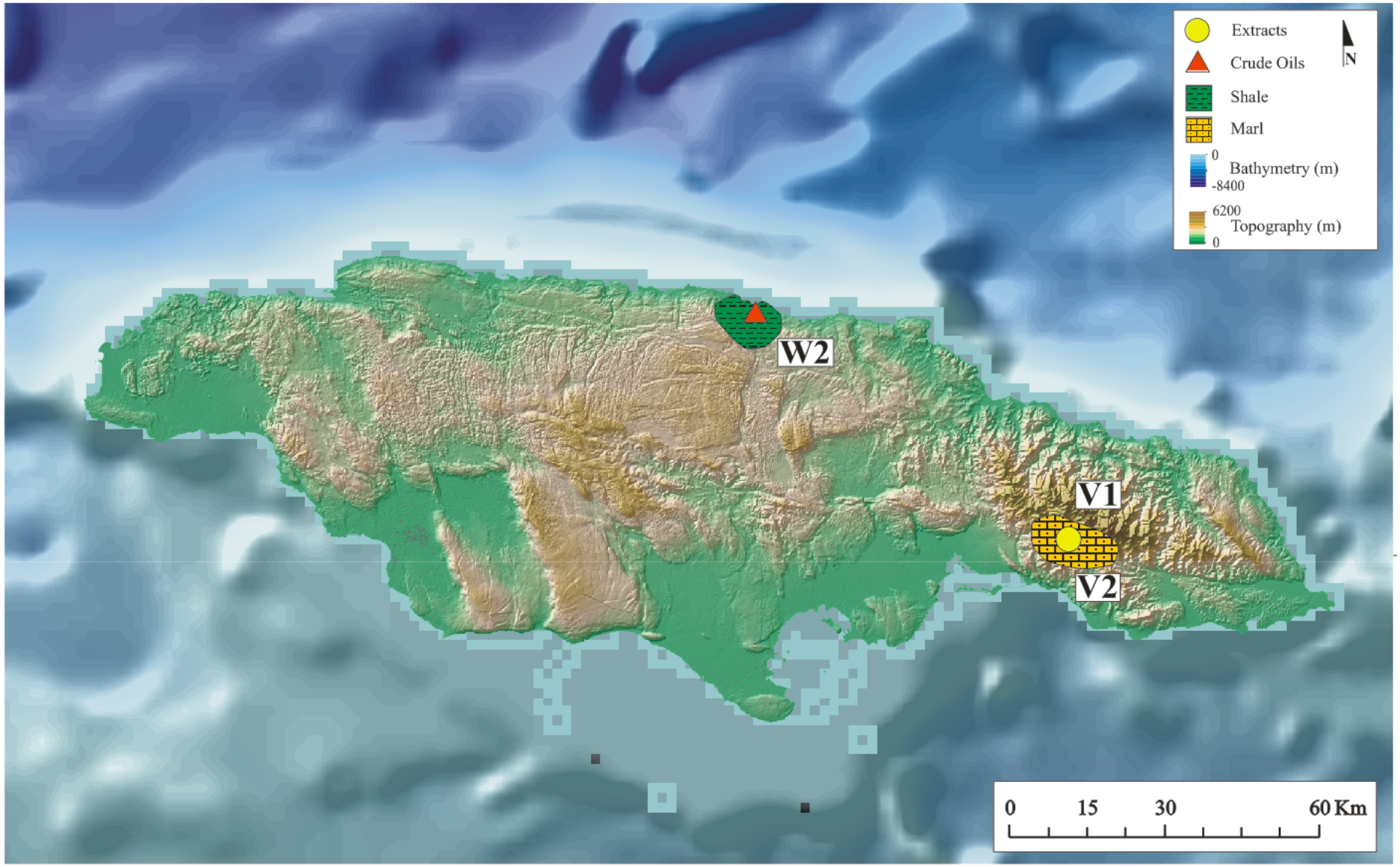

Figure 38 *Interpretations of the lithofacies of the source rocks generating the oils in Jamaica. The oil sample W2 is derived from a shaly source rock, whereas the samples V1 and V2 originate from marls.*

5.2.3.2 Light Oil Fraction

5.2.3.2.1 Correlation Star-diagram (C7-OSCD)

The correlation star-diagrams of Halpern (1995) use compounds that are least affected by biodegradation in the light oil fraction. The star-diagram relates the light oil fraction to the oils source-related origin. If the different oils originate from the same or a similar source rock, the oils will have an identical or similar trend in the star-diagram. The correlation ratios C2 and C5 can be used to differentiate carbonate from more clastic derived oils, where higher values of the two ratios would indicate the oil originate from a more calcareous source rock (Halpern, 1995).

Two different patterns can be identified in Figure 39 A. Samples 5, 6, and 14 (northwestern Cuba) in Figure 39 B display higher values of C5 relative to the other samples (samples 7, 9, 10, 11, and 12) (northwestern and central Cuba) in Figure 40 A. This indicates that the light oil fraction from these samples originates from a carbonate source rock, whereas samples 7 (northwestern Cuba), 9, 10, 11, and 12 (central Cuba) have a clastic origin, plausibly shales. The light oil fraction of the remaining samples (samples 1, 2, 4, 8 (northwestern Cuba) and W2 (Jamaica)) do not follow any of the two previously described patterns (Figure 40 B), which may suggest that the light fraction of these oils represent mixtures of light fractions from different source rocks.

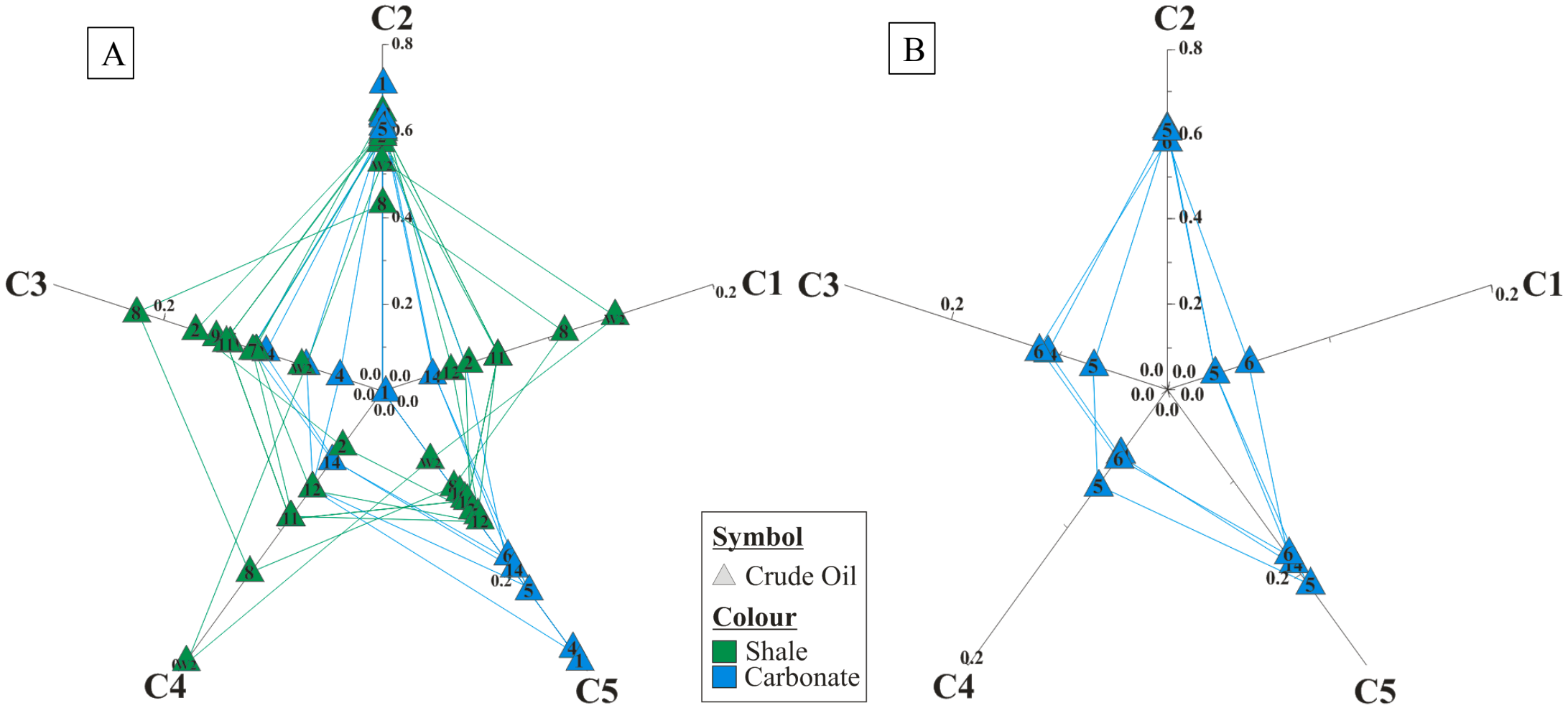

Figure 39 A *Correlation (C) star-diagram (Halpern, 1995) illustrating the lithofacies correlation of the light oil fraction, where some similarities can be observed.* ***B*** *the carbonate derived oil samples 5, 6, and 14 show similar patterns in the correlation star-diagram.*

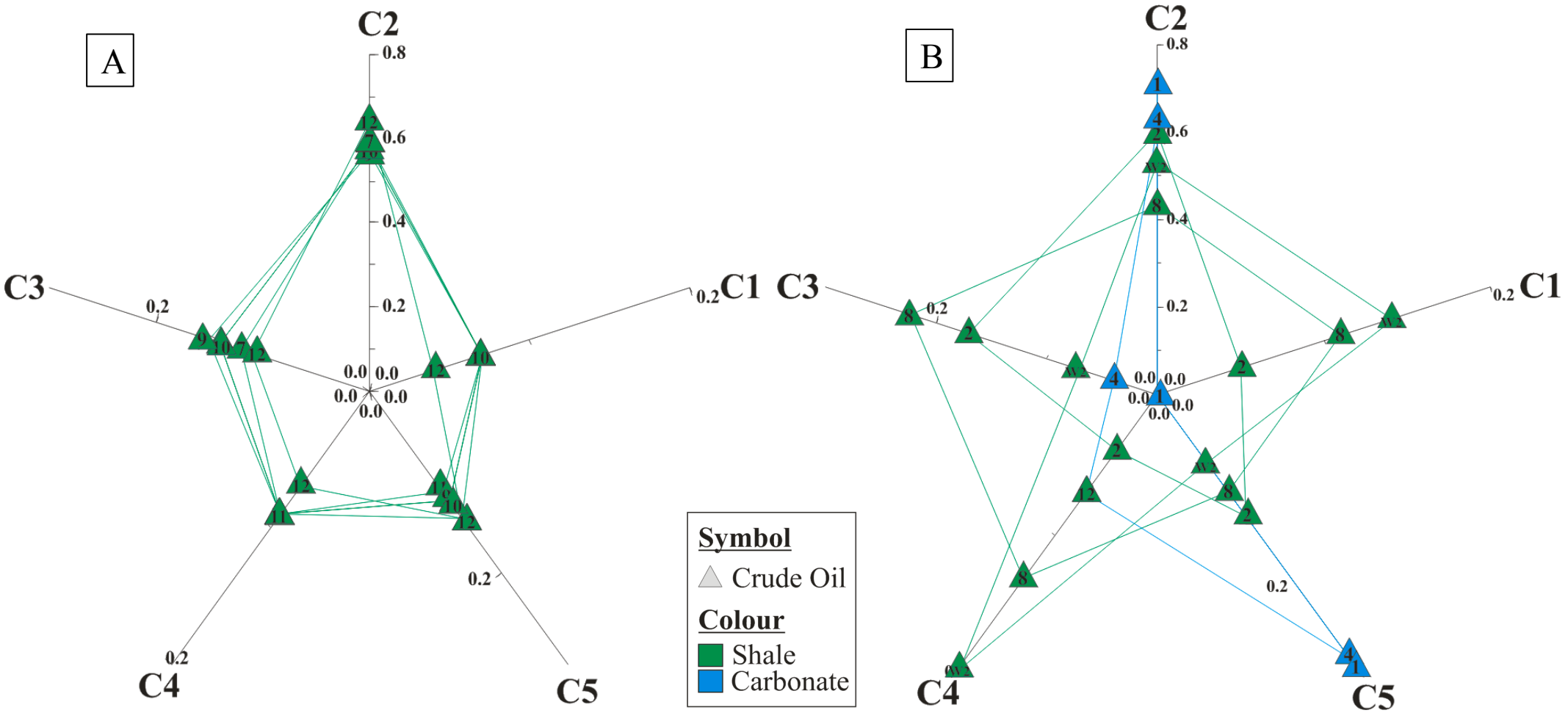

Figure 40 A *correlation star-diagram with shale derived samples 7, 9, 10, 11, and 12 show similar patterns.* ***B*** *the remaining samples 1, 2, 4, 8, and W2, which does not correlate with the two previous patterns in Figure 39B and Figure 40A.*

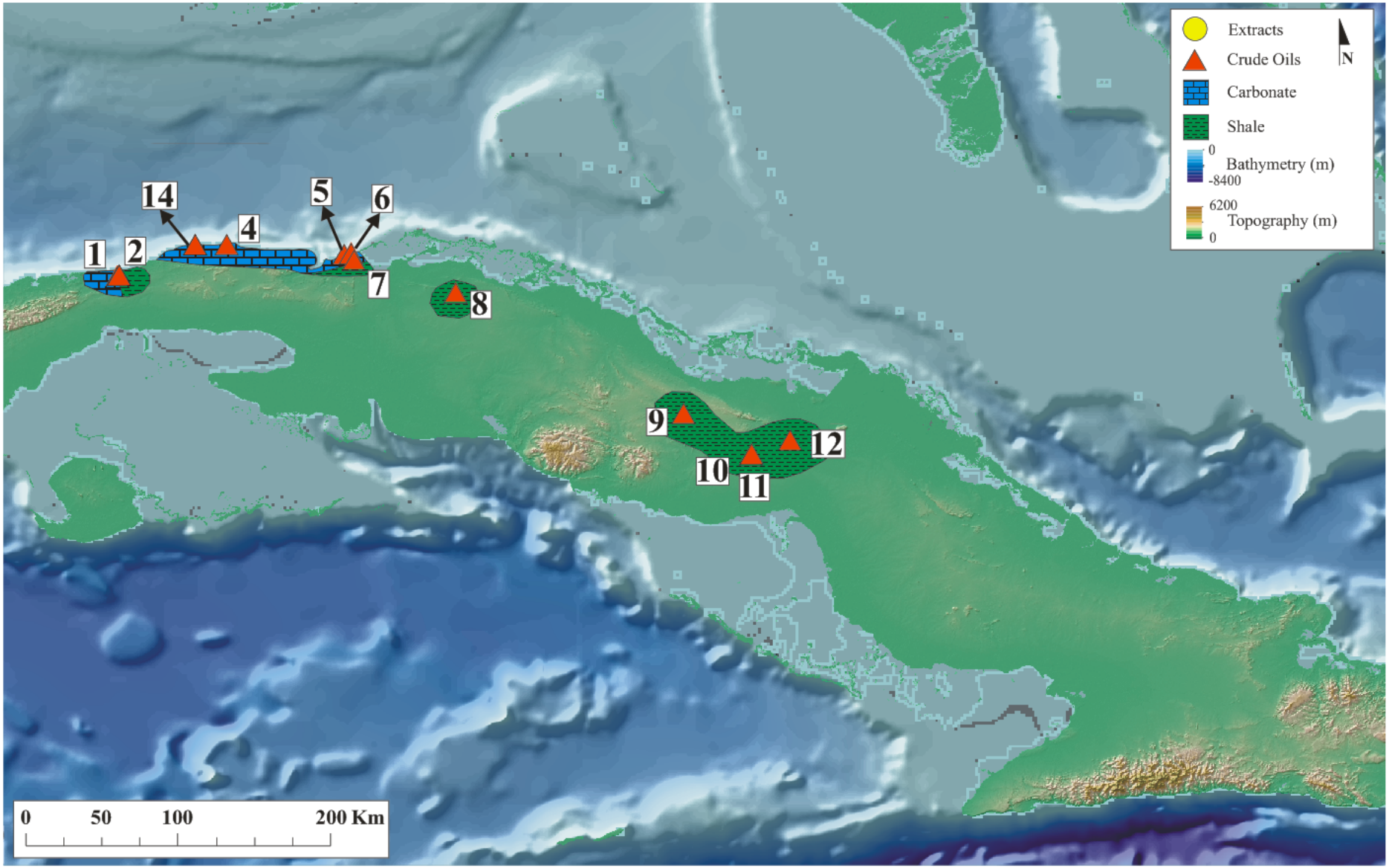

Figure 41 *The lithofacies interpretation of the light oil fraction. The crude oil samples in central Cuba show to originate from shaly source rocks, whereas the samples in northwestern Cuba are, generally, derived from carbonates.*

5.2.4 Organofacies

5.2.4.1 Heavy Oil Fraction

5.2.4.1.1 C19-C21 Tricyclic Terpanes

In general, the samples have low concentrations of the C19, C20, and C21 tricyclic terpanes, which is in accordance with early to mid-mature oils. An increasing trend in the height of the peaks from C19 to C21 is, however, observed for most of the samples (exemplified in Figure 42 by sample 14). This suggest marine organofacies for the source rocks generating these oils (Peters et al., 2005). The exception is the crude oil sample W2 (Jamaica) where the peaks have the same height (Figure 43), indicating the oil derived from a source rock influenced by more terrestrial input relative to the other samples.

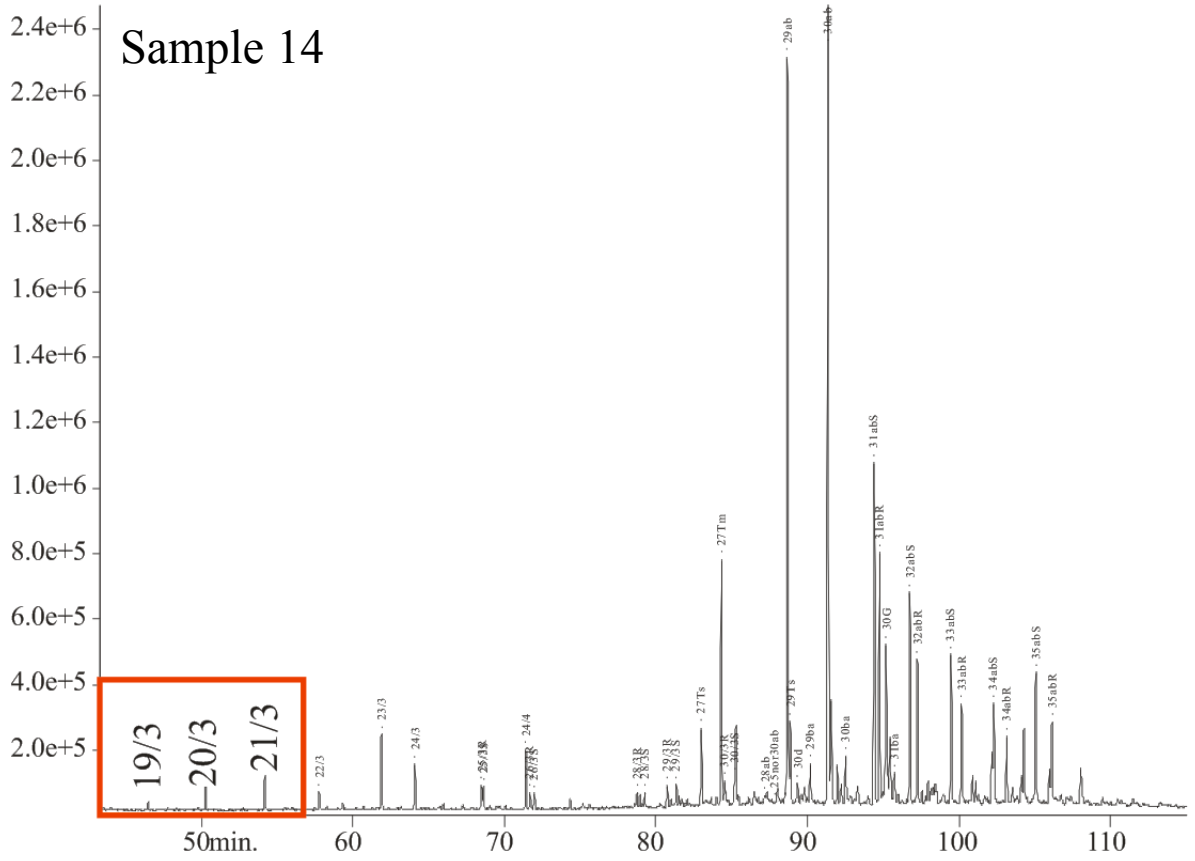

Figure 42 *GC-MS (m/z 191) of sample 14 representing the general trend of increasing peak height from C19 to C21 tricyclic terpanes for majority of the samples, suggesting marine organofacies.*

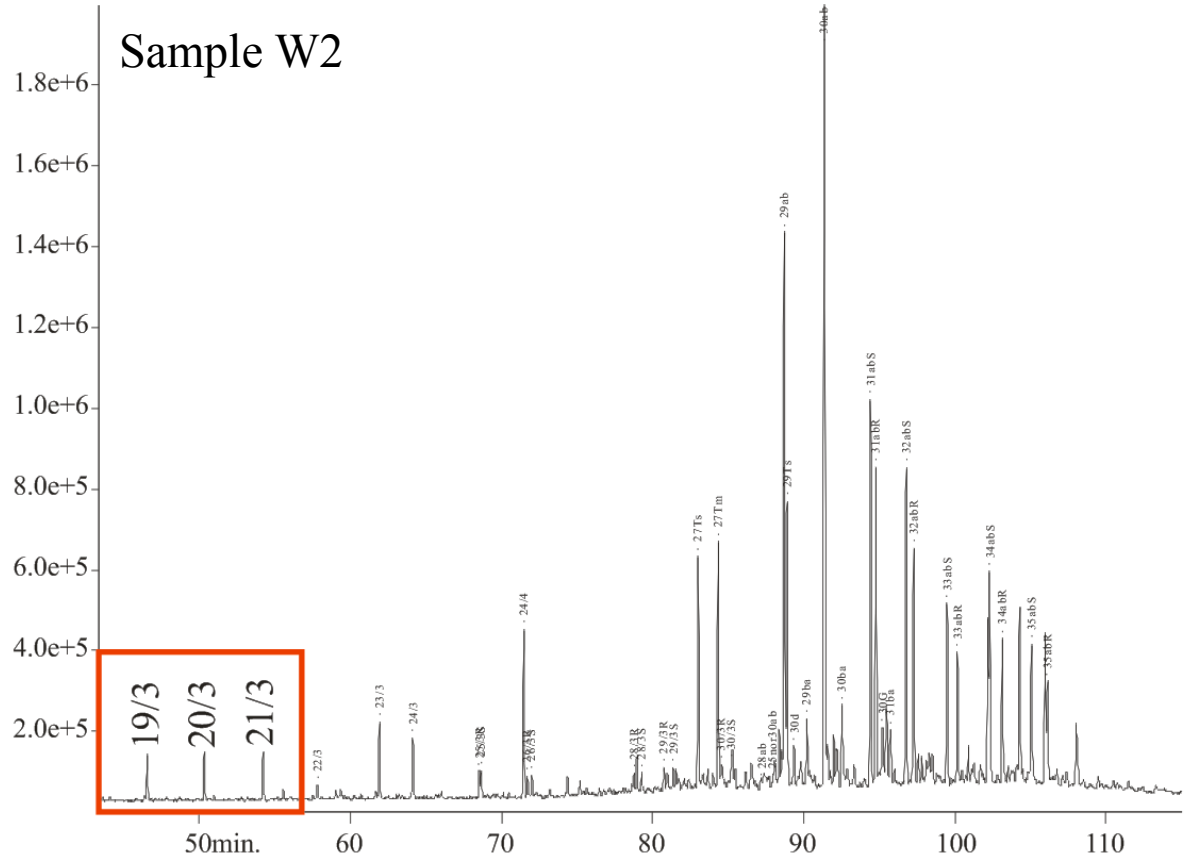

Figure 43 *GC-MS (m/z 191) of sample W2 showing the same peak height for the C19-21 tricyclic terpanes, indicating the sample W2 originate from a source rock influenced by more terrestrial input compared to the other samples (exemplified by sample 14 in Figure 42).*

5.2.4.1.2C19/C23 Tricyclic

The C19 tricyclic terpane is mainly derived from higher plants, whereas the C23 tricyclic terpane is predominantly derived from algal and bacterial organic matter (Simoneit, 1977, Alberdi-Genolet and Tocco, 1999). Thus, high values of the ratio indicate oils derived from source rocks containing significant amounts of land plants-derived organic matter, whereas oils derived from algal organic material show low values. All the extract and crude oil samples, except sample W2 from Jamaica, have low values of the C19/C23 (0.01 to 0.3) (Table 11), suggesting that the source rocks that generated the oils are dominated by marine organic material. The sample W2 (Jamaica), however, has a value of 0.6 (Table 11), which indicates that this oil originated from a more terrigenous dominating source rock.

Table 11 *Biomarker ratios used to assess the organofacies of the source rocks generating the analysed oils. The Cuban sample names are coloured in blue and the Jamaican sample names are coloured in green.* ***TT****: Tricyclic terpanes;* ***%C30 diasteranes****: 24-propyldiacholestane ratio* ***δ ARO:*** *Aromatic isotope fraction;* ***δ SAT****: Saturate isotope fraction;* ***TPP****: Tetracyclic polyprenoid ratio;* ***H****: Heptane value;* ***I****: Isoheptane value.*

Sample	Heavy Fraction							Whole Oil		Light Fraction	
	C19/C23 TT	C30 sterane index	ββ-Steranes			TPP	%C30 Diasteranes	δ ARO	δ SAT	H	I
			%C27	%C28	%C29						
1	0.27	5.71	31.43	27.03	41.54			-28.1	-26.6	20.04	1.16
2	0.21	5.69	32.39	25.07	42.55	0.27	2.5	-28.4	-27.1	15.66	0.78
3	0.14	7.31	40.40	28.29	31.31			-27.3	-26.9		
4	0.18	7.05	39.63	26.97	33.40			-27.1	-26.2	20.9	1.36
5	0.12	9.59	48.27	24.36	27.37			-26.8	-25.9	5.93	0.93
6	0.12	8.79	48.10	24.84	27.06			-27.2	-26	9.02	1.32
7	0.22	6.18	29.53	27.15	43.32			-28.6	-28.1	9.09	0.77
8										19.24	2.18
9	0.16	7.26	34.34	25.97	39.70			-27.7	-27.3	17.81	1.63
10	0.27	5.40	31.57	27.92	40.51			-27.6	-27	6.98	1.27
11	0.30	5.50	32.55	27.33	40.11			-27.8	-27	22.89	2.1
12	0.28	5.72	32.97	28.84	38.19	0.19	2.42	-27.4	-27.5	28.9	2.81
13								-26.2	-25.9		
14	0.11	8.02	46.54	25.51	27.95			-26.9	-26	36.15	3.14
15	0.19	21.96	28.88	24.41	46.71						
16								-27.2	-26.9		
17	0.09	10.31	31.19	22.72	46.09						
18	0.07	9.86	32.12	22.71	45.17						
19	0.07	10.00	31.31	22.75	45.94						
20	0.09	8.97	32.53	23.59	43.88						
21	0.07	9.58	32.39	23.27	44.34						
22	0.09	8.92	32.18	22.02	45.80						
23	0.09	10.26	30.23	22.91	46.85						
24	0.06	9.57	32.39	22.83	44.78						
26	0.09	9.64	32.43	22.88	44.69						
X1	0.03	11.15	24.84	23.96	51.20			-28.9	-27.5		
Y1								-26.9	-25.8		
A1								-28.6	-27		
A2								-26.7	-25.3		
A3								-26.9	-25.6		
C1			22.05	22.49	55.46			-27.7	-26.9		

W2	0.60	6.77	33.76	21.04	45.20	0.35	2.30	-25.2	-23.7	3.76	0.39
D2			28.57	19.13	52.30			-28.4	-27.3		
V1	0.01	12.07	29.08	18.66	52.25	0.31	6.70	-27.9	-27.6		
V2	0.01	12.60						-27.9	-27.7		
P1								-25.7	-25.8		

C30 sterane index: *100*C30/C27-30 regular steranes;* ***%C27:****100*C27ββ/(C27ββ+C28ββ+C29ββ);* ***%C28:*** *100*C28/(C27ββ+C28ββ+C29ββ);* ***%C29:*** *100*C29ββ/(C27ββ+C28ββ+C29ββ);* ***TPP:*** *2*C30 tetracyclic polyprenoid-R/(2*tetracyclic polyprenoid-R+C26 27-norcholestanes);* ***%C30 diasteranes:*** *C30/C27-C30 ββ-diasteranes.*

5.2.4.1.3 C30 Sterane Index

The C30 sterane originate from 24-*n*-propylcholesterols which are common in marine invertebrates (Raederstorff and Rohmer, 1984) and is a good indicator for marine algal input to the source rocks (Moldowan et al., 1985, Peters et al., 1986). Thus, the presence of C30 steranes in all the samples imply various contributions of marine algae (Table 11). The C30 steranes index (C30/C27-30) was plotted against the C19/C23 tricyclic ratio in Figure 44. The Figure clearly shows the expected inverse correlation.

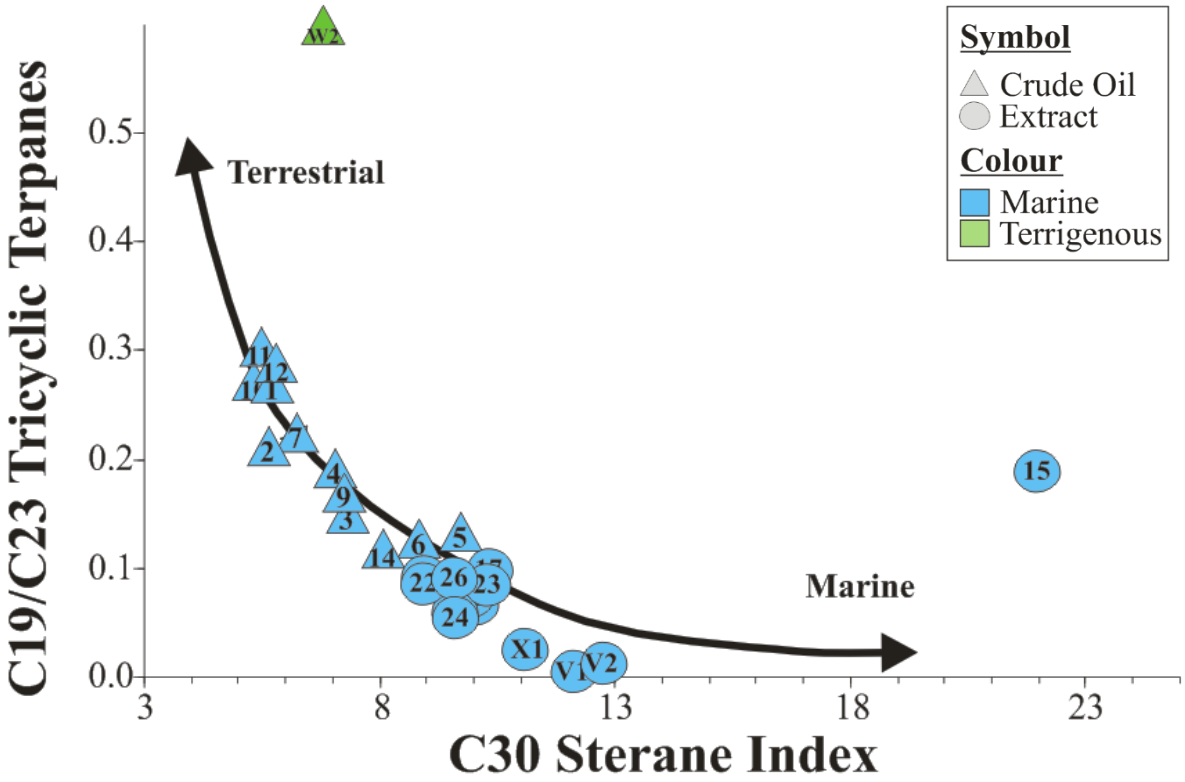

Figure 44 *The C30 sterane index is plotted against the C19/C23 tricyclic terpanes ratio illustrating the organofacies of the source rocks generating the oils. Most of the oils show to be derived from source rocks influenced by marine organic material, whereas the sample W2 plot to be more influenced by terrestrial input.*

5.2.4.1.4 Tetracyclic Polyprenoid Ratio and 24-Propyldiacholestane Ratio

As mentioned in the methodology chapter (Chapter 3.3), four oil samples were chosen to represent different areas in Cuba and Jamaica for GC-MSMS. Sample 2 from northwest Cuba, sample 12 from central Cuba, and V1 and W2 from Jamaica.

The C30 tetracyclic polyprenoid (TPP) is common in lacustrine environments. However, they are also found in marine environments. In the tetracyclic polyprenoid ratio (TPP: 2*C30 tetracyclic polyprenoid-R/(2*tetracyclic polyprenoid-R+C26 27-norcholestanes), the C30 TPP is compared to the C26 27-norcholestanes, as the C26 27-norcholestanes is common in marine systems and occurs with low concentrations in none-marine systems (Holba et al., 2000). When comparing the TPP ratio to the 24-propyldiacholestane ratio (%C30 diasteranes: C30/C27-C30 ββ-diasteranes), which is the most consistent indicator of marine algal input (Moldowan et al., 1990), the oils can be differentiated between marine, lacustrine, and mixed marine-lacustrine oils. In Figure 45, the samples 2 (northwest Cuba) and 12 (central Cuba), and sample V1 show to be mainly influenced by marine organic material. In contrast, sample W2 plot with values indicating that this oil is a mixture of marine and non-marine organic material.

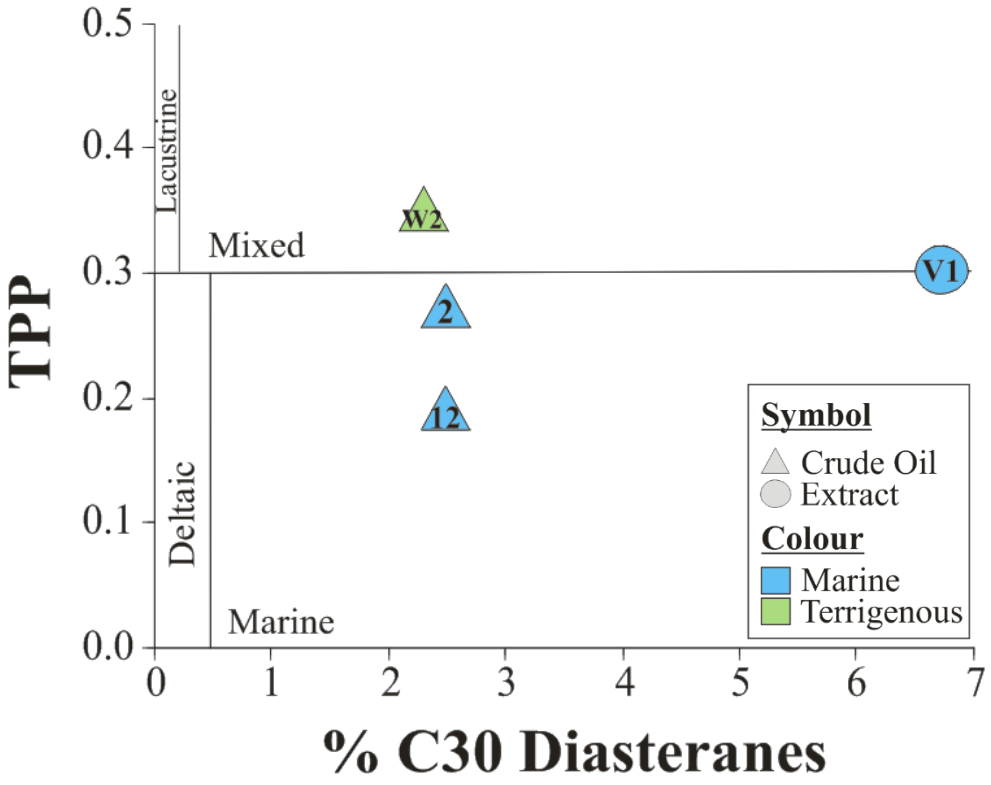

Figure 45 *Illustration of the organofacies of the source rock deriving the oils based on the cross-plot of tetracyclic polyprenoid ratio (TPP) against 24-Propyldiacholestane ratio (%C30 diasteranes) ((Holba et al., 2000)). The source rocks generating the oil samples 2 (northwest Cuba), 12 (central Cuba), and V1 (Jamaica) show to be influenced by marine organic material, whereas sample W2 is suggested to originate from a mixed source rock.*

5.2.4.1.5 %C27 %C28 %C29

The relative percentage of the C27%, C28%, and C29% steranes can help to distinguish between depositional settings. Only samples 3, 4, 5, 6, and 14 from northwest Cuba have a relatively higher percentage of C27, ranging from 40 to 48% (Table 11). The C27 steranes is dominant in most planktons (Grantham and Wakefield, 1988) and is therefore a good indicator of marine contribution. The remaining samples have relatively higher percentages of the C29, ranging from 38 to 52% (Table 11). In almost all higher plants, the C29 is a dominant sterol (Huang and Meinschein, 1979, Czochanska et al., 1988). Thus, it is tempting to suggest that these oils were generated from source rocks containing mainly higher plants, which contradicts previous interpretations. However, this sterol is also known to be synthetized by brown and green algae (Grantham and Wakefield, 1988), which may explain the relatively higher percentage of C29.

5.2.4.1.6 Aromatic and Saturate Isotope Fractions

The saturated and aromatic hydrocarbon fractions from purely marine kerogen is suggested to differ less in terms of $\delta^{13}C$ values than oils derived from terrigenous kerogen (Sofer, 1984). When plotting the carbon isotope values of the saturated and aromatic hydrocarbons of the oils according to Sofer (1984), all the oils plot as influenced by marine derived organic material (Figure 31). This further suggest that the relatively higher percentages of the C29 steranes (Table 11) could be due to high content of green and brown algae. The W2 oil from Jamaica suggested by the biomarkers to be influenced by terrigenous organic material is, however, suggested to have a marine source by the isotope values of the saturated and aromatic fractions. This could be a result of the biomarkers only representing a small part of the oil, whereas the isotopic fractions represent the whole oil.

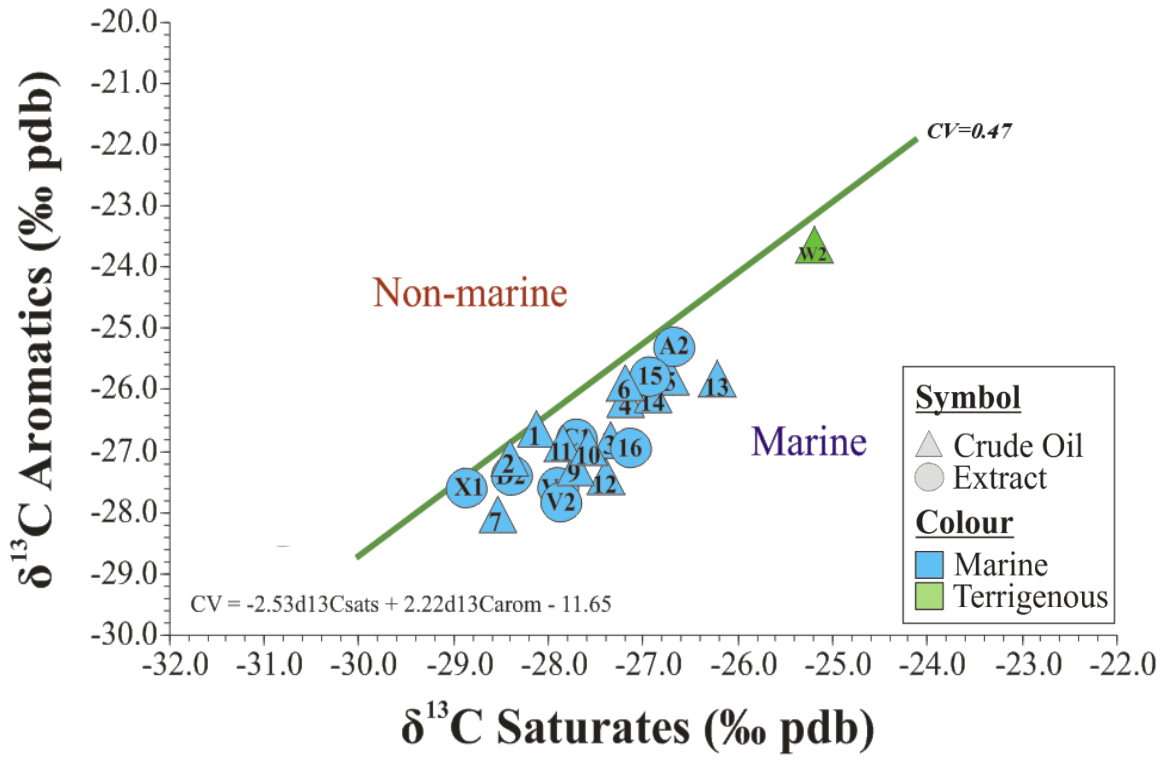

Figure 46 *Cross-plot of the aromatic isotope fraction against the saturate isotope fraction. According to Sofer (1984) all the samples plot as marine derived. This differ from previous interpretations of sample W2 (Figure 44 and Figure 45). However, the isotope fractions represent the whole oil, whereas the biomarkers only represent a small part of the oil.*

5.2.4.2 Light Oil Fraction

5.2.4.2.1 Thompson H-I Diagram

The Heptane (H) and Isoheptane (I) values can be used to differentiate between kerogen types II and III, as the H and I values for oil samples that have experienced identical catagenetic histories differ slightly according to the kerogen type (Thompson, 1983). In the H-I plot (***Figure 47***), five of the oils samples (1, 2, 4, 14 (northwestern Cuba), and 12 (central Cuba)) are shown to originate from aliphatic source rocks of kerogen type II. Samples 9 and 11 from central Cuba show slightly higher content of aromatic organic matter, suggesting a mixture of kerogen types II and III. Additionally, the condensate sample (8) plots as an aromatic type III kerogen. These differences in kerogen types suggest that the source rocks generating the light fractions were deposited in different environments. The remaining samples (5, 6, 7 (northwestern Cuba), 10 (central Cuba), and W2 (Jamaica)) show anomalously low values, most likely resulting from biodegradation as previously discussed.

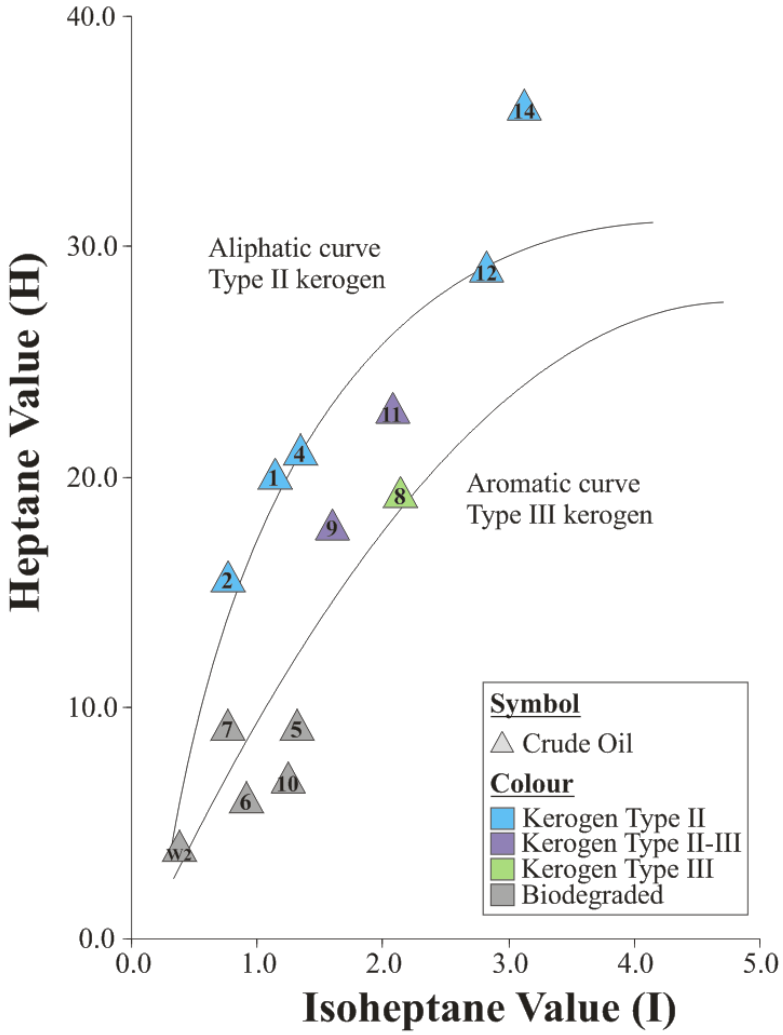

Figure 47 *cross-plot of the Heptane value against the Isoheptane value to determine kerogen type. The samples show to be derived from both the kerogen type II and III.*

5.2.5 Age of the Source Rocks Generating the Oils

5.2.5.1 Heavy Fraction

5.2.5.1.1 C28/C29 Steranes

The relative content of C28 steranes increases while C29 steranes decreases through geological time in marine petroleum (Moldowan et al., 1985, Grantham and Wakefield, 1988). Such behaviour is probably caused by the diversification of phytoplankton assemblages in the Jurassic and Cretaceous period (Peters et al., 2005). The C28/C29 steranes values (Table 12) was plotted in the Grantham and Wakefield plot (1988) (Figure 48). Crude oil samples 3, 4, 5, 6, 14 (northwestern Cuba), and 12 (central Cuba) plot as oils generated by Cretaceous aged source rocks. The crude oil samples 1, 2, 7 (northwestern Cuba), 9, 10, and 11 (central Cuba) are suggested to be derived from source rocks of Jurassic ages. The remaining extract samples from southern Cuba (samples 15, 17-24, 26, and X1), as well as the crude oil W2 and the extract samples V1 and V2 from Jamaica plot as Triassic and Carboniferous sourced oils. Rocks of this age are not present on Cuba and Jamaica, consequently the low ratios of these samples must have a different explanation. As was previously discussed in the organofacies chapter (Chapter 5.2.4.1.5), these samples could have been affected by high amounts of terrestrial or green and blue algal input as shown by high C29%. These oils, hence, most likely originated from Jurassic or younger aged source rocks.

5.2.5.1.2 Extended Tricyclic Terpanes

The extended tricyclic terpanes ratio (ETR) ((C28+C29 tricyclic terpanes)/Ts) can be used to distinguish Jurassic or younger aged source rocks (ETR<2) from Triassic or older source rocks (ETR>2) (Holba et al., 2001). The difference in ETR content between Triassic and Jurassic have been related to the increase in diatom bloom in connection to upwelling in the Triassic. In Figure 49, the ETR is plotted against the C28/C29 sterane ratio. Based on the ETR values, all the samples are suggested to be derived from Jurassic or younger aged source rocks. This substantiates the previous conclusion the low values of the C28/C29 sterane ratio for the extract samples as discussed in the previous section are a result of organofacies.

Table 12 *Biomarker ratios used to evaluate the age of the source rocks from which the oils originate.* ***Reg.Ster****: Regular Steranes;* ***ETR****: Extended tricyclic terpanes;* ***TA****: Triaromatic;* ***DMC****: Dimethylcholesteroids;* ***NDR****: Nordiacholestane.*

Samples	C28/C29 Reg.Ster.	ETR	TA-DMC	TA-Dinosteroids	NDR
1	0.65	0.44	0.08	0.64	
2	0.59	0.45	0.09	0.67	0.24
3	0.90	0.66	0.24	0.86	
4	0.81	0.60	0.12	0.83	
5	0.89	0.67	0.28	0.87	
6	0.92	0.67	0.28	0.87	
7	0.63	0.49	0.08	0.70	
8	0.71	0.63	0.20	0.71	
9	0.65	0.39	0.29	0.77	
10	0.69	0.44	0.08	0.67	
11	0.68	0.47	0.07	0.67	
12	0.76	0.44	0.08	0.69	0.18
14	0.91	0.57	0.27	0.87	
15	0.52	0.36	0.12	0.45	
17	0.49	0.37	0.13	0.82	
18	0.50	0.43	0.12	0.81	
19	0.50	0.36	0.15	0.86	
20	0.54	0.42	0.13	0.79	
21	0.52	0.43	0.16	0.84	
22	0.48	0.38	0.12	0.82	
23	0.49	0.45	0.15	0.82	
24	0.51	0.39	0.12	0.80	
26	0.76	0.83	0.14	0.80	
X1	0.51	0.41	0.12	0.79	
W2	0.47	0.29	0.07	0.68	0.17
V1	0.41	0.30	0.34	0.68	0.10
V2	0.37	0.55	0.01	0.19	

ETR: *(C28/C29 tricyclic terpanes)/Ts;* ***TA-DMC:*** *TA (23,24-dimethylcholesteroid/(23,24-dimethylcholesteroid+24-ethylcholesteroid 20S));* ***TA-Dinosteroids****: TA(dinosteroids 1-6)/(dinosteroids 1-6+4-methylstigmastanes);* ***NDR****:C26 (24/(24+27)nordiacholestanes.*

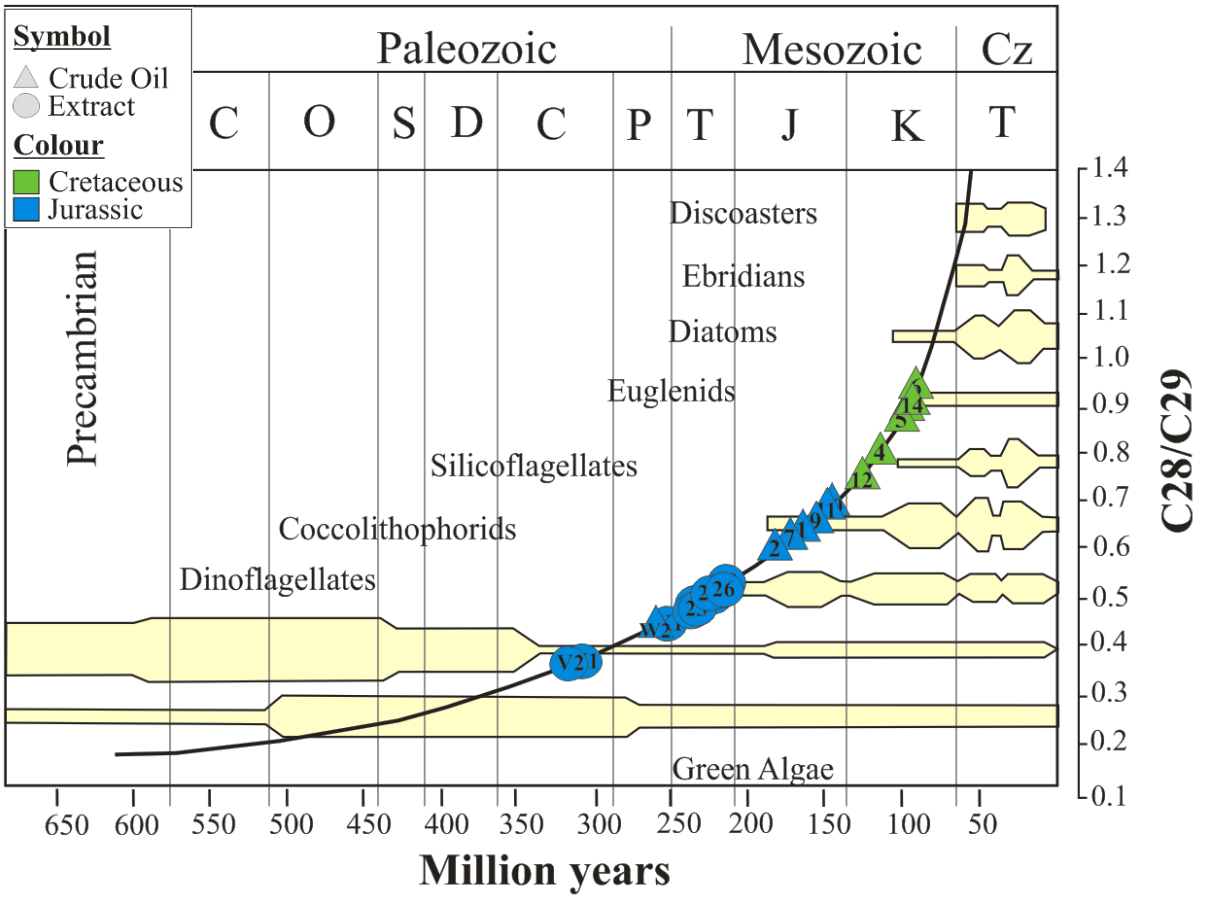

Figure 49 *Evaluation of the source rock age based on C28/C29 regular steranes (Grantham and Wakefield, 1988) indicating Carboniferous to Cretaceous ages for the samples. However, the samples which plot with Carboniferous and Triassic ages could be influenced by organofacies.*

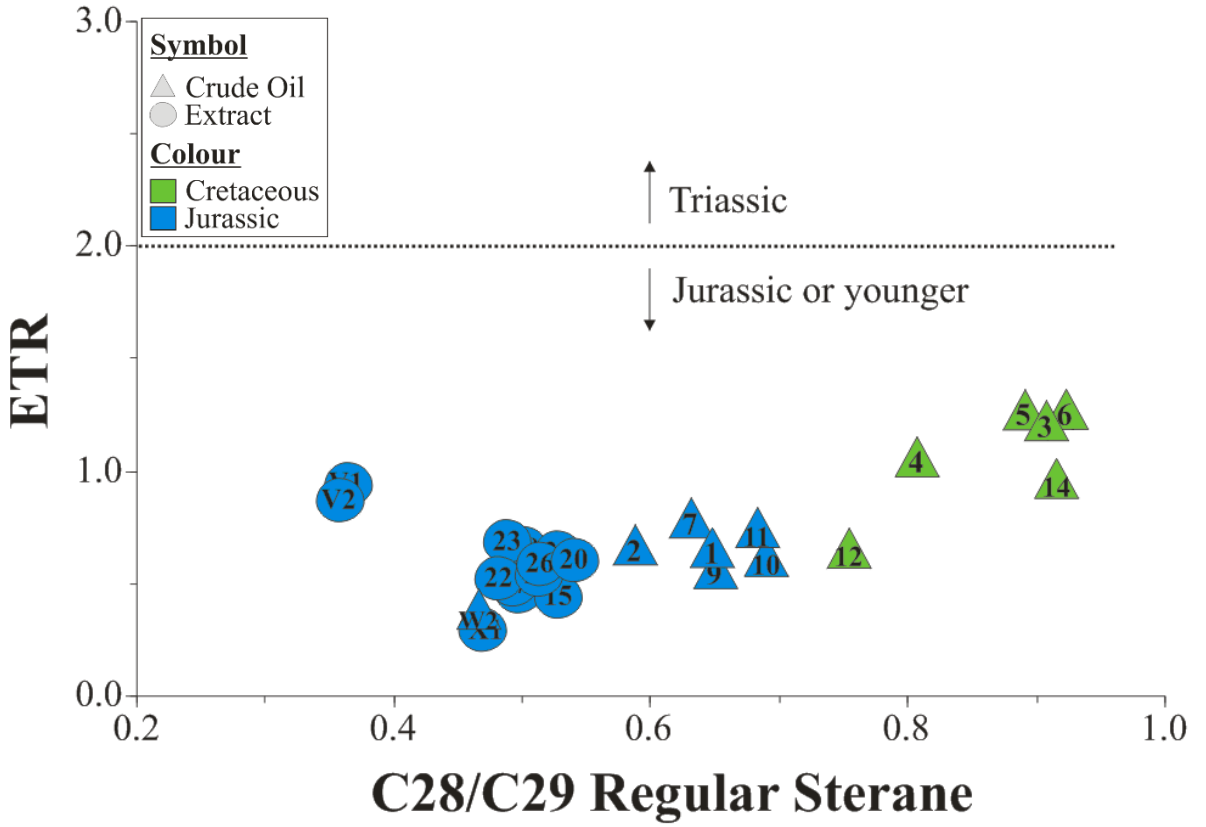

Figure 48 *Evaluation of source rock age based on extended tricyclic triterpanes (ETR) (Holba et al., 2001) indicating Jurassic or younger ages for the Cuban and Jamaican samples.*

5.2.5.1.3 Triaromatic-Dimethylcholesteroids and Triaromatic-Dinosteroids

The triaromatic 23,24-dimethylcholesteroids (TA-DMC: 23,24-dimethylcholesteroid/(23,24-dimethylcholesteroid+24-ethylcholesteroid-S)) can be used together with the triaromatic dinosteroids (TA-dinosteroids: (dinosteroids 1-6)/(dinosteroids 1-6+4-methylstigmastanes)) to distinguish Paleozoic from Mesozoic ages of the source rocks generating the oils (Barbanti et al., 2011). Dinosteranes are derived from dinosterols, which are typically found in dinoflagellate (Withers, 1987) with a paleontological record from Triassic to present (Moldowan and Talyzina, 1998, Talyzina et al., 2000). The TA-DMC are also found in dinoflagellates, as well as diatoms and haptophyte (Volkman et al., 1981, Withers, 1987, Volkman et al., 1993). Both dinoflagellates and haptophytes have existed from Triassic to present, which is similar to the TA-dinosteroids. The TA-DMC is, however, also found in more than 100 diatom species dated to Jurassic and younger ages (Rampen et al., 2009).

In Figure 50, the samples are separated into two groups (marked with blue and green circles), which is generally consistent with the Grantham and Wakefield plot (Figure 49). The Jurassic sourced oils plot as a cluster between 0.05 and 0.15 TA-DMC ratio (Table 12) marked with a blue circle in Figure 50. Samples 3, 5, 6, and 14 (northwestern Cuba), previously interpreted as derived from Cretaceous source rocks, plot as a cluster with values around 0.25 to 0.3 encircled with green colour in Figure 50. Sample 9 from central Cuba, however, does not plot as a Jurassic sourced oil as suggested by the C28/C29 steranes ratio (Figure 49). In addition, samples 4 and 12, which are suggested to derive from source rocks of Cretaceous ages in Figure 49, plot with similar values as the oils derived from Jurassic source rocks (Figure 50). The remaining sample 15 from southern Cuba, as well as the samples V1 and V2 from Jamaica, plot as outliers in Figure 50. As will later be mentioned in the principal component analysis (Chapter 5.2.7), samples V1 and V2 appear to belong to a different oil family than the other oils. Sample 15 has also previously shown different trends relative to the other samples.

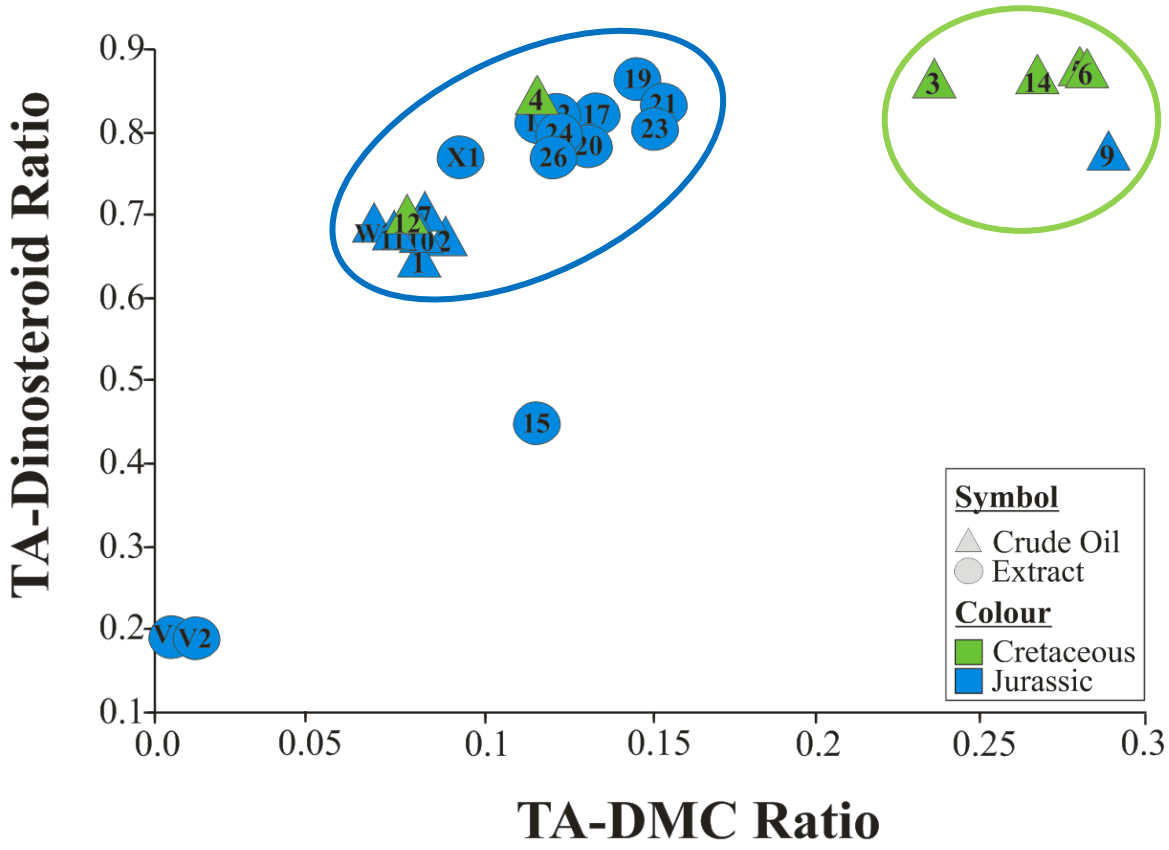

Figure 50 *The triaromatic dimethylcholesteroids ratio (TA-DMC) plotted against the triaromatic dinosteroids ratio (TA-dinosteroid). The samples generally plot in two clusters. The samples encircled in blue colour representing the suggested oils generated by Jurassic source rocks(Figure 48), whereas the samples encircled in green represents the oil suggested to originate from Cretaceous ages (Figure 48). Samples 4 (northwestern Cuba) and 12 (central Cuba) previously suggested as oils originating from Cretaceous source rocks in* ***Figure 48*** *are plotting with the proposed Jurassic derived oils, whereas sample 9 (central Cuba) show the opposite. Three samples plot as outliers (samples 15 (central Cuba), V1, and V2 (Jamaica).*

5.2.5.1.4 Nordiacholestane Ratio

The nordiacholestane ratio (NDR: C26 (24/(24+27) nordiacholestanes) calculated from the 24- and 27-nordiacholestanes can be used to indicate the age of the organic material in the source rocks generating the oils (Holba et al., 1998). The 24-nordiacholestane compound is suggested to be related to diatoms, which increased rapidly in abundance during the Cretaceous. High values of the ratio, thus, indicate Cretaceous ages. The Grantham and Wakefield plot showed a Cretaceous age for sample 12. Thus, it is expected that the NDR ratio would show the highest NDR value for sample 12 among the GC-MSMS analysed samples (2 (northwestern Cuba), 12 (central Cuba), W2, and V1 (Jamaica)). However, as can be observed in Figure 51, sample 2 plots with the highest value. This could indicate that sample 12 was in fact derived from a Jurassic aged source rock as shown in the dinosteroids plot (Figure 50).

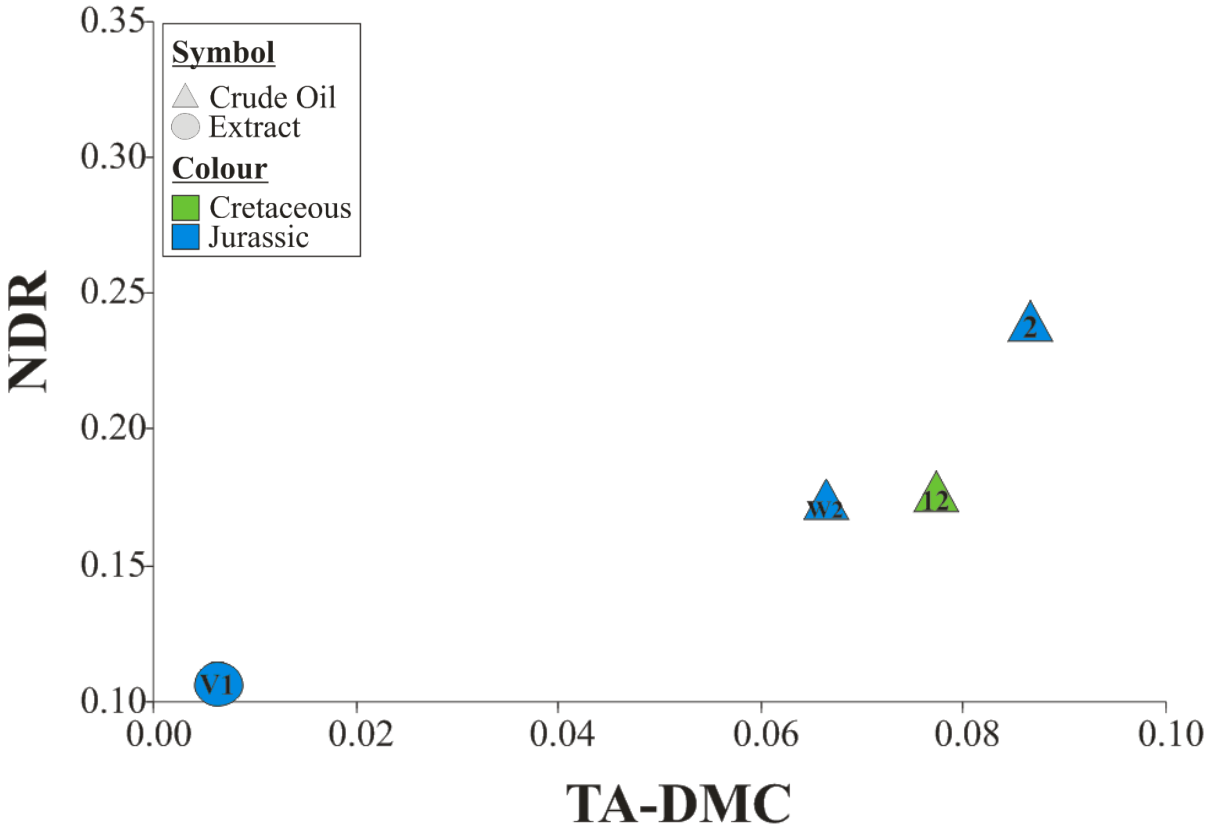

Figure 51 *Cross-plot showing the triaromatic dimethylcholesteroids ratio (TA-DCM) against the nordiacholestane ratio (NDR). Sample 12 (central Cuba), previously suggested to be derived from a Cretaceous source rock (Figure 48), show lower values of the NDR ratio than sample 2 (northwest Cuba), which is suggested to originate from a Jurassic source rock. This could indicate sample 12 was derived from a Jurassic source rock, coinciding with the dinosteriod plot (Figure 50).*

5.2.5.1.5 Distribution

In Figure 52 and Figure 53, the interpreted ages for the source rocks that generated the analysed oils are visualised. The oils from southern part of Cuba (***Figure 52***) and Jamaica (***Figure 53***) appear to be derived from Jurassic aged source rocks, whereas the oils from northwestern and central Cuba are suggested to have both Cretaceous and Jurassic origins (Figure 52). Regarding the three Jamaican samples suggested to stem from Jurassic aged source rock, this is problematic as Jurassic rocks are not known from Jamaica (Lithostratigraphy Chapter 2.2.2). As previously mentioned in the geological setting chapter (Chapter 2.1), the Jamaican island arc collided with the Chortis block during the Latest Cretaceous (Pindell, 1994), which could have led to the attachment of Jurassic source rocks from the North American plate (Cameron et al., 2004).

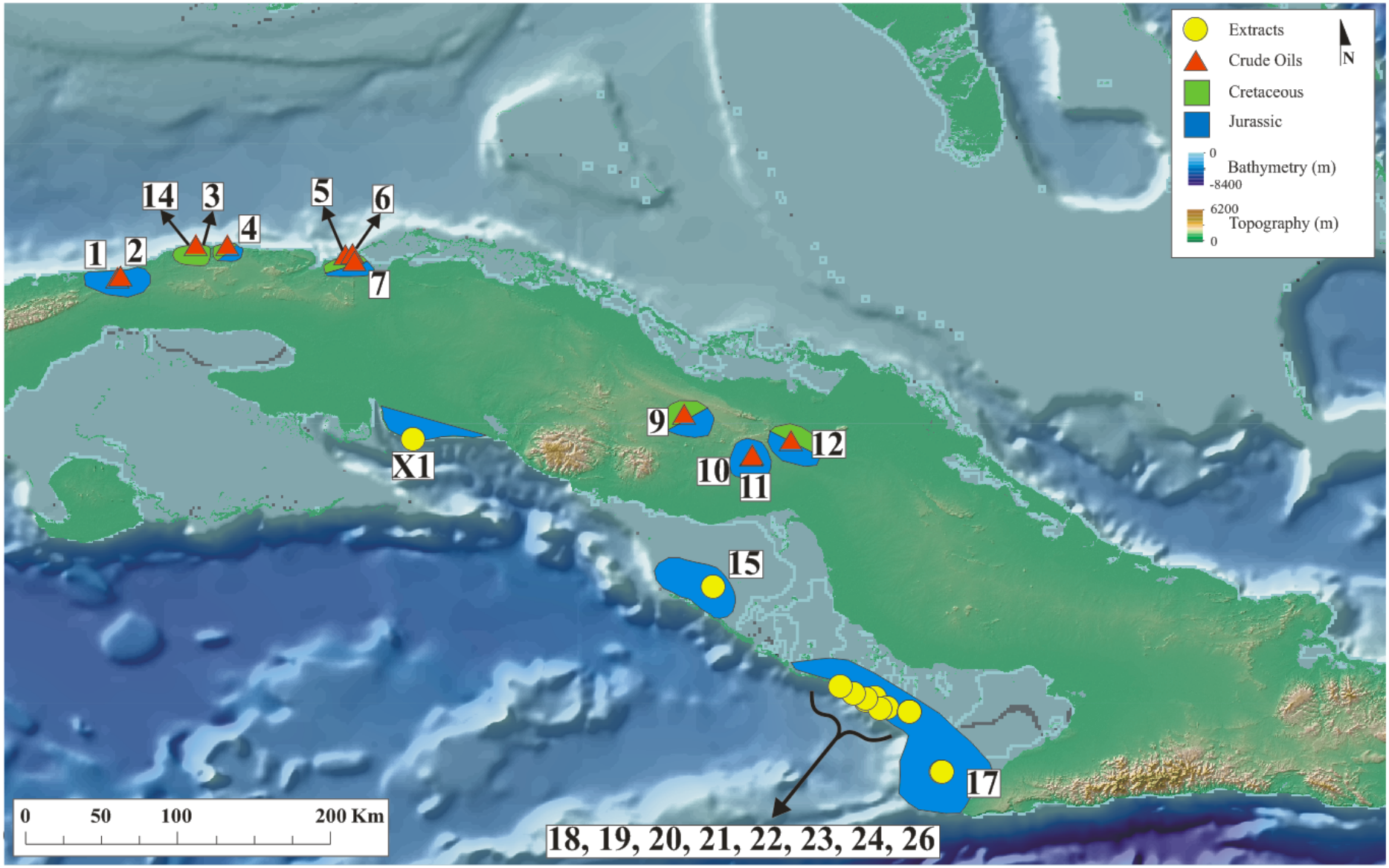

Figure 52 *Distribution of the suggested ages for the source rocks generating the different oils. The samples in central and northwestern Cuba appear to originate from source rocks of both Cretaceous and Jurassic ages, whereas the samples from southern Cuba are suggested to be generated by Jurassic source rocks.*

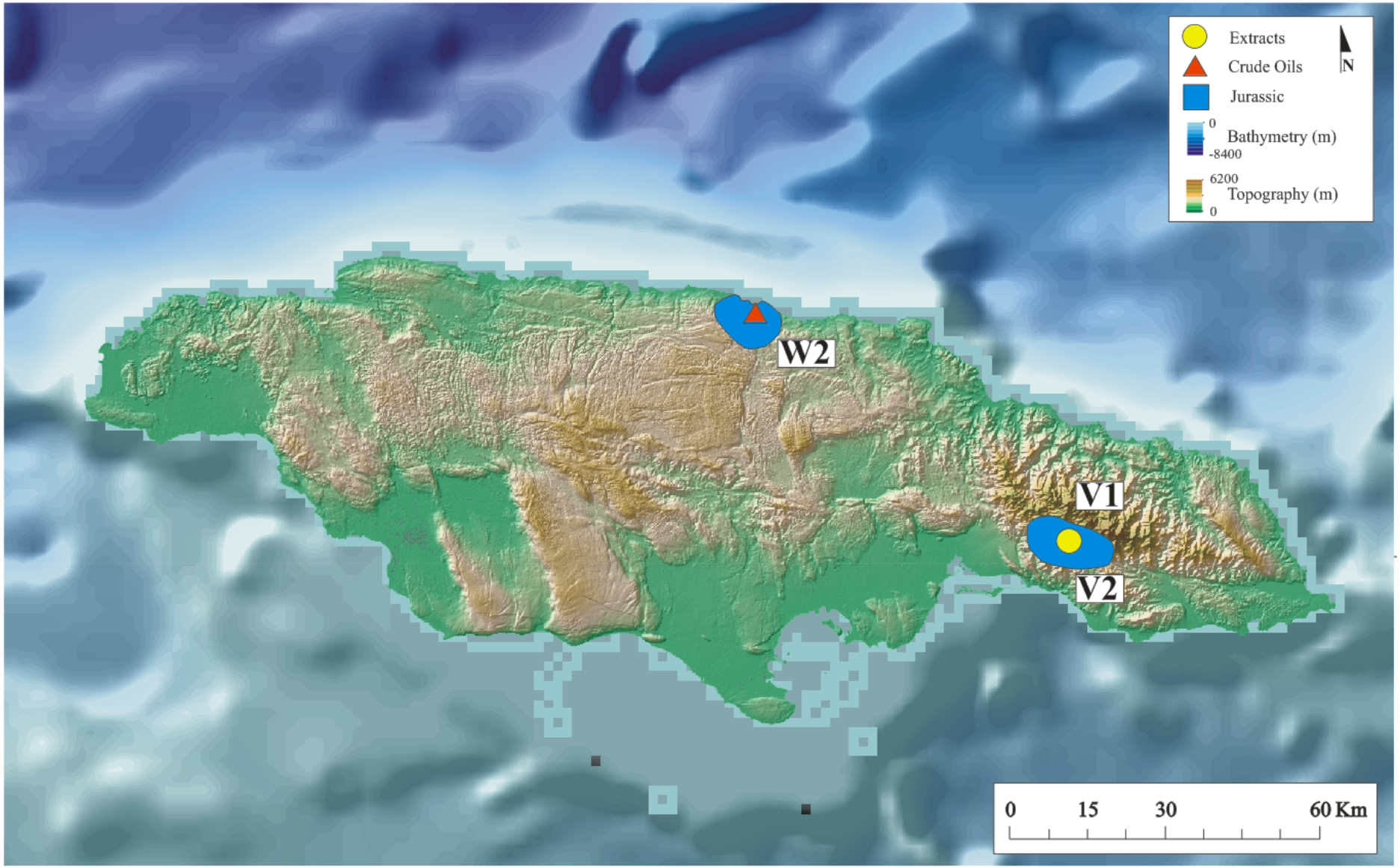

Figure 53 *The oils in Jamaica are suggested to be derived from source rocks of Jurassic ages. However, from the lithostratigraphy (Chapter 2.2.2) the oldest rocks known on Jamaica are of Early Cretaceous ages. The collision between Jamaica and the Chortis block during the late Early Cretaceous could have led to the attachment of Jurassic source rocks from the North American plate (Cameron et al., 2004).*

5.2.6 Compound Specific Isotope Analysis

Compound Specific Isotope Analysis (CSIA) can be a useful tool in terms of oil-oil correlation. Individual n-alkanes are suggested to arise from different precursors (Tissot and Welte, 1984) and given that these precursors may be isotopically distinct (Schoell, 1984, Collister et al., 1992, Collister et al., 1994), the source variation should be reflected in the n-alkane isotope profile (Murray et al., 1994).

As shown in Figure 54, none of the oils plot with identical patterns. The oils plot with surprisingly large variations in isotope values between the different n-alkanes, with sample 4 (northwestern Cuba) displaying the largest diversity. This scattering may reflect that the analysed oils represent mixtures of various oils. Several of the samples (1, 2 (northwest Cuba), 11, and 12 (central Cuba)) also show a significant drop in the δ^{13}C10 to δ^{13}C12 n-alkane range (Figure 54), which suggests a different source for the light oil fraction. Some similarities between the samples may, however, be observed. Samples 1 and 2 from northwestern Cuba show profiles with fairly similar trends (Figure 55). These differ from the other samples by being the isotopically lightest. Furthermore, samples 9, 11, 12 (central Cuba), and 14 (northwestern Cuba) show some similarities in the profiles (Figure 56), where samples 9 and 11 plot almost identical in the C15 to C30 range. This suggests that these oils (oil fractions) originate from the same source rocks. Minor contributions of oils from other source rocks may explain the somewhat different isotope patterns seen in the oil samples 12 and 14. The significantly variation seen in the light n-alkane fraction hints on contribution from different source rocks, or may be a result of alteration effects, as the isotope values generally gets heavier with increasing biodegradation level.

Sample W2 from Jamaica is seen to be the isotopically heaviest oil in the dataset. This could be a result of biodegradation or higher maturity. However, sample W2 has a low biodegradation level (level 1) and roughly the same maturity as the other samples (see Chapters 5.2.1 and 5.2.2). Thus, this could indicate that sample W2 is derived from a different petroleum system than the analysed oils from Cuba.

Samples 1 and 2 that show a similar isotope pattern (Figure 55 and Figure 56) are previously shown to originate from shales (Lithofacies Chapter 5.2.3). The isotope values of these oils suggest that corresponding shales represent the same source rock interval. Samples 9, 11, 12 (central Cuba), and 14 (northwestern Cuba) originate from carbonate (Chapter 5.2.3). Hence the CSIA (Figure 54-56) may reflect some of the previously made interpretations regarding lithofacies.

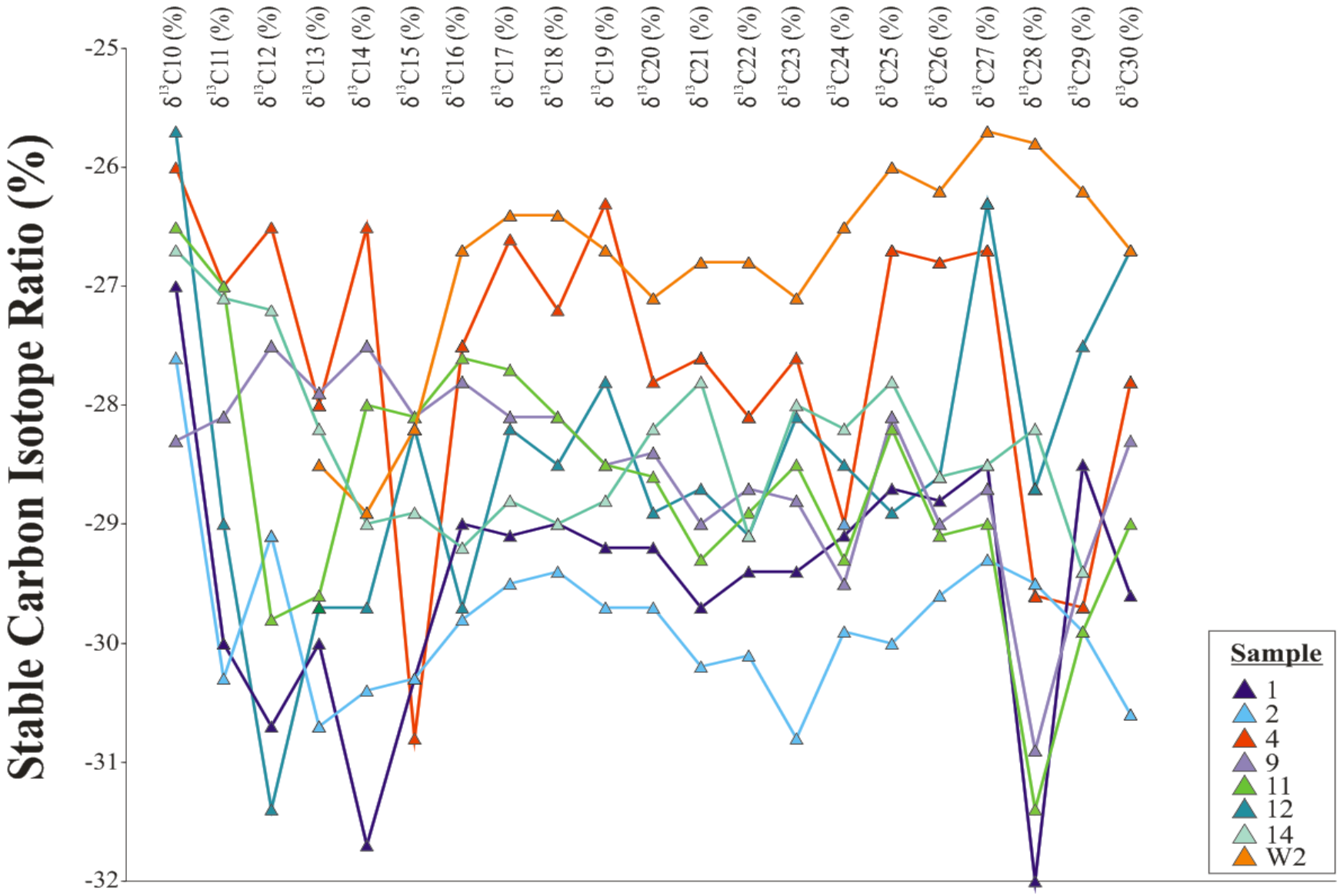

Figure 54 *Compound specific isotope profile for the less biodegraded crude oils. A large spread is seen in the isotope values of the individual n-alkanes for different oils. This indicates that different petroleum systems exists. Some of the samples show, however, similar patterns (samples 1 and 2 (Figure 55), as well as samples 9, 11, 12, and 14 (Figure 56)). This suggest that these grouped samples belong to the same petroleum systems*

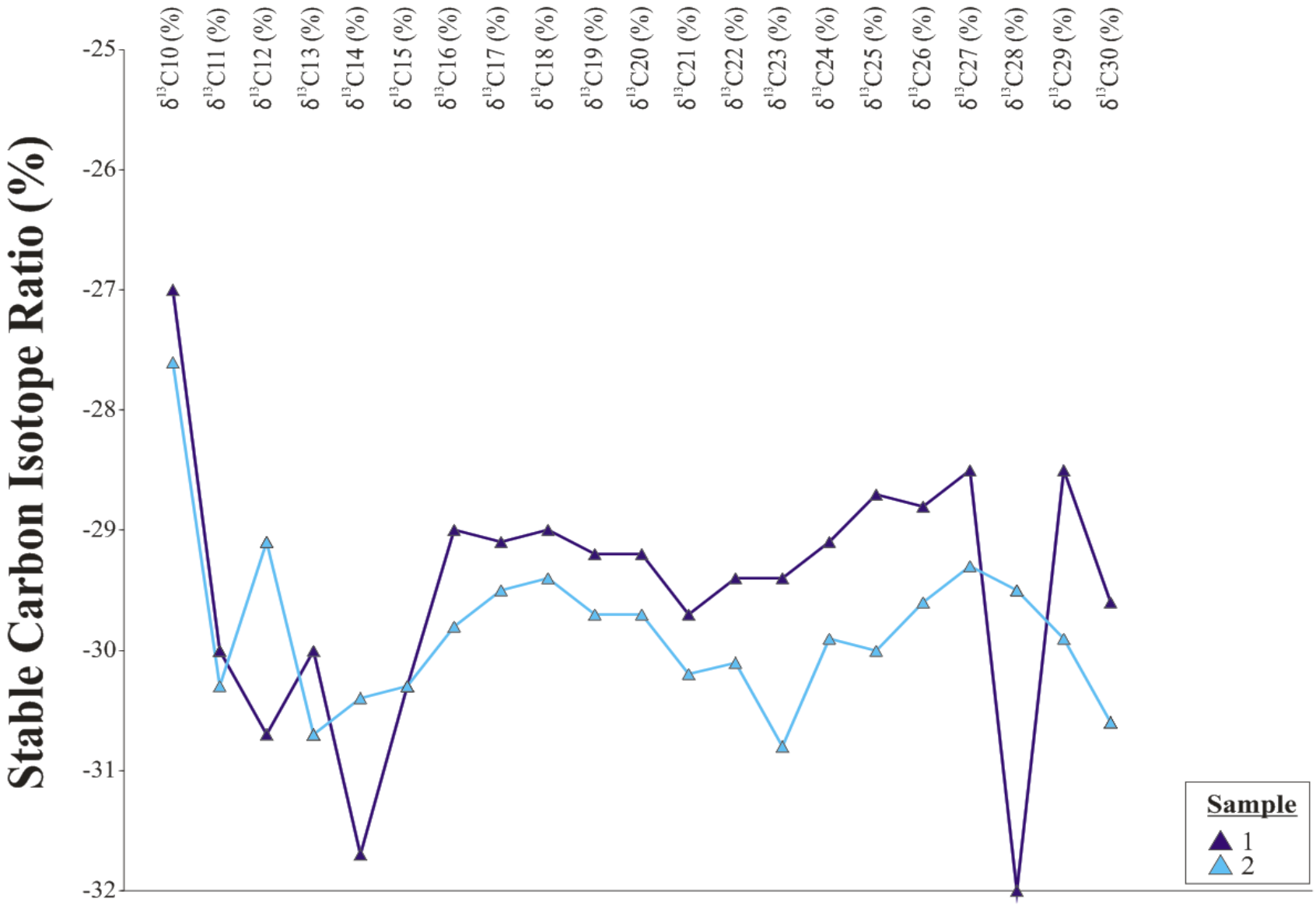

Figure 55 *Compound specific isotope profile showing samples 1 and 2 from northwest Cuba with similar patterns.*

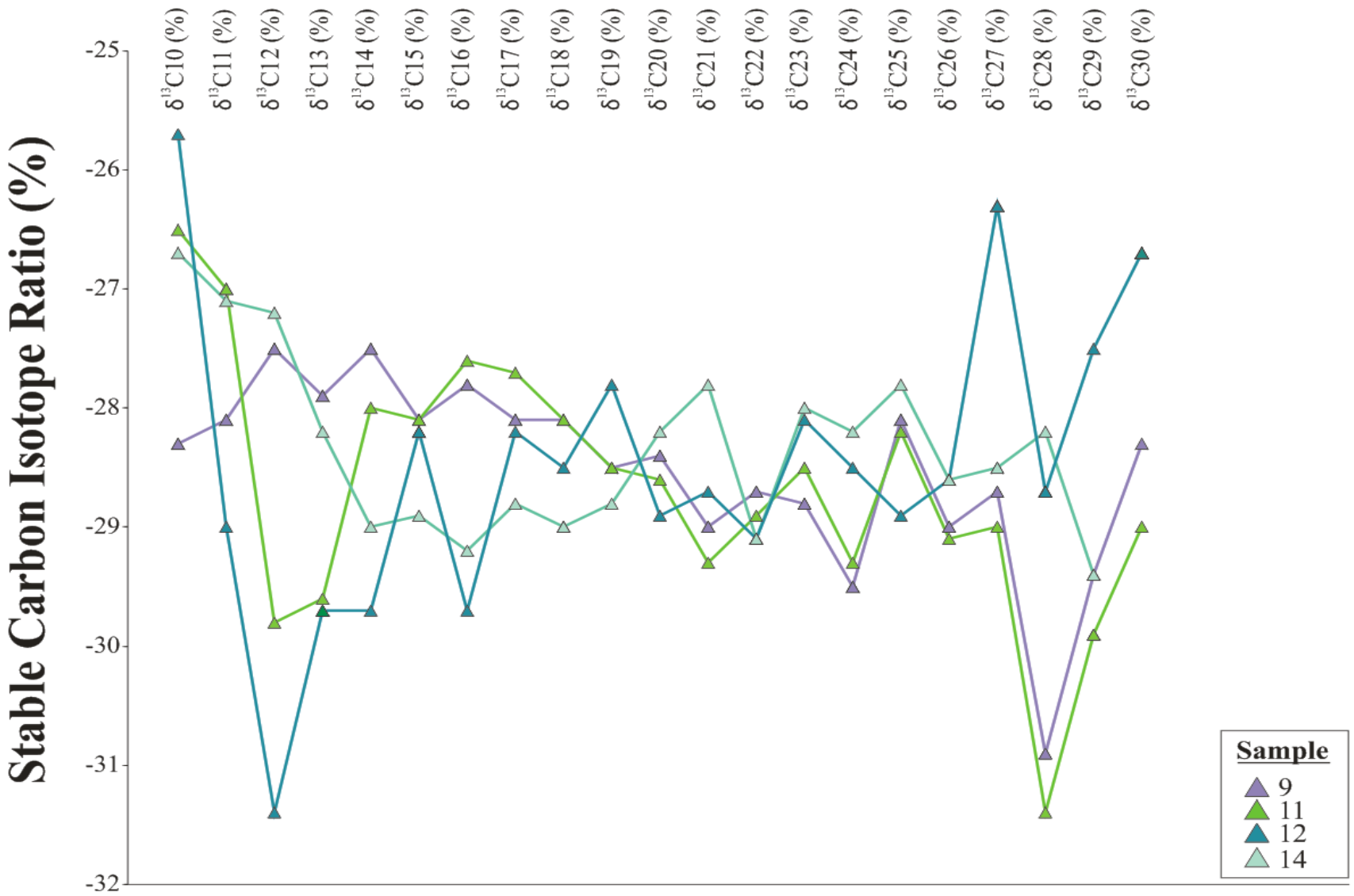

Figure 56 *Fairly similar isotope values are seen for samples 9, 11, and 12 from central Cuba, as well as sample 14 from northwestern Cuba. Sample 9 and 11 show the largest similarity particularly in the C15-C30 range, which suggest charge from the same source rock. The isotope values of the shorter chained n-alkanes from these samples varies a lot and indicates contribution from different source rocks or indicate some biodegradation of this fraction as the isotope values generally gets heavier. Samples 12 and 14, although isotopically having more similarities to sample 9 and 11 than the other analysed oils (Figure 54) plot with larger variations than sample 9 and 11, which indicates mixture of different oils.*

5.2.7 Principal Component Analysis

5.2.7.1 Heavy Fraction

Principal component analysis (PCA) is a multivariate statistical technique used to reduce a high-dimensional data (dataset described by n numbers of variables) into a lower dimensional space (2 or 3 dimensional) to extract the maximum variance in the dataset. Principal component (PC) 1 describes most of the variance, PC 2 the second most etc. (Johnson and Wichern, 2003). For the PCA in this dataset, 22 facies and age sensitive biomarkers were loaded (Table 13). Maturity sensitive parameters were discarded as these might mask the information obtained from the facies and age biomarkers. However, as discussed in the maturity chapter (Chapter 5.2.2), the maturity parameters derived from the terpanes are strongly influenced by lithofacies and are, therefore, included in the PCA.

PC1 to 3 describe ~77 % of the total variance in the dataset and the various cross plots can be seen in Figure 57. From the analysis, five oil families can be identified, as well as three outliers:

- Family I consists of the samples 1, 2, and 7 from northwestern Cuba
- Family II comprise the samples 3, 4, 5, 6, and 14 from northwestern Cuba
- Family III represents the samples 10, 11, and 12 from central Cuba
- Family IV consist of the samples 17-24, 26, and X1 from southern Cuba
- Family V includes the samples V1 and V2 from Jamaica
- The remaining samples (9 (central Cuba), 15 (southern Cuba), and W2 (Jamaica) plot as outliers

The distribution of the different families can be seen on maps of Cuba (Figure 58) and Jamaica (Figure 59). The PCA correlates well with the previous interpreted lithofacies (chapter 6.3) and ages (chapter 5.2.5) for the source rocks generating the oils. Family I comprises the shale derived oils in northwestern Cuba. Samples 1 and 2 also showed similar isotope patterns in the CSIA (Figure 55) and were interpreted to originate from the same source rock. Family II consists of the oils originating from the marls in northwestern Cuba. The previously interpreted carbonate sample 14 is, however, also included with the marls in Family II. This could indicate that sample 14 is derived from a marly source rock rather than a carbonate, as the PCA is based on all facies parameters and not only the few parameters assessed in the biomarker chapters (see Chapters 5.2.3-5.2.5). On the other hand, according to the CSIA, sample 14 show a similar isotopic profile as the carbonate derived oils from central Cuba (samples 9, 11, and 12). The

diversity in the isotope values does, however, suggest contribution of oils from more than one source rock, and the saturate fraction, which makes up most of the oils, may reflect the carbonate derived oil. The biomarkers, which describes only a minor percentage of the oils may in this case, however, reflect a marly origin. Family III (Figure 58) consist of the carbonate derived oils in central Cuba. The fourth family (Family IV) includes the carbonate derived oils in southern Cuba (Figure 58), and Family V is comprised of the Jamaican oils derived from marls (Figure 59).

The remaining samples 9, 15, and W2 plot as outliers in Figure 57. Sample 9 from central Cuba has previously been shown to have almost identical isotopic values as sample 11 from central Cuba (Figure 56). However, as discussed for sample 14, the biomarkers could represent mixtures of oils representing different source rock. The shale derived oil sample 15 from southern Cuba is seen to differentiate from the other shale derived oils in northwestern Cuba, as this sample generally plot as an outlier in the many of the plots (Figure 36, Figure 44, and Figure 50). Sample W2 from Jamaica has also been interpreted to originate from a shaly source rock. However, based on the biomarkers, this samples is shown to be the most terrigenous influenced oil in the data set (Organofacies Chapter 5.2.4). This is supported by its heavy isotope values (Figure 54). Based on CSIA and PCA oil sample W2 is suggested to belong to a different petroleum system than the Cuban oils.

Table 13 *The 22 facies and age dependent biomarker ratios used in the principal component analysis and their correlation with the principal components. The biomarker ratios which show the largest magnitude (farthest from zero in either direction) are strongly correlated with the principal components.*

Biomarker Ratios	Principal Component		
	1	2	3
Ts/Tm	0.903		-0.366
C29Ts/(C29Ts+C29 hopane)	0.867		
C35/C34 hopanes	-0.834		
C26/C25 tricyclic terpanes	0.782		
C30 diahopane/C30 hopane	0.761		0.466
C30 diahopane/(C30 diahopane+C30 moretane)	0.656		0.622
C29/C30 hopanes	-0.653	0.513	-0.433
TA-DCM (TA(23,24-dimethylcholesteroid/(23,24-dimethylcholesteroid+24-ethylcholesteroid-S))	-0.637	-0.384	
C30 hopane/C30 moretane	-0.562	-0.433	
TA-Dinosteriods (TA(dinosteroids 1-6)/(dinosteroids 1-6+4-methylstigmastanes))	-0.552		
diasterane/(diasteranes+regular steranes) (C27 diasteranes/(C27 diasteranes +C27 regular steranes)	0.547	0.492	0.488
C30 sterane index (C30/C27-30)	0.476	-0.473	-0.454
C24 tetracyclic/ C23 tricyclic terpanes		-0.865	0.313
C24 tetracyclic terpane/C30 hopane		0.847	
C24 tetracyclic/ C26 tricyclic terpanes	-0.460	0.788	
Gammacerane index (C30 gammacerane/C30 hopane)	-0.405	-0.690	0.428
C20/C21 tricyclic terpanes	-0.312	0.690	0.400
C23-29 tricyclic terpanes/C30 hopane		0.667	0.389
ETR ((C28+C29 tricyclic terpanes)/Ts)	-0.302	-0.666	0.532
C24/C23 tricyclic terpanes	0.564		0.785
C28/C29 regular steranes	-0.533		0.773
C19/C23 tricyclic terpanes		0.632	0.641

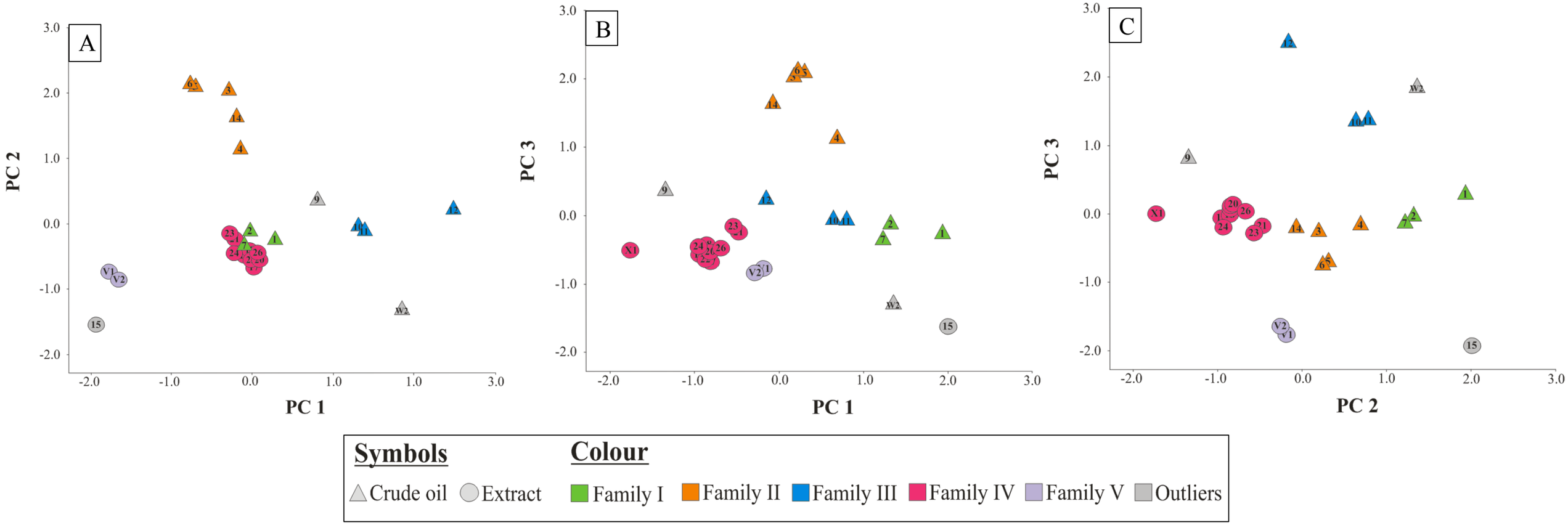

Figure 57 *Principal component analysis (PCA) group the samples into five oil families. Plots of PC1 versus PC2, PC1 versus PC3, and PC2 versus PC3 are presented. These illustrate the variance in the dataset in a three dimensional space. Family I consist of the samples originating from shales in northwest Cuba (1, 2, and 7). Family II comprises the marl derived oils from northwest Cuba (samples 3, 4, 5, and 6) in addition to the carbonate derived oil sample 14 also from northwest Cuba. Family III includes the carbonate derived oils from central Cuba (samples 10, 11, and 12). Family IV represents the oils originating from marls on Jamaica (samples V1 and V2). The three remaining samples (9 (central Cuba), 15 (southern Cuba), and W2 (Jamaica)) plot as outliers.*

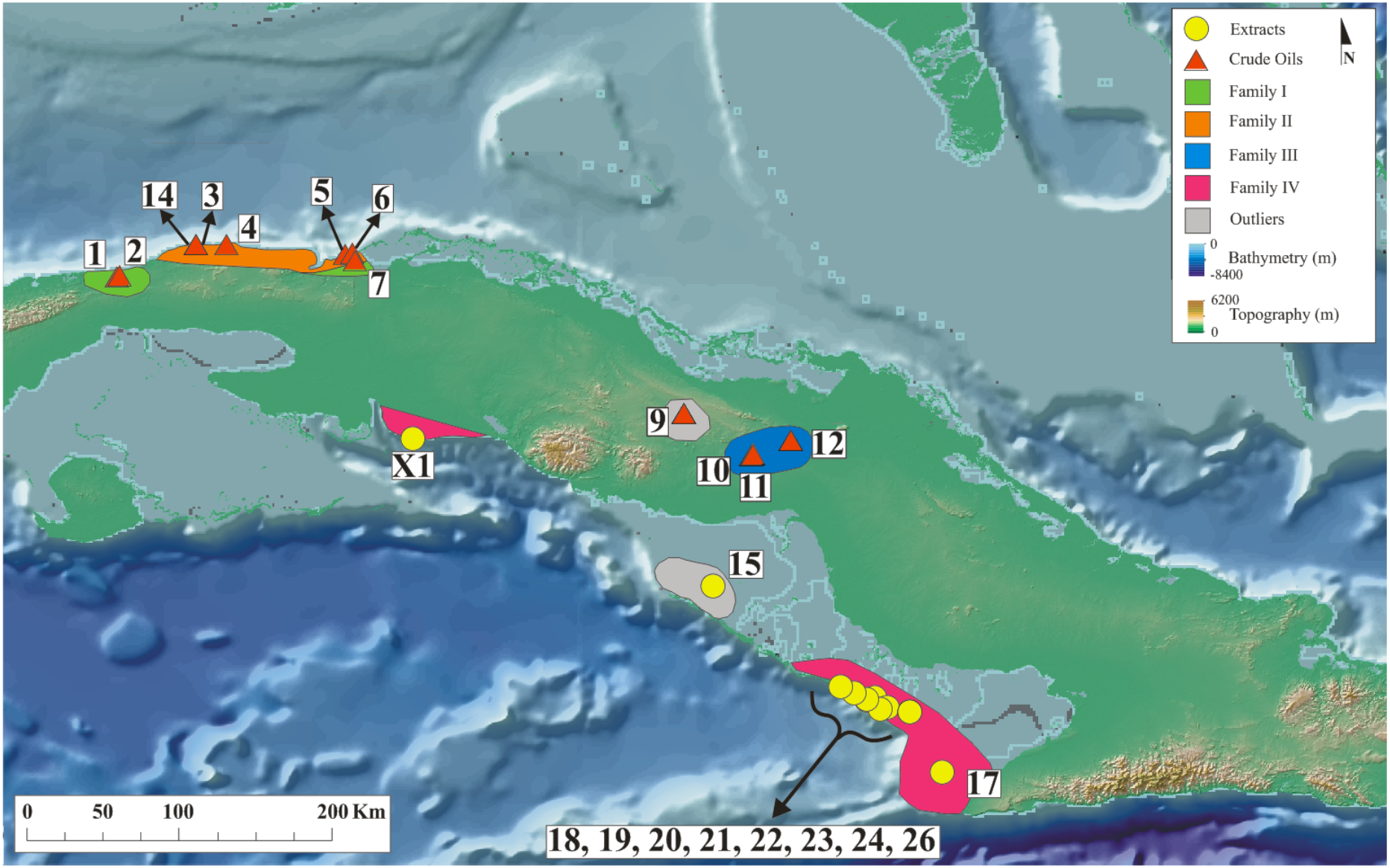

Figure 58 *Map illustrating the distribution of the different PCA families in Cuba. Two families (Family I and II) are located in northwest, Family III in central, and Family IV is in the south. Samples 9 and 15 are not related to the other families, plotting as outliers.*

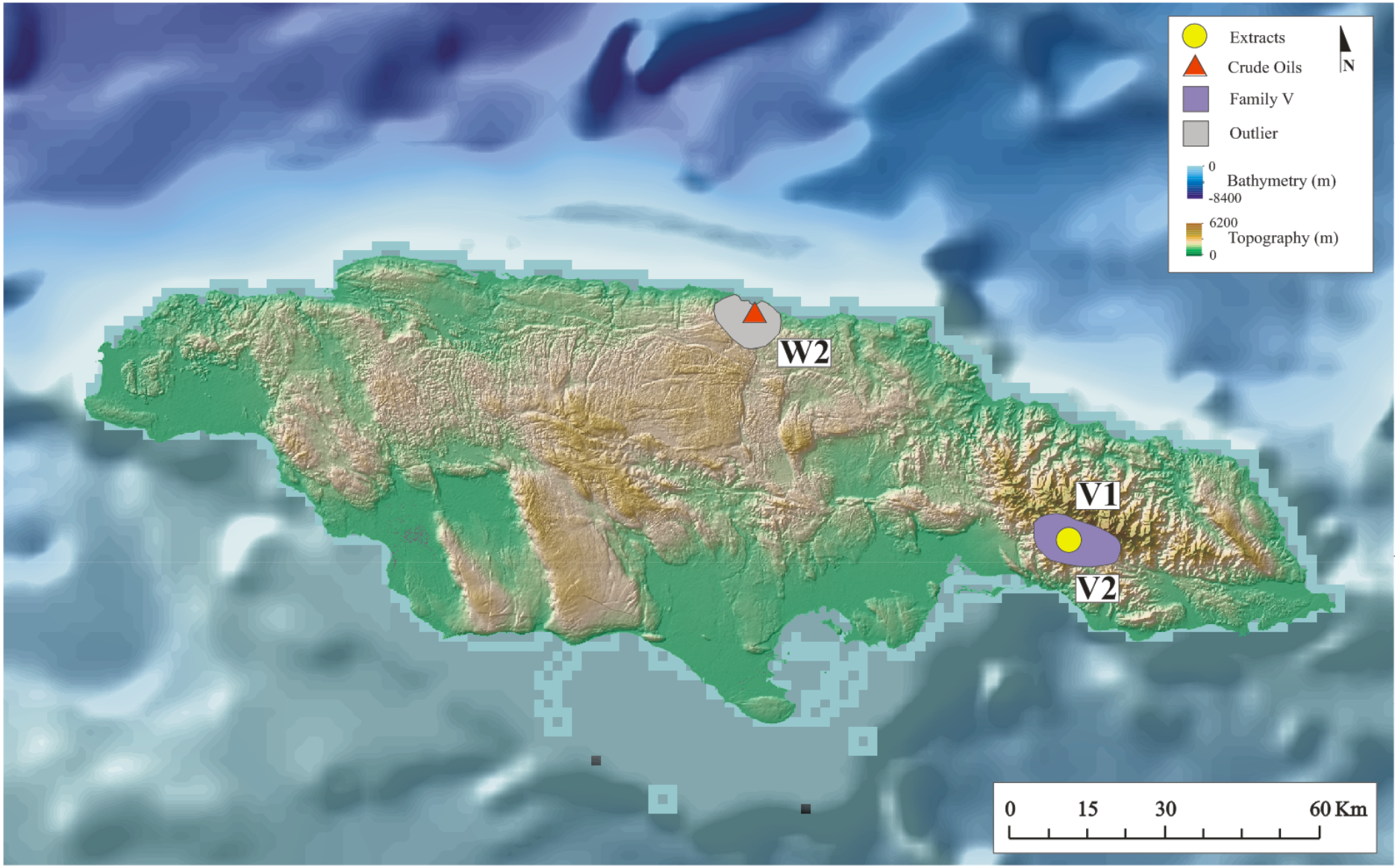

Figure 59 *Map of Jamaica showing the location of Family V in eastern Jamaica. Sample W2 appear to not be related to any of the families.*

5.2.8 Comparison of the Oil Fractions

The Caribbean convergence with the North American plate during the Paleocene to Eocene led to the development of a fold and thrust belt in northern Cuba and a set of normal faults in the south (Figure 2). Due to the folding and thrusting the same source rock may be present at different depths, as well as different stages of maturity and will generate and expel oils reflecting these maturity differences. Faults associated with the folding and thrusting represent likely migration pathways from the source rock to the reservoirs. The mix of oils from different source rocks, maturities and the, in some cases, recent recharge of light hydrocarbon to biodegraded oils demonstrate the petroleum system is very dynamic.

In Figure 60 and Figure 61, the samples generally show higher maturities for the light and medium oil fractions compared to the heavy fraction. This indicates recharge of lighter hydrocarbons. In contrast, the medium oil fraction in sample X1 (central Cuba) appears to have a lower maturity than the heavy oil fraction (Figure 60), which indicates contribution of a less mature source rock. The medium oil fraction in sample 9 (central Cuba, outlier sample) has a very low maturity compared to the light and heavy oil fractions. This could be a result of leaching, where migration of later mature light oil dissolve and pick-up components from an immature source rock.

Further evidences of ongoing charges of hydrocarbons may be observed in the biodegraded oil samples 5, 6, 7 (northwestern Cuba), and 10 (central Cuba), which have higher concentrations of light and medium oil fractions (exemplified by samples 5 and 7 in Figure 62). Differences in lithologies between the light and heavy oil fractions have also been interpreted for several of the samples (Figure 63). The heavy oil fraction shows the samples from southern and central Cuba to mainly originate from carbonate source rocks and the samples from northwestern Cuba to be derived from a mixture of clastic and carbonate source rocks. However, the light fraction shows the opposite with the samples in central Cuba being derived from clastic source rocks and the samples in northwestern Cuba originating from carbonate source rocks. This indicate the presence of at least two petroleum systems in both central and northwestern Cuba.

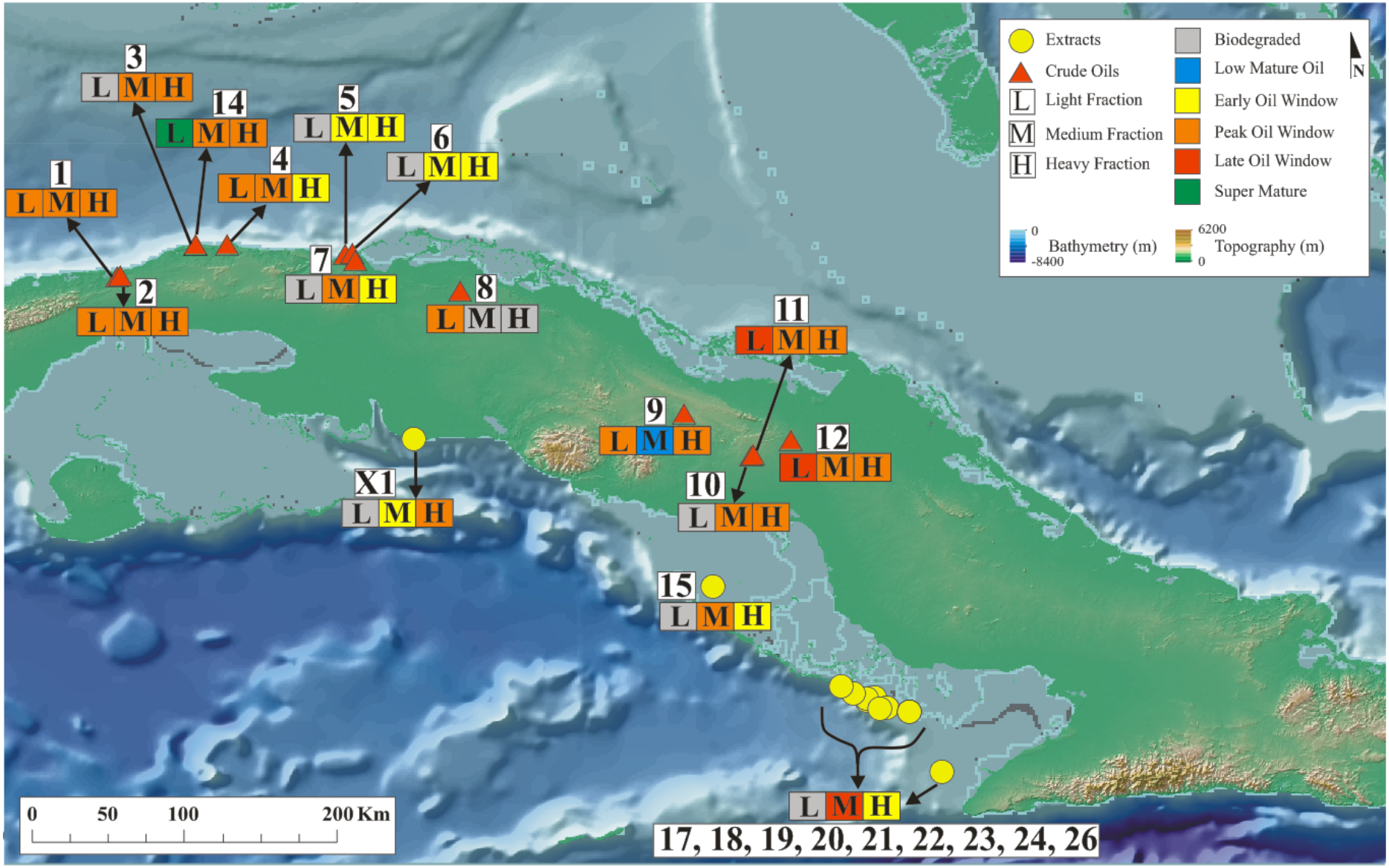

Figure 60 *Comparison of the interpreted maturities between the different oil fractions. The light and medium oil fractions are shown to, generally, have higher maturities compared to heavy oil fraction, indicating recharge of lighter hydrocarbons.*

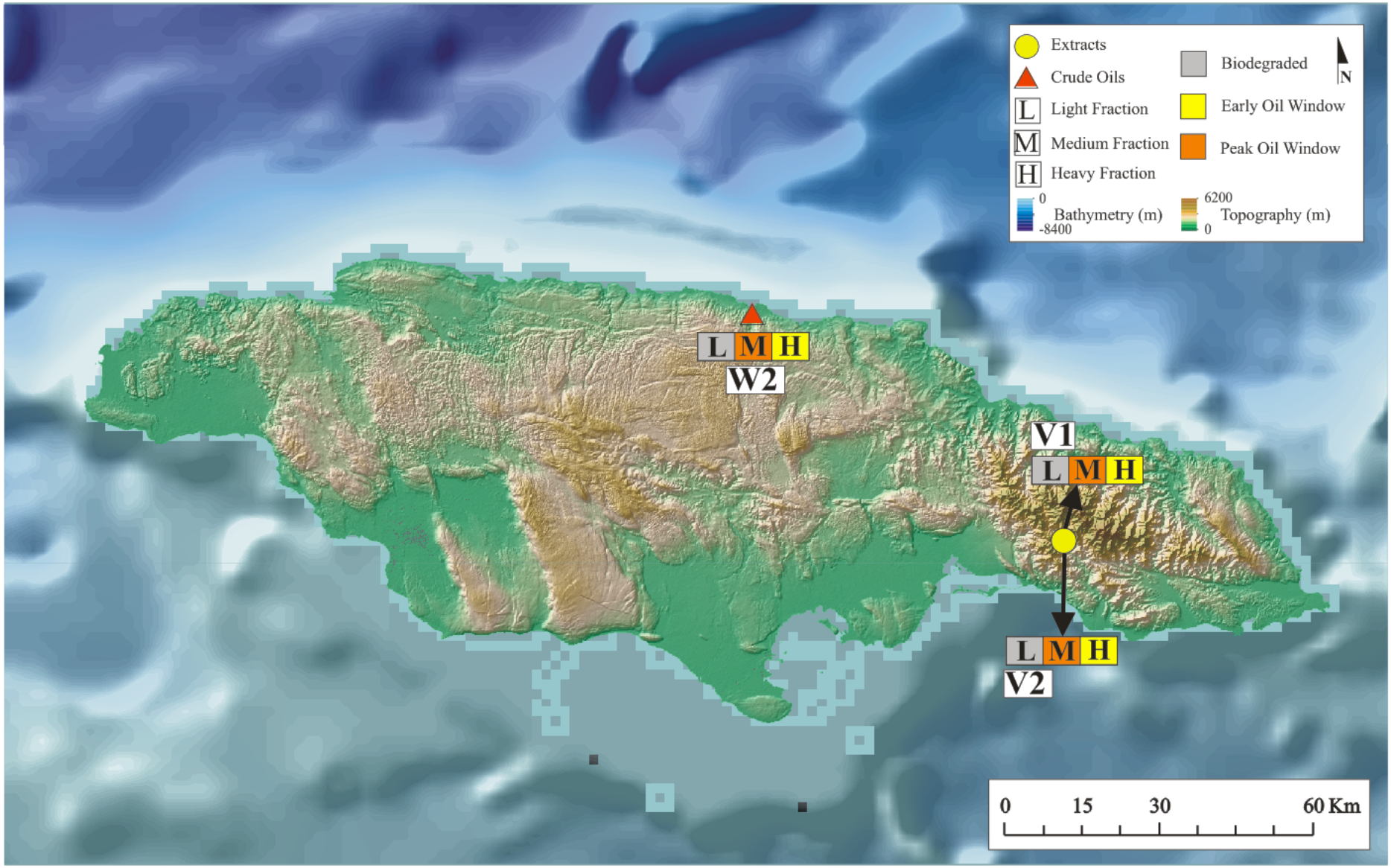

Figure 61 *All the samples from Jamaica show to have higher maturity for the medium oil fraction compared to the heavy oil fraction, indicating more than one charge of hydrocarbons.*

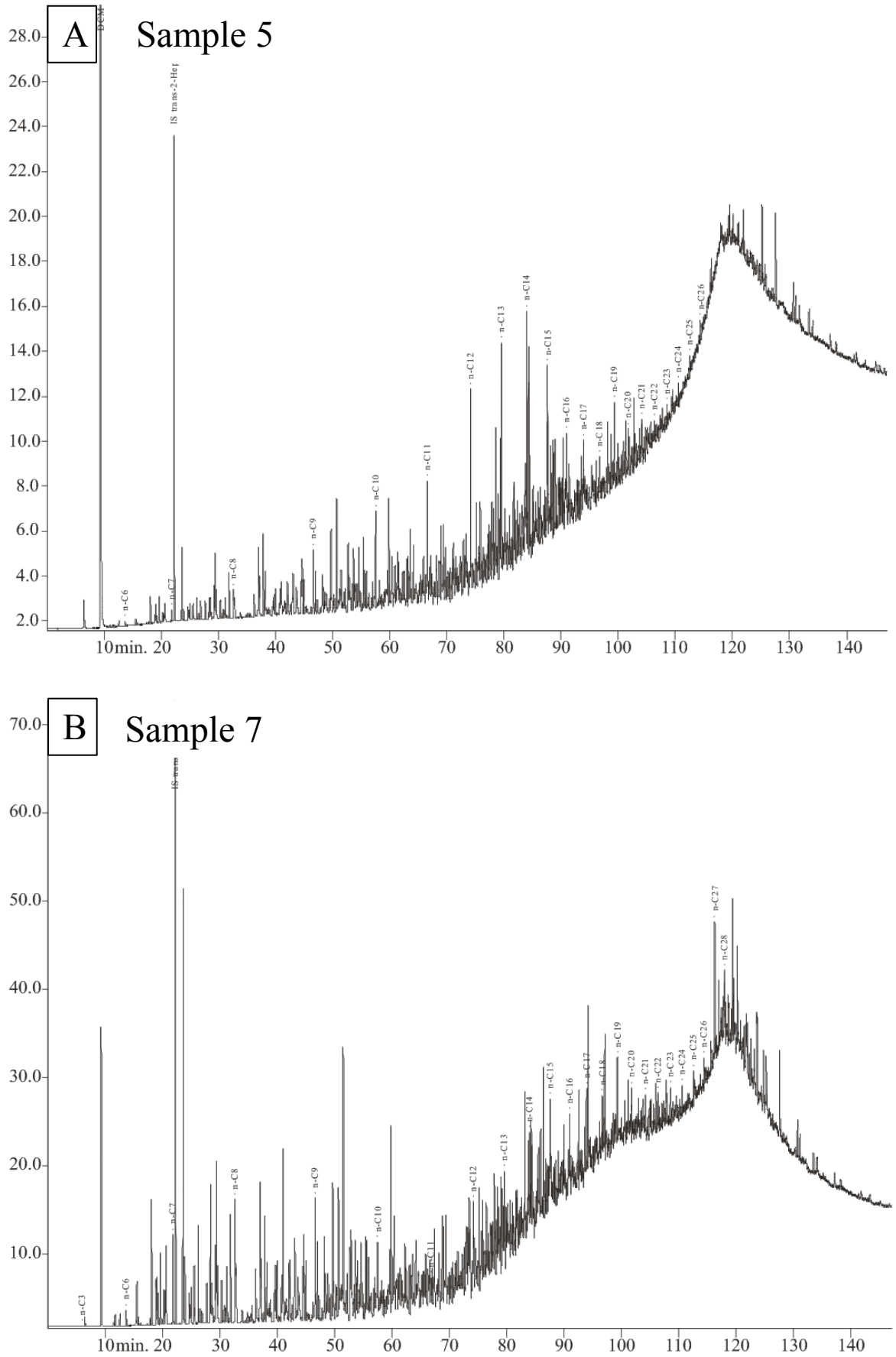

Figure 62 *GC-FID chromatographs of samples 5 (**A**) and 7 (**B**) from northwestern Cuba. The higher concentration of the light and medium oil fractions indicate ongoing recharge of lighter hydrocarbons.*

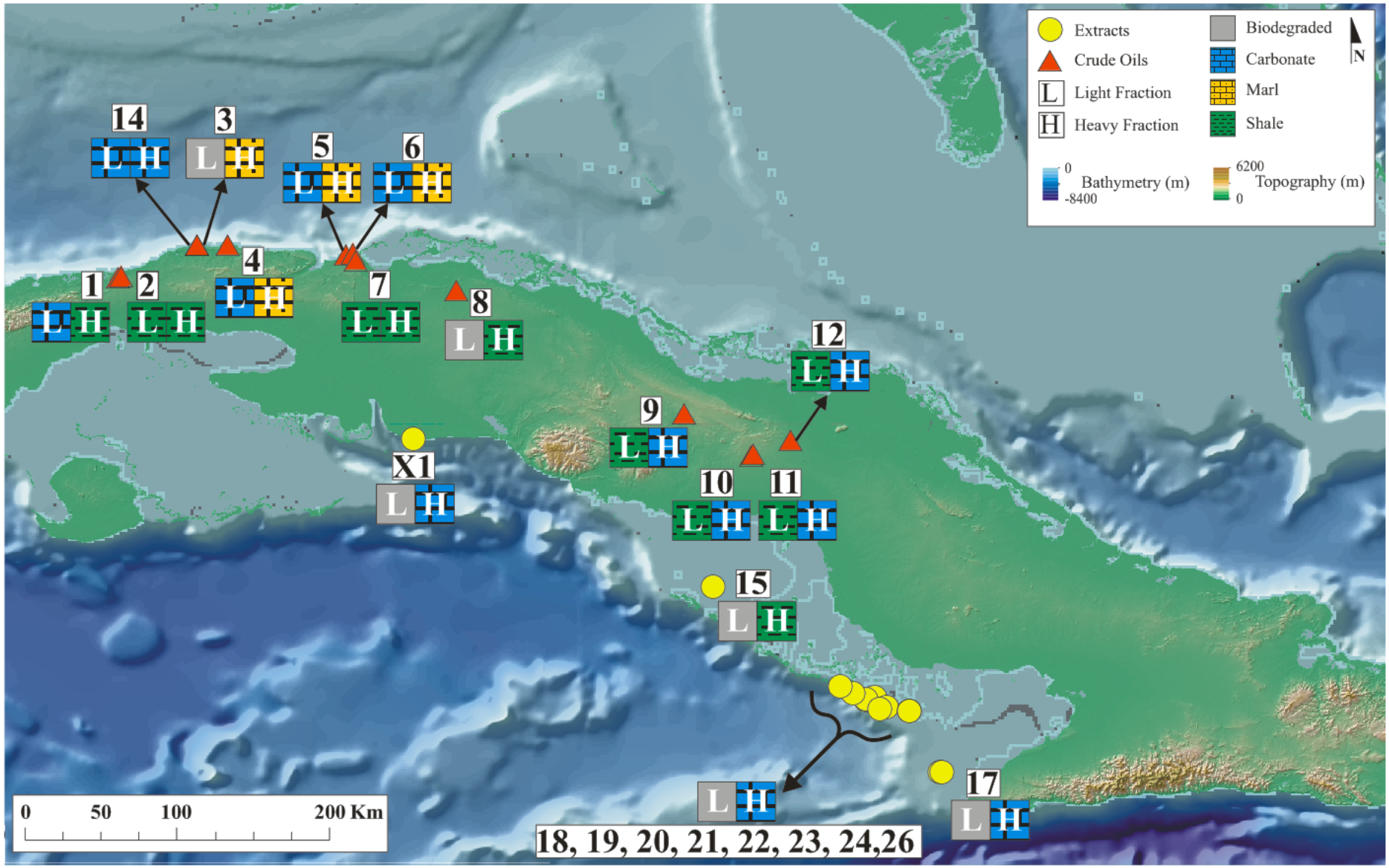

Figure 63 *Comparison of lithofacies between the different oil fractions. The heavy oil fractions of samples from southern and central Cuba are interpreted to be derived from carbonate source rocks, whereas the samples from northwest show to be generated by both clastic and calcareous source rocks. The light oil fraction, however, show an opposite trend. The samples from central Cuba are suggested to be derived from clastic source rocks, whereas the samples from northwestern Cuba appear to originate from carbonates. This indicates the presence of at least two petroleum systems.*

6 Regional Comparison

As described in the geological setting chapter (Chapter 2.1), the geological history of Cuba is generally related to the Caribbean plate. However, at present day, this northern boundary of the Caribbean plate is thrusted over the southern margin of the North American plate. Jamaica, however, is separated from Cuba by the Cayman trough. Thus, it is of significant importance to establish whether petroleum occurrences on Cuba and Jamaica belong to a GOM, northern South American, Caribbean or a completely different petroleum system. To obtain a regional overview, the analysed sampleset is compared with published biomarker analytical data from the GOM and oils from the southern rim of the Caribbean plate (Barbados, Venezuela, and southeastern South America).

6.1 Comparison with the northern area (Gulf of Mexico)

The oils from Cuba and Jamaica were plotted in the C30 diahopane/C30 hopane versus C29/C30 hopane plot (Figure 64). In a similar plot, Cole et al. (2001) distinguished oils from central and east-central GOM. Oils from these areas clustered into two groups; clastic (encircled in green colour) and marls (encircled in orange colour) (Figure 64). Several of the samples from Cuba (1, 2, 3, 4, 5, 6, 7 (northwestern Cuba), and 15 (southern Cuba)) and the samples from Jamaica (samples V1, V2, and W2) are seen to plot along with the GOM oils. Figure 65 illustrate that the majority of the samples that plot together with the GOM oils are located in northwestern Cuba. According to Galloway (2009), marls of Jurassic to Cretaceous ages generate the majority of the hydrocarbons in the GOM. This coincides with the interpreted Jurassic to Cretaceous ages for the oils originating from marly source rocks in the analysed dataset. In addition, prolific shales of Jurassic ages are known in the GOM area (Mancini et al., 2008), coinciding with the Jurassic ages suggested for shale derived oils. The analysed dataset suggests that the GOM petroleum system also is working on northwestern Cuba. Regarding the samples from Jamaica, they are all suggested to be derived from Jurassic source rocks (Age Chapter 5.2.5) even though the oldest rocks known on Jamaica are of Lower Cretaceous ages (Lithostratigraphy Chapter 2.2.2). These petroleum occurrences are suggested to be a result of the collision between Jamaica and the Chortis block during the Latest Cretaceous (Cameron et al., 2004).

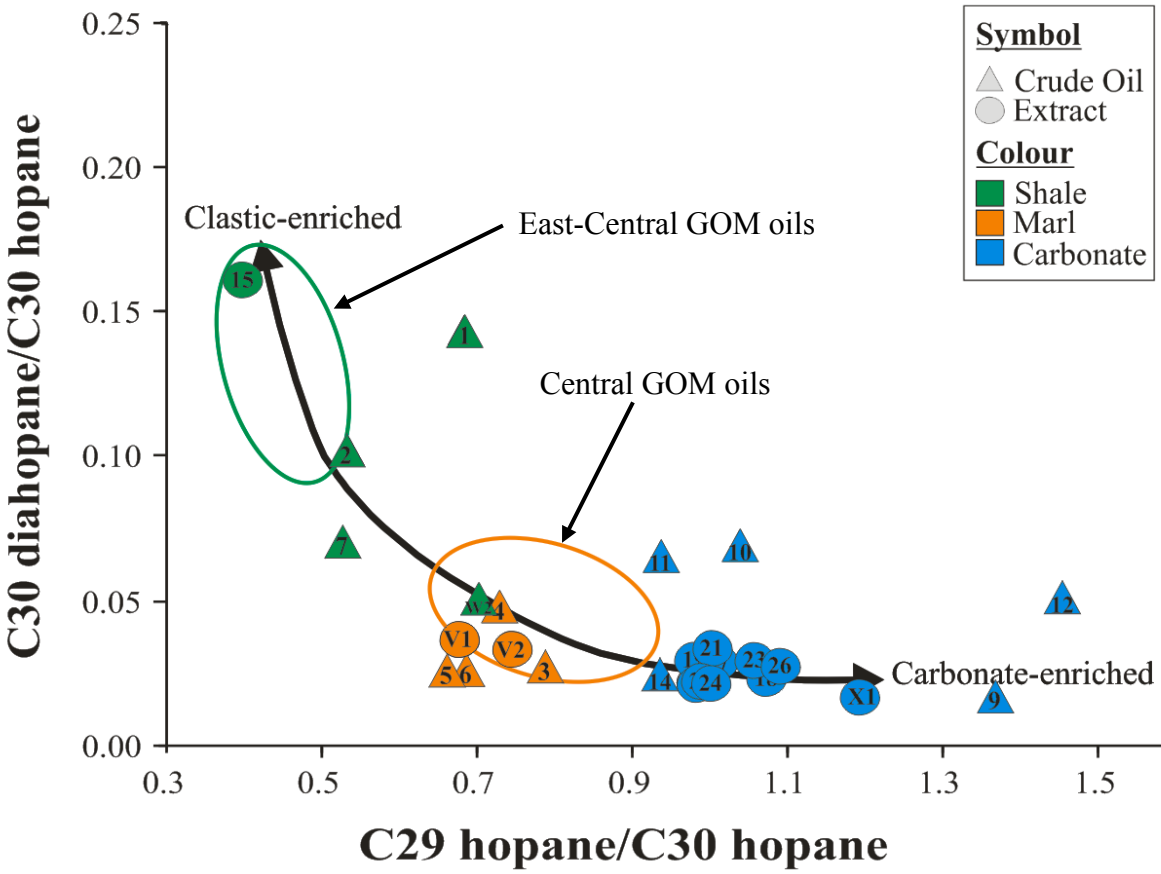

Figure 64 *Cross-plot of C29/C30 hopanes versus C30 diahopane/C30 hopane comparing Cuban and Jamaican oils with oils from central (encircled in orange) and east-central (encircled in green) Gulf of Mexico (GOM) published by Cole et al. (2001). Several of the samples are seen to plot along with the oils from GOM.*

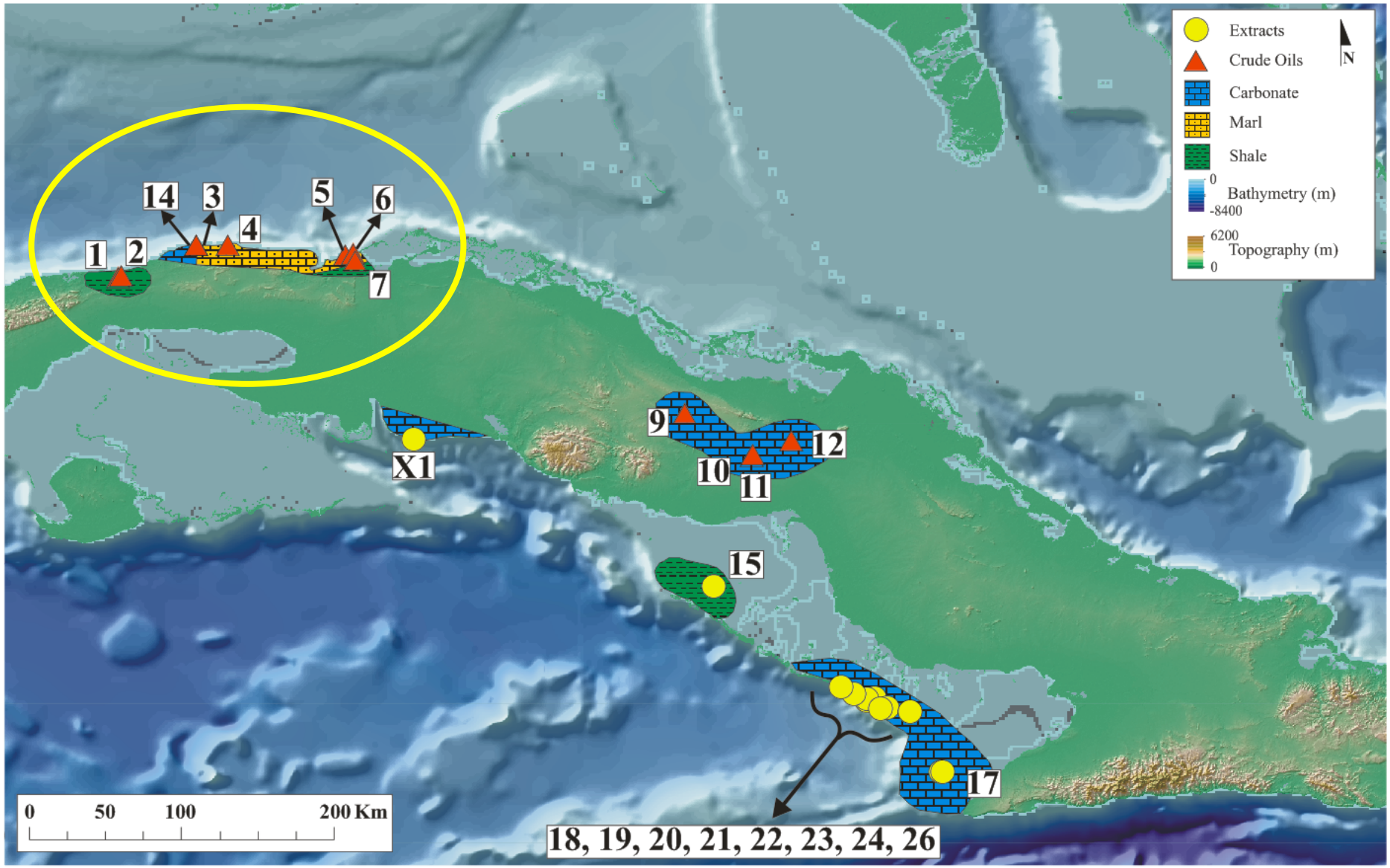

Figure 65 *The distribution of the interpreted lithofacies of the heavy oil fraction on Cuba. The majority of the samples that show similar lithologies as the oils from central and east-central Gulf of Mexico (Figure 64) are located in northwest Cuba (encircled in yellow colour).*

6.2 Comparison with the Southern Area (Barbados, Venezuela, and southeastern South America)

The Cuban and Jamaican oils were compared to oils from Barbados, Venezuela and southeastern South America using PCA with 24 facies, age dependent parameters (Table 14). In Figure 66 plot of PC1 to 3 are visualized. The three first PC's represents 58% of the total variance in the data set. The samples are seen to plot in two different clusters; the oils from Jamaica and Cuba comprises a first cluster, whereas a second cluster consists of the samples from the south. Thus, based on these biomarker ratios (Table 14), the Cuban and Jamaican oils appear to belong to a different petroleum system compared to the samples from the southern rim of the Caribbean plate.

Table 14 *The 24 facies and age dependent biomarker ratios used in the principal component analysis and their correlation with the principal components. The biomarker ratios which show the largest magnitude (farthest from zero in either direction) are strongly correlated with the principal components.*

Biomarker Ratios	Principal Component		
	1	2	3
C30 hopane/C30 moretane	-0.863	-0.306	
C30 diahopane/C30 hopane	0.802		
Diasteranes/(diasteranes+regular steranes)	0.749		
(C27diasteranes/(C27 diasteranes+C27 regular steranes)			
C29/C30 hopanes	-0.742		
C30 sterane index (C30/C27-30)	-0.721		0.516
C28/C29 regular steranes	-0.704	-0.411	
Bisnorhopane	0.69		
ETR ((C28+C29tricyclic terpanes)/Ts)	0.635	-0.552	
C27 Ts/C27 Tm	0.634		0.633
C24/C23 tricyclic terpanes	0.516	-0.323	
C30 diahopane/(C30 diahopane+C29 moretane)			
C19/C23 tricyclic terpanes		0.919	
C20/C21 tricyclic terpanes		0.905	
C24 tetracyclic/C26 tricyclic terpanes	-0.446	0.867	
C24 tetracyclic/C23 tricyclic terpanes	-0.428	0.743	
C35/C34 hopanes		0.597	-0.545
C30 diahopane/(C30 diahopane+C30 moretane)	0.575	0.591	
Gammacerane index (C30 gammacerane/C30 hopane)	-0.341	-0.403	
C25 norhopane		0.373	
C24 tetracyclic terpane/C30 hopane	-0.333	0.371	
C29 Ts/(C29 Ts+C29 hopane)	0.318	0.316	0.783
C26/C25 tricyclic terpanes			0.723
TA-DCM (23,24-dimethylcholesteroid/(23,24-dimethylcholesteroid+24-ethylcholesteroid-S))		-0.412	-0.615
TA-Dinosteroids (TA(dinosteroids 1-6)/(dinosteroids 1-6+4-methylstigmastanes))		-0.415	-0.469

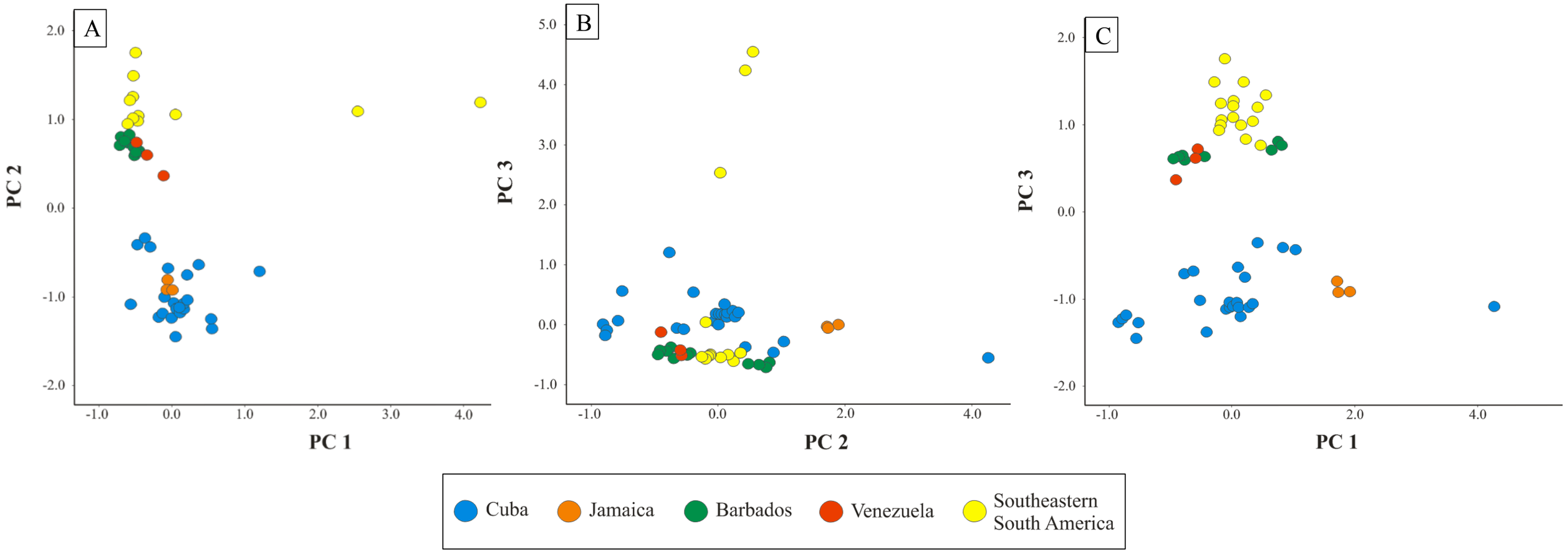

Figure 66 *Principal component analysis (PCA) of oil samples from Cuba, Jamaica, Barbados, Venezuela, and southeast Caribbean based on the principal components (PC) 1, 2, and 3. Oils from Cuba and Jamaica show to plot separately from the oils in the southern margin of the Caribbean plate.*

7 Conclusion

Detailed geochemical characterisation of oils and sediment samples from Cuba and Jamaica leads to the following conclusions:

- Variations in the maturity and facies between the light and the heavy fractions suggest contributions from at least two different source rocks.
- The compound specific isoptope analyses suggest that most of the analysed oils consist of mixtures of various oils.
- Oils in Cuba and Jamaica are interpreted to be derived from both clastic and carbonaceous source rocks;
    - The heavy oil fraction of the analysed oils in central and southern Cuba originates from carbonate source rocks, whereas the oils from northwestern Cuba originates from a mixture of carbonate and clastic source rocks.
    - The light oil fraction, however, show an opposite trend with clastic derived oils in central Cuba and carbonate derived oils in northwestern Cuba.
    - The heavy oil fraction of the Jamaican oils is derived from marls and clastic source rocks.
- High concentrations of the light oil fraction in biodegraded oils suggest an ongoing charge of light hydrocarbons.
- Oils from northwestern and central Cuba are suggested to come from Jurassic and Cretaceous source rocks, whereas oils from southern Cuba appear to only originate from Jurassic source rocks.
- Biomarkers also suggest the Jamaican oils to have a Jurassic source. However, the oldest rocks known from Jamaica are of Lower Cretaceous ages. The collision with the Chortis block during the Latest Cretaceous has been suggested to result in the attachment of Jurassic source rocks.
- PCA suggest five oil families generally supporting the facies interpretation and three outliers;

- **Family I** consists of the shale derived oil samples from northwestern Cuba.
- **Family II** comprises the marls and carbonate derived oils from northwestern Cuba.
- **Family III** includes three out of the four carbonate derived samples from central Cuba.
- **Family IV** comprises the oil samples in southern Cuba generated by carbonates
- **Family V** consists of the oils originating from marls in Jamaica

- Oils from northwestern Cuba and Jamaica show lithofacies similarities to GOM oils.
- Oils from Cuba and Jamaica appear to belong to a different petroleum system than oils from the southern margin of the Caribbean plate.
- The immature source rock samples from Jamaica indicate that they, when buried deep, may generate and expel petroleum.

8 References

ALBERDI-GENOLET, M. & TOCCO, R. 1999. Trace metals and organic geochemistry of the Machiques Member (Aptian–Albian) and La Luna Formation (Cenomanian–Campanian), Venezuela. *Chemical Geology,* 160**,** 19-38.

BARBANTI, S. M., MOLDOWAN, J. M., WATT, D. S. & KOLACZKOWSKA, E. 2011. New triaromatic steroids distinguish Paleozoic from Mesozoic oil. *Organic Geochemistry,* 42**,** 409-424.

BASKIN, D. K. & PETERS, K. E. 1992. Early Generation Characteristics of a Sulfur-Rich Monterey Kerogen {1}. *AAPG Bulletin,* 76**,** 1-13.

BEAUMONT, C., BOUTILIER, R., MACKENZIE, A. S. & RULLKOTTER, J. 1985. Isomerization and aromatization of hydrocarbons and the paleothermometry and burial history of Alberta foreland basin. *AAPG Bulletin,* 69**,** 546-566.

BRALOWER, T. J. & ITURRALDE-VINENT, M. A. 1997. Micropaleontological dating of the collision between the North American Plate and the Greater Antilles Arc in western Cuba. *Palaios***,** 133-150.

BROWN, I. & MITCHELL, S. F. 2010. Lithostratigraphy of the Cretaceous succession in the Benbow Inlier, Jamaica. *Caribbean Journal of Earth Science,* 41.

BURKE, K. 1988. Tectonic evolution of the Caribbean. *Annual Review of Earth and Planetary Sciences,* 16**,** 201-230.

CAMERON, N., MILSOM, J., MATCHETTE-DOWNES, C., MITCHELL, S. F., WRIGHT, R. & ZUMBERGE, J. E. 2004. Jamaica found to have play types analogous to Sumatra, NW Java. *Oil & Gas Jurnal***,** 49-53.

CEDENO , A. F. M. 2017. *Geochemical analysis of oils from Barbados and basin modeling of Paleozoic units in the southern Llanos basin, Colombia.* University of Stavanger, Norway.

CLARK, J. P. & PHILP, R. P. 1989. Geochemical characterization of evaporite and carbonate depositional environments and correlation of associated crude oils in the Black Creek Basin, Alberta. *Bulletin of Canadian Petroleum Geology,* 37**,** 401-416.

COLE, G. A., REQUEJO, R., DEVAY, J., YU, A., PEEL, F., TAYLOR, C. H., BROOKS, J., BERNARD, B., ZUMBERGE, J. & BROWN, S. The deepwater GOM petroleum system: insights from piston coring, defining seepage, anomalies, and background. Proceedings of the 21st Annual GCS-SEPM Foundation Research Conference–Petroleum systems of deep-water basins: Global and Gulf of Mexico Experience. SEPM, Houston, TX, 2001.

COLLISTER, J. W., RIELEY, G., STERN, B., EGLINTON, G. & FRY, B. 1994. Compound-specific d13C analyses of leaf lipids from plants with differing photosynthetic pathways. *Organic Geochemistry,* 21**,** 619-627.

COLLISTER, J. W., SUMMONS, R. E., LICHTFOUSE, E. & HAYES, J. M. 1992. An isotopic biogeochemical study of the Green River oil shale. *Organic Geochemistry,* 19**,** 265-276.

CUBAPETROLEO 2002. The oil industry in Cuba—opportunities

in the new century: Havana, Cuba, Comercial Cupet S.A.**,** 18 p.

CZOCHANSKA, Z., GILBERT, T. D., PHILP, R. P., SHEPPARD, C. M., WESTON, R. J., WOOD, T. A. & WOOLHOUSE, A. D. 1988. Geochemical application of sterane and triterpane biomarkers to a description of oils from the Taranaki Basin in New Zealand. *Organic Geochemistry,* 12**,** 123-135.

DENNY, W. M., AUSTIN JR, J. A. & BUFFLER, R. T. 1994. Seismic stratigraphy and geologic history of middle Cretaceous through Cenozoic rocks, southern Straits of Florida. *AAPG bulletin,* 78**,** 461-487.

DRAPER, G. 2008. Some speculations on the Paleogene and Neogene tectonics of Jamaica. *Geological Journal,* 43**,** 563-572.

DRAPER, G. & BARRAOS, J. A. 1994. Cuba. *In:* DONOVAN, S. K. & JACKSON, T. A. (eds.) *Caribbean Geology: An Introduction.* Kingston, Jamaica: The University of the West Indies Publishers' Association (UWIPA).

ESCALONA, A. & NORTON, I. Quantitative Plate Tectonic and Paleogeographic Reconstructions of the Caribbean Region. 77th EAGE Conference and Exhibition 2015, 2015.

GALLOWAY, W. E. 2009. Gulf of Mexico.

GRANTHAM, P. J. & WAKEFIELD, L. L. 1988. Variations in the sterane carbon number distributions of marine source rock derived crude oils through geological time. *Organic Geochemistry,* 12**,** 61-73.

HACZEWSKI, G. 1976. Sedimentological reconnaissance of the San Cayetano Formation: An accumulative continental margin in the Jurassic of Western Cuba. *Acta Geologica Polonica,* 26**,** 331-354.

HAKIMI, M. H. & ABDULLAH, W. H. 2013. Organic geochemical characteristics and oil generating potential of the Upper Jurassic Safer shale sediments in the Marib-Shabowah Basin, western Yemen. *Organic Geochemistry,* 54**,** 115-124.

HAKIMI, M. H., ABDULLAH, W. H. & SHALABY, M. R. 2012. Geochemical and petrographic characterization of organic matter in the Upper Jurassic Madbi shale succession (Masila Basin, Yemen): origin, type and preservation. *Organic Geochemistry,* 49**,** 18-29.

HALPERN, H. I. 1995. Development and applications of light-hydrocarbon-based star diagrams. *AAPG Bulletin,* 79**,** 801-815.

HOLBA, A. G., ELLIS, L., DZOU, I. L., HALLAM, A., MASTERSON, W. D., FRANCU, J. & FINCANNON, A. L. Extended tricyclic terpanes as age discriminators between Triassic, Early Jurassic and Middle-Late Jurassic oils. 20th International Meeting on Organic Geochemistry, 2001. EAOG Nancy, France, 464.

HOLBA, A. G., TEGELAAR, E., ELLIS, L., SINGLETARY, M. S. & ALBRECHT, P. 2000. Tetracyclic polyprenoids: Indicators of freshwater (lacustrine) algal input. *Geology,* 28**,** 251-254.

HOLBA, A. G., TEGELAAR, E. W., HUIZINGA, B. J., MOLDOWAN, J. M., SINGLETARY, M. S., MCCAFFREY, M. A. & DZOU, L. I. P. 1998. 24-norcholestanes as age-sensitive molecular fossils. *Geology,* 26**,** 783-786.

HUANG, W. Y. & MEINSCHEIN, W. G. 1979. Sterols as ecological indicators. *Geochimica et cosmochimica acta,* 43**,** 739-745.

HUGHES, W. B. 1984. Use of thiophenic organosulfur compounds in characterizing crude oils derived from carbonate versus siliciclastic sources.

HUNT, J. M. 1996. *Petroleum geochemistry and geology*, WH Freeman New York.

ITURRALDE-VINENT, M. A., GARCÍA-CASCO, A., ROJAS-AGRAMONTE, Y., PROENZA, J. A., MURPHY, J. B. & STERN, R. J. 2016. The geology of Cuba: A brief overview and synthesis. *GSA Today,* 26**,** 4-10.

ITURRALDE-VINENT, M. A. & LIDIAK, E. G. 2006. Caribbean tectonic, magmatic, metamorphic and stratigraphic events. Implications for plate tectonics. *Geologica Acta: an international earth science journal,* 4.

ITURRALDE-VINENT, M. A., OTERO, C. D., GARCÍA-CASCO, A. & VAN HINSBERGEN, D. 2008. Paleogene foredeep basin deposits of north-central Cuba: a

record of arc-continent collision between the Caribbean and North American Plates. *International Geology Review,* 50**,** 863-884.
ITURRALDE-VINENT, M. A. 1994. Cuban geology: a new plate-tectonic synthesis. *Journal of Petroleum Geology,* 17**,** 39-69.
JAMES-WILLIAMSON, S. A. & MITCHELL, S. F. 2012. Revised lithostratigraphy of the Coastal Group of south-eastern St. Thomas, Jamaica. *Caribbean Journal of Earth Science,* 44**,** 9-17.
JOHNSON, R. A. & WICHERN, D. 2003. *Applied multivariate stastistical analysis*, Prentice-Hall of India Private Limited.
JORDAN, T. H. 1975. The present-day motions of the Caribbean plate. *Journal of Geophysical Research,* 80**,** 4433-4439.
LAFARGUE, E. & BARKER, C. 1988. Effect of water washing on crude oil compositions. *AAPG Bulletin,* 72**,** 263-276.
LEROY, S., MAUFFRET, A., PATRIAT, P. & MERCIER DE LÉPINAY, B. 2000. An alternative interpretation of the Cayman trough evolution from a reidentification of magnetic anomalies. *Geophysical Journal International,* 141**,** 539-557.
MACKENZIE, A. S. & MCKENZIE, D. 1983. Isomerization and aromatization of hydrocarbons in sedimentary basins formed by extension. *Geological Magazine,* 120**,** 417-470.
MACKENZIE, A. S., RULLKOTTER, J., WELTE, D. H. & MANKIEWICZ, P. 1985. Reconstruction of oil formation and accumulation in North Slope, Alaska, using quantitative gas chromatography-mass spectrometry: source rock evaluation including isotopes and biomarkers.
MAGNIER, C., MORETTI, I., LOPEZ, J. O., GAUMET, F., LOPEZ, J. G. & LETOUZEY, J. 2004. Geochemical characterization of source rocks, crude oils and gases of Northwest Cuba. *Marine and Petroleum Geology,* 21**,** 195-214.
MAKEEN, Y. M., ABDULLAH, W. H., HAKIMI, M. H. & MUSTAPHA, K. A. 2015. Source rock characteristics of the Lower Cretaceous Abu Gabra Formation in the Muglad Basin, Sudan, and its relevance to oil generation studies. *Marine and Petroleum Geology,* 59**,** 505-516.
MANCINI, E. A., OBID, J., BADALI, M., LIU, K. & PARCELL, W. 2008. Sequence-stratigraphic analysis of Jurassic and Cretaceous strata and petroleum exploration in the central and eastern Gulf coastal plain, United States. *Aapg Bulletin,* 92**,** 1655-1686.
MANN, P. 1999. Caribbean sedimentary basins: Classification and tectonic setting from Jurassic to present. *Sedimentary Basins of the World.* Elsevier.
MANN, P., DEMETS, C. & WIGGINS-GRANDISON, M. 2007. Toward a better understanding of the Late Neogene strike-slip restraining bend in Jamaica: geodetic, geological, and seismic constraints. *Geological Society, London, Special Publications,* 290**,** 239-253.
MANN, P., DRAPER, G. & BURKE, K. 1985. Neotectonics of a strike-slip restraining bend system, Jamaica.
MANN, P., SCHUBERT, C. & BURKE, K. Review of Caribbean neotectonics. IN: The geology of North America. Vol. H-The Caribbean region. Boulder, CO, Geological Society of America, 1990, p. 307-338. Research supported by University of Texas, CONICIT, and Universidad de Los Andes., 1990. 307-338.
MELLO, M. R., GAGLIANONE, P. C., BRASSELL, S. C. & MAXWELL, J. R. 1988a. Geochemical and biological marker assessment of depositional environments using Brazilian offshore oils. *Marine and petroleum Geology,* 5**,** 205-223.
MELLO, M. R., TELNAES, N., GAGLIANONE, P. C., CHICARELLI, M. I., BRASSELL, S. C. & MAXWELL, J. R. 1988b. Organic geochemical characterisation of depositional

palaeoenvironments of source rocks and oils in Brazilian marginal basins. *Organic Geochemistry In Petroleum Exploration.* Elsevier.
MITCHELL, S. F. 2003. Lithostratigraphy and palaeogeography of the White Limestone Group. *Cainozoic Research,* 3**,** 5-29.
MITCHELL, S. F. 2006. Timing and implications of Late Cretaceous tectonic and sedimentary events in Jamaica. *Geologica Acta: an international earth science journal,* 4.
MITCHELL, S. F., MILLER, D. J. & MAHARAJ, R. 2003. Field guide to the geology and geomorphology of the Tertiary limestones of the Central Inlier and Cockpit Country. *Caribbean Journal of Earth Science,* 37**,** 39-48.
MOLDOWAN, J. M., FAGO, F. J., LEE, C. Y., JACOBSON, S. R., WATT, D. S., SLOUGUI, N. E., JEGANATHAN, A. & YOUNG, D. C. 1990. Sedimentary 12-n-propylcholestanes, molecular fossils diagnostic of marine algae. *Science,* 247**,** 309-312.
MOLDOWAN, J. M., SEIFERT, W. K. & GALLEGOS, E. J. 1985. Relationship between petroleum composition and depositional environment of petroleum source rocks. *AAPG bulletin,* 69**,** 1255-1268.
MOLDOWAN, J. M., SUNDARARAMAN, P. & SCHOELL, M. 1986. Sensitivity of biomarker properties to depositional environment and/or source input in the Lower Toarcian of SW-Germany. *Organic Geochemistry,* 10**,** 915-926.
MOLDOWAN, J. M. & TALYZINA, N. M. 1998. Biogeochemical evidence for dinoflagellate ancestors in the Early Cambrian. *Science,* 281**,** 1168-1170.
MOLNAR, P. & SYKES, L. R. 1969. Tectonics of the Caribbean and Middle America regions from focal mechanisms and seismicity. *Geological Society of America Bulletin,* 80**,** 1639-1684.
MORETTI, I., TENREYRO, R., LINARES, E., LOPEZ, J. G., LETOUZEY, J., MAGNIER, C., GAUMET, F., LECOMTE, J. C., LOPEZ, J. O. & ZIMINE, S. 2003. Petroleum system of the Cuban northwest offshore zone.
MURRAY, A. P., SUMMONS, R. E., BOREHAM, C. J. & DOWLING, L. M. 1994. Biomarker and n-alkane isotope profiles for Tertiary oils: relationship to source rock depositional setting. *Organic Geochemistry,* 22**,** 521-542.
PETERS, K. E. & CASSA, M. R. 1994. Applied source rock geochemistry: chapter 5: Part II. Essential elements.
PETERS, K. E. & MOLDOWAN, J. M. 1991. Effects of source, thermal maturity, and biodegradation on the distribution and isomerization of homohopanes in petroleum. *Organic geochemistry,* 17**,** 47-61.
PETERS, K. E. & MOLDOWAN, J. M. 1993. *The Biomarker Guide–Interpreting molecular fossils in petroleum and ancient sediments., 1993*, Prentice Hall, Englewood Cliffs, New Jersey.
PETERS, K. E., MOLDOWAN, J. M., SCHOELL, M. & HEMPKINS, W. B. 1986. Petroleum isotopic and biomarker composition related to source rock organic matter and depositional environment. *Organic Geochemistry,* 10**,** 17-27.
PETERS, K. E., WALTERS, C. C. & MOLDOWAN, J. M. 2005. *The biomarker guide*, Cambridge university press.
PHILIPPI, G. T. 1975. The deep subsurface temperature controlled origin of the gaseous and gasoline-range hydrocarbons of petroleum. *Geochimica et Cosmochimica Acta,* 39**,** 1353-1373.
PHILIPPI, G. T. 1977. On the depth, time and mechanism of origin of the heavy to medium-gravity naphthenic crude oils. *Geochimica et Cosmochimica Acta,* 41**,** 33-52.
PINDELL, J. & DEWEY, J. F. 1982. Permo-Triassic reconstruction of western Pangea and the evolution of the Gulf of Mexico/Caribbean region. *Tectonics,* 1**,** 179-211.

PINDELL, J. L. 1994. Evolution of the Gulf of Mexico and the Caribbean. *Caribbean geology: an introduction*, 13-39.

PSZCZÓŁKOWSKI, A. 1999. The exposed passive margin of North America in western Cuba. *Sedimentary basins of the world.* Elsevier.

RADKE, M. 1988. Application of aromatic compounds as maturity indicators in source rocks and crude oils. *Marine and Petroleum Geology,* 5, 224-236.

RAEDERSTORFF, D. & ROHMER, M. 1984. Sterols of the unicellular algae Nematochrysopsis roscoffensis and Chrysotila lamellosa: isolation of (24E)-24-n-propylidenecholesterol and 24-n-propylcholesterol. *Phytochemistry,* 23, 2835-2838.

RAMANAMPISOA, L., RADKE, M., SCHAEFFER, R. G., LITTKE, R., RULLKÖTTER, J. & HORSFIELD, B. 1990. Organic-geochemical characterisation of sediments from the Sakoa coalfield, Madagascar. *Organic Geochemistry,* 16, 235-246.

RAMPEN, S. W., SCHOUTEN, S., HOPMANS, E. C., ABBAS, B., NOORDELOOS, A. A. M., VAN BLEIJSWIJK, J. D. L., GEENEVASEN, J. A. J. & DAMSTÉ, J. S. S. 2009. Diatoms as a source for 4-desmethyl-23, 24-dimethyl steroids in sediments and petroleum. *Geochimica et Cosmochimica Acta,* 73, 377-387.

ROBINSON, E. 1994. Jamaica. *In:* DONOVAN, S. K. & JACKSON, T. A. (eds.) *Caribbean geology: an introduction.* Kingston: University of the West Indies Publishers' Association.

RUBINSTEIN, I., SIESKIND, O. & ALBRECHT, P. 1975. Rearranged sterenes in a shale: occurrence and simulated formation. *Journal of the Chemical Society, Perkin Transactions 1*, 1833-1836.

SCHENK, C. J. 2008. Jurassic-Cretaceous Composite Total Petroleum System and geologic models for oil and gas assessment of the North Cuba Basin, Cuba. *U.S. Geological Survey North Cuba Basin Assessment Team, Jurassic-Cretaceous Composite Total Petroleum System and geologic assessment of oil and gas resources of the North Cuba Basin, Cuba: U.S. Geological Survey Digital Data Series DDS–69–M,* .

SCHOELL, M. 1984. Recent advances in petroleum isotope geochemistry. *Organic Geochemistry,* 6, 645-663.

SEIFERT, W. K. & MOLDOWAN, J. M. 1978. Applications of steranes, terpanes and monoaromatics to the maturation, migration and source of crude oils. *Geochimica et Cosmochimica Acta,* 42, 77-95.

SEIFERT, W. K. & MOLDOWAN, J. M. 1986. Use of biological markers in petroleum exploration. *Methods in geochemistry and geophysics,* 24, 261-290.

SIESKIND, O., JOLY, G. & ALBRECHT, P. 1979. Simulation of the geochemical transformations of sterols: superacid effect of clay minerals. *Geochimica et Cosmochimica Acta,* 43, 1675-1679.

SIMONEIT, B. R. T. 1977. Diterpenoid compounds and other lipids in deep-sea sediments and their geochemical significance. *Geochimica et Cosmochimica Acta,* 41, 463-476.

SINTON, C. W., DUNCAN, R. A., STOREY, M., LEWIS, J. & ESTRADA, J. J. 1998. An oceanic flood basalt province within the Caribbean plate. *Earth and Planetary Science Letters,* 155, 221-235.

SOFER, Z. 1984. Stable carbon isotope compositions of crude oils: application to source depositional environments and petroleum alteration. *AAPG bulletin,* 68, 31-49.

SYKES, R. & SNOWDON, L. R. 2002. Guidelines for assessing the petroleum potential of coaly source rocks using Rock-Eval pyrolysis. *Organic Geochemistry,* 33, 1441-1455.

TALUKDAR, S. C., DETONI, B., MARCANO, F., SWEENEY, J. & RANGEL, A. 1993. Upper Cretaceous source rocks of northern South America. *AAPG Bulletin (American Association of Petroleum Geologists);(United States),* 77.

TALYZINA, N. M., MOLDOWAN, J. M., JOHANNISSON, A. & FAGO, F. J. 2000. Affinities of Early Cambrian acritarchs studied by using microscopy, fluorescence flow cytometry and biomarkers. *Review of Palaeobotany and Palynology,* 108**,** 37-53.

THOMPSON, K. F. M. 1979. Light hydrocarbons in subsurface sediments. *Geochimica et Cosmochimica Acta,* 43**,** 657-672.

THOMPSON, K. F. M. 1983. Classification and thermal history of petroleum based on light hydrocarbons. *Geochimica et Cosmochimica Acta,* 47**,** 303-316.

TISSOT, B. P. & WELTE, D. H. 1984. *Petroleum formation and occurrence*, Springer.

VAN HINSBERGEN, D. J. J., ITURRALDE-VINENT, M. A., VAN GEFFEN, P. W. G., GARCÍA-CASCO, A. & VAN BENTHEM, S. 2009. Structure of the accretionary prism, and the evolution of the Paleogene northern Caribbean subduction zone in the region of Camagüey, Cuba. *Journal of Structural Geology,* 31**,** 1130-1144.

VOLKMAN, J. K., BARRETT, S. M., DUNSTAN, G. A. & JEFFREY, S. W. 1993. Geochemical significance of the occurrence of dinosterol and other 4-methyl sterols in a marine diatom. *Organic Geochemistry,* 20**,** 7-15.

VOLKMAN, J. K., SMITH, D. J., EGLINTON, G., FORSBERG, T. E. V. & CORNER, E. D. S. 1981. Sterol and fatty acid composition of four marine Haptophycean algae. *Journal of the Marine Biological Association of the United Kingdom,* 61**,** 509-527.

WAPLES, D. W. & MACHIHARA, T. 1991. Biomakers for geologist. *American Association of Petroleum GeologistsMethods in Exploration Series*.

WEBER, J. C., DIXON, T. H., DEMETS, C., AMBEH, W. B., JANSMA, P., MATTIOLI, G., SALEH, J., SELLA, G., BILHAM, R. & PÉREZ, O. 2001. GPS estimate of relative motion between the Caribbean and South American plates, and geologic implications for Trinidad and Venezuela. *Geology,* 29**,** 75-78.

WILHELMS, A., LARTER, S. R., HEAD, I., FARRIMOND, P., DI-PRIMIO, R. & ZWACH, C. 2001. Biodegradation of oil in uplifted basins prevented by deep-burial sterilization. *Nature,* 411**,** 1034.

WITHERS, N. 1987. In: Toylor, F. J. R. (Ed.). The biology of Dinoflagellates, Botanical Monographs. *Blackwell Scientific,* 21**,** 16-359.

ZUMBERGE, J. E. 1987. Prediction of source rock characteristics based on terpane biomarkers in crude oils: A multivariate statistical approach. *Geochimica et Cosmochimica Acta,* 51**,** 1625-1637.